# ANALYSIS OF INTER-CARRIER INTERFERENCE CANCELLATION TECHNIQUE AND CHANNEL CAPACITY OF OFDM COMMUNICATION SYSTEM

**by**

**Vivek Kumar Dwivedi**

a thesis submitted for fulfillment of the requirements

for the degree of

## Doctor of Philosophy

in

## Electronics and Communication Engineering



**DEPARTMENT OF ELECTRONICS AND COMMUNICATION ENGINEERING**

**JAYPEE UNIVERSITY OF INFORMATION TECHNOLOGY**

**WAKNAGHAT, SOLAN - 173234**

**INDIA**

**Roll No. 086001**                                      **February 2012**

# CERTIFICATE

This is to certify that the work reported in the Ph.D. thesis entitled "**ANALYSIS OF IINTER-CARRIER INTERFERENCE CANCELLATION TECHNIQUE AND CHANNEL CAPACITY OF OFDM COMMUNICATION SYSTEM**", submitted by **Vivek Kumar Dwivedi** at **JAYPEE UNIVERSITY OF INFORMATION TECHNOLOGY, WAKNAGHAT**, **INDIA,** is a bonafide record of his / her original work carried out under my supervision. This work has not been submitted elsewhere for any other degree or diploma.

Prof. (Dr.) Ghanshyam Singh
(Associate Professor)
Department of Electronics and Communication Engineering
Jaypee University of Information Technology
Waknaghat, Solan-173234, India

(Advisor)

3$^{rd}$ Feb. 2012

**Dedicated to my parents and my family**

# ACKNOWLEDGMENT

First of all, I express most sincere gratitude to my advisor, Prof. (Dr.) Ghanshyam Singh for his guidance, support and encouragement. His vast experience and deep understanding of the subject proved to be immense help to me, and also his profound view-points and extraordinary motivation enlightened me in many ways. I am highly indebted for his guidance, support and cooperation. I shall always remain grateful to him.

My sincere thank to the "COO", Jaypee Education System, the Vice-Chancellor, Director, and Head ECE Department, JUIT, Solan for providing me all the needed support to complete this work. I also sincerely thank to the every member of the Department of Electronics and Communication Engineering and Administration of the JIIT Noida for their kind support. My special acknowledgement goes to Mr. Pankaj K. Yadav and Mr. Shyam Pratap Singh for all of their support in writing this dissertation.

I cannot finish without mentioning my parents, who have been offering all round support during the period of my studies and research. It is the boundless blessings of my parents, endless sacrifice of my wife Nidhi, daughter Shambhvi, son Ishan and brother-in-law Nitin, who gave me enough strength to complete this work. They have shown extreme patience and supported me in every possible way. Words alone can never express my gratitude to them. I express my thanks to my uncles and aunts, all the relatives and friends for their blessings and encouragement for my academic pursuit.

In the last but not least, I thank the ultimate source of energy of every particle in the universe, the Almighty (Lord Shiv and Shiva) and beloved Baba Ji, for giving me enough energy to complete the work.

(Vivek Kumar Dwivedi)

# PUBLICATIONS

**JOURNALS**

[1] Vivek K Dwivedi and G Singh, "A novel marginal MGF based analysis of the channel capacity over correlated Nakagami-m fading with maximal-ratio combining diversity", *Progress In Electromagnetic Research B*, vol. 41, pp. 333-356, 2012.

[2] Vivek K Dwivedi and G Singh, "A novel MGF-based performance analysis of maximal ratio combining diversity receivers in the generalized-K fading channels", *Progress In Electromagnetic Research C*, vol. 26, pp.153-165, Dec. 2011.

[3] Vivek K Dwivedi and G Singh, "Repeated correlative coding scheme for mitigation of inter-carrier interference in an orthogonal frequency division multiplexing system," *IET Communication*, vol. 6, no. 6, pp. 599-603, April 2012.

[4] Vivek K Dwivedi and G Singh, "A novel moment generating function based performance analysis over correlated Nakagami-m fading", *Journal of Computational Electronics*, vol. 10, no. 4, pp. 373-381, Dec. 2011.

[5] Vivek K Dwivedi and G Singh, "Error-rate analysis of OFDM communication system in correlated Nakagami-*m* fading channel using maximal ratio combining diversity", *International Journal of Microwave and Wireless Technologies*, vol. 3, no. 6, pp. 717-726, Dec. 2011.

[6] Vivek K Dwivedi and G Singh, "A novel bit error rate analysis and improved ICI reduction of OFDM communication systems", *Journal of Infrared, Millimeter and Terahertz Waves*, vol. 30, no. 11, pp. 1170-1180, Nov. 2009.

**Submitted/Under Review/Revision**

[7] Vivek K Dwivedi and G Singh, "Analysis of channel capacity of the generalized-K fading based on marginal moment generating function with maximal ratio combing diversity", *Wireless Networks*, (Revision Incorporated), Jan. 2012.

[8] Vivek K Dwivedi and G Singh, "MGF-Based performance analysis of maximal-ratio combining diversity receivers in the generalized-K fading channels", *Digital Signal Processing*, (Revision Incorporated), May. 2012.

**INTERNATIONAL CONFERENCES/SYMPOSIUM**

[9] Vivek K Dwivedi and G Singh, "Analysis of channel capacity of generalized-K fading with maximal ratio combining diversity receivers," *Proc. International Conference on Communication System and Networking technology* (CSNT-2011), 3-5 June 2011, India, pp. 550-553.

[10] Vivek K Dwivedi, Richansh Kumar, Abhinav Gupta, and G Singh, "Performance analysis of Coded OFDM system using various coding schemes," *Proc.*

*Progress In Electromagnetic Research Symposium* (PIERS-2009), 18-21 August, 2009**,** Russia, pp. 1249-1253**.**

[11] Akhil Kamboj, Abhinav Keshari, Vivek K Dwivedi, and G Singh, "Bandwidth Efficient Inter-carrier Interference Cancellation Technique for OFDM Digital Communication Systems," *Proc. Progress In Electromagnetic Research Symposium* (PIERS-2009), 18-21 August, 2009**,** Russia, pp. 1244-1248**.**

[12] Vivek K Dwivedi and G Singh, **"**An efficient BER analysis of OFDM systems with ICI conjugate cancellation method," *Proc. Progress In Electromagnetic Research Symposium* (PIERS 2008), July 2-6, 2008, Cambridge, USA, pp. 166-171.

[13] Vivek K Dwivedi and G Singh, "A LMMSE approach for frequency offset estimation in OFDM systems," *Proc. 5th International Conference on Intelligent Systems and Networks* (ISN2008), Feb. 22-24, 2008, India, pp. 264-266.

[14] V K Dwivedi, P Kumar, and G Singh, **"**A novel blind frequency offset estimation method of OFDM systems", *Proc. Int. Conf. on Recent Advances in Microwave Theory and Applications* (Microwave-08), Nov. 21-24, 2008, India, pp. 668-670.

[15] V K Dwivedi and G Singh, "Improved BER analysis of OFDM communication system on correlated Nakagami fading channel", *Proc. Int. Conf. on Recent Advances in Microwave Theory and Applications* (Microwave-08), Nov. 21-24, 2008, India, pp. 536-539.


**NATIONAL CONFERENCES/SYMPOSIUM**

[16] Vivek K Dwivedi and G Singh, "Inter-carrier-interference cancellation in OFDM systems", *Proc. National Conference on Wireless and Optical Communication* (WOC-2007), pp. 245-248, PEC Chandigarh, India.

# TABLE OF CONTENTS

# LIST OF TABLE

# ABSTRACT

Orthogonal Frequency Division Multiplexing (OFDM) is a multicarrier modulation technique, which is widely used in various communication systems and standards due to its high-data rate, high-spectral efficiency and robustness to the frequency selective channels. However, one of the major disadvantages of OFDM communication is its sensitivity against carrier frequency offset, which causes inter-carrier-interference (ICI) and degrades the performance of system. The carrier frequency offset is caused by the mismatch of frequencies between the oscillators of transmitter and receiver, or from the Doppler spread due to the relative movement between the transmitter and receiver as well as phase noise arises predominantly due to imperfections of the local oscillator in the transceiver. However, the ICI induced by phase noise and timing offset can be completely compensated or corrected. Since the Doppler spread or frequency shift is random, so we can only mitigate its impact in the system. A simple and most effective method, which is known as self-cancellation scheme, reduces the ICI at the cost of transmission rate with little additional computational complexity. The main idea used in this scheme is to modulate the input data symbol onto a group of subcarriers with predefined coefficients such that the generated ICI signals within that group cancel each other, hence named as self-cancellation. Due to this reason, the bandwidth efficiency becomes half, which is the major drawback of this technique. Frequency domain equalization for ICI cancellation, which is very simple but the short coming of this technique is that it can only reduce the ICI caused by multipath fading distortion. Moreover, it is only suitable for flat-fading channels but in the mobile communication the channels are frequency selective fading in nature. Another effective technique is conjugate cancellation, in which two sequences are transmitted in each data symbol. First sequence is original received sequence and another sequence is conjugate of the original sequence. Thus the two sequences are conjugate of each other rather than adjacent subcarriers with opposite polarities in order to cancel the ICI.

In this thesis, we have investigated an efficient ICI cancellation technique and developed a novel mathematical model to improve the bit-error-rate and carrier-to-interference ratio compared to the other techniques as reported in literature. In the

proposed OFDM system, at the transmitter, IFFT is performed for first part of the data and FFT for the second part of data. At the receiver, FFT is performed for first part of the data and IFFT for the second part of data. These combined operation forms an ICI cancellation scheme for the OFDM system. We analyze the subcarrier index before and after cancellation of the frequency offset and discuss the carrier-to-interference ratio. The average carrier-to-interference power ratio is used as the ICI level indicator and theoretically carrier-to-interference ratio expression is derived for the proposed scheme. The proposed scheme provides significant carrier-to-interference ratio improvement, which has been studied theoretically and supported by simulations.

A repeated correlative coding scheme is also proposed to combat ICI caused by the frequency offset in OFDM communication systems. This proposed scheme combine two ideas of the well-known methods, which are the coding of adjacent subcarriers with antipodal of the same data symbol (ICI self-cancellation) and correlative coding. A mathematical expression for the carrier-to-interference ratio by using this proposed repeated correlative coding scheme is derived. The carrier-to-interference ratio for proposed scheme is significantly improved compared to the correlative coding as well as self-cancellation scheme. The bit-error-rate of proposed scheme is also compared with the ICI self-cancellation scheme and correlative coding scheme, which is comparable to that of the ICI self-cancellation scheme and better than correlative coding scheme. The proposed theoretical analysis and simulation results prove that the ICI caused by multicarrier frequency offset can be cancelled efficiently by using the proposed repeated correlative coding scheme for the OFDM communication system.

OFDM transmission over mobile/wireless channels, the electromagnetic waves experience different effect like diffraction, scattering, reflection, and absorption because of interaction with surface irregularities, which create a continuum of scattered partial waves. The reflections caused when the electromagnetic waves impinge upon surface having dimensions much larger than the wavelength of the impinging wave. The diffractions are caused due to effects of sharp edges in the path of the radio waves between the transmitter and receiver. The scattering is caused when the electromagnetic waves encounter objects of dimension much smaller than the wave in the propagation medium. The amplitudes and phases variations of these

partially refracted, scattered and reflected waves depend on the physical properties of the surfaces such as geometrical proportions and electromagnetic reflection properties. These partial waves create irregular electromagnetic field after interfering with each other and with the direct wave. On the other hand, the transmitted signal power decreases with the traveled distance and because of existence of large number of refracting, scattering and reflecting objects between transmitter and receivers, introduces random variations of the local mean of the envelope or equivalently the local mean power. Therefore, to statistically model the wireless channels, it is a very common practice to consider two independent propagation models, the small-scale propagation model for random amplitude and phase variations and large-scale propagation model for power (shadowing and path loss) variation. Several distributions have been discussed to model the small-scale fading such as the Rayleigh, Rician and Nakagami-m in detail. The Rayleigh and Rician distributions are used to characterize the channel envelop of faded signal over small geographical areas or short term fades.

Recently, the Nakagami-m fading channel model has received considerable attention due to its great flexibility and accuracy. In studying the performance of wireless communication system, it is usually assumed that two signals are independent of one another, however, there are number of real-life scenario in which this assumption is not valid, for example, insufficient antenna spacing in small-size mobile units equipped with space and polarization antenna diversity. Therefore, the effect of correlated fading on the performance of a diversity combining receiver has received a great deal of research interest. We have analyzed the performance of correlated Nakagami-m fading channel by using the maximal-ratio combining diversity at the receiver. A closed-form mathematical expression is derived for the average bit-error-rate, symbol-error-rate and outage probability for various modulation scheme in terms of the higher transcendental function such as Appell hypergeometric function by using the well-known moment generating function (MGF) based approach with arbitrary fading index for OFDM communication systems. The diversity path greater than two (M ≥ 2) at the receiver hence the average bit-error-rate performance of the OFDM system is improved significantly. The proposed mathematical analysis is used to study various novel performance evaluation

results with parameters of interest such as fading severity and correlation coefficients, which is very significant for the design consideration of the OFDM communication systems.

We have explored the marginal moment generating function (MMGF) for the correlated Nakagami-m fading channel by using maximal-ratio combining diversity scheme at receiver for the computation of the channel capacity for various adaptive transmission schemes such as: 1) optimal simultaneous power and rate adaptation, 2) optimal rate adaptation with constant transmit power, 3) channel inversion with fixed rate, and 4) truncated channel inversion with fixed rate. An analytical expression for the channel capacity as a function of signal-to-noise ratio over the correlated Nakagami-m fading channel with maximal-ratio combining diversity at the receiver is obtained, which is valid for arbitrary value of the fading parameters $m$. We have also analyzed the effect of correlation on the channel capacity. Due to their simple forms, these results offer a useful analytical tool for the accurate performance evaluation of the various communication systems of practical interest.

In addition to the multipath fading, the quality of signal in the wireless communication environment is also affected due to shadowing from various obstacles in propagation path. The Nakagami-$m$ and Rayleigh-lognormal (Suzuki) are well known composite statistical distribution to model the multipath fading and shadowing. The Gamma probability density function (PDF) was proposed for shadowing instead of the lognormal and the resultant PDF is called generalized-K distribution for the shadowed fading channel and the $K$-distribution when the short term fading is modeled by using the Rayleigh instead of the Nakagami-m PDF. The K-distribution is derived as a special case of the generalized-K distribution by letting $m = 1$. The generalized-K distribution fading model characterizes the confined effect of fast and slow fading in the received signal by using two shaping parameters $m$ and $k$, where $m$ is the Nakagami fading parameters for the short term fading and $k$ is the parameter of the Gamma distribution for the received average power due to shadowing. In the wireless communication systems, the fading is important phenomena, which limits the channel capacity.

We have also investigated a simple and novel MMGF based channel capacity analysis approach over generalized-K fading channel with maximal-ratio combining

diversity. Initially, an analytical expression for the MMGF of received signal-to-noise ratio with M-branch maximal-ratio combining diversity is obtained and utilizes it to derive the mathematical expression for the channel capacity under the different power and rate adaptation policies for arbitrary value of shaping parameters. The result of proposed methods is compared with other reported literature to support the analysis. We have derived the expression for the channel capacity with optimal rate adaptation ($C_{ORA}$) which is valid for arbitrary values of the shaping parameters $k$ and $m$. Moreover, we derived an expression for the capacity for channel inversion with fixed rate ($C_{CIFR}$). The $C_{ORA}$ and $C_{CIFR}$ are very easily computed by using the MGF based approach. We also derived the marginal MGF based channel capacity for truncated channel inversion with fixed rate ($C_{TCIFR}$) and channel capacity for optimal rate and power adaptation $^{(C_{OPRA})}$ schemes for the Generalized-K fading channel, which is a simple and novel approach that can be applied to other fading channels also. The contributions and implications of this work for future research are also discussed.

# INTRODUCTION

## 1.1 OVERVIEW OF OFDM

The concept of Orthogonal Frequency Division Multiplexing (OFDM) was first introduced by Chang [1, 2] in 1966 for dispersive fading channels. For long time, the application was very limited because of the implementation complexity. Weinstein and Ebert [3] have suggested an OFDM implementation based on the discrete Fourier transform (DFT) to replace the banks of sinusoidal generators and demodulators. This work dramatically reduced the implementation complexity of OFDM systems but it was able to reach towards sufficient maturity for employment in standard communication systems during the 1990s. Recently, it has been selected as the high performance local area network's (HIPERLAN) transmission technique as well as becoming part of the IEEE 802.11 Wireless Local Area Network (WLAN), IEEE 802.16 WiMax [2] and 3GPP Long Term Evolution (LTE) standards [4-5]. OFDM is improved form of Frequency Division Multiplexing (FDM). It extends the concept of single carrier modulation by using multiple subcarriers within the same single channel as shown in Figure 1.1. The total data rate to be sent in the channel is divided between the various subcarriers. Advantages include using separate modulation/demodulation customized to a particular type of data, or sending out bunch of dissimilar data that can be sent in best manner by using multiple and possibly different modulation schemes. FDM offers an advantage over single-carrier modulation in terms of narrowband frequency interference since this interference will affect only one of the frequency sub-bands and other subcarriers (the carriers used to modulate the individual message signals are called sub-carriers) will not be affected by the interference. Since each subcarrier has a lower information rate, the data symbol periods in a digital system will be longer, adding some additional immunity to impulse noise and reflections. FDM systems usually require a guard band between modulated subcarriers to prevent interference one subcarrier from other. These guard bands lower the system's effective information rate when compared to a single carrier system with similar modulation scheme. At the receiving end the signal is applied to a

bank of band-pass filters, which separates individual frequency channels. The band pass filter outputs are then demodulated and distributed to different output channels. To ensure that the signal of one channel did not overlap with the signal from an adjacent one, guard band was provided between different channels which lead to inefficiencies as shown Figure 1.1.
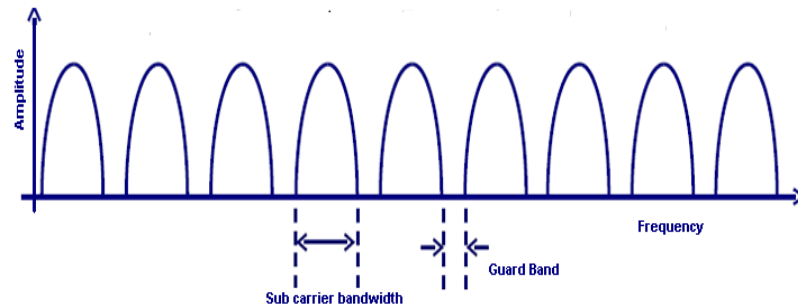


Figure 1.1 Conventional frequency division multiplexing.
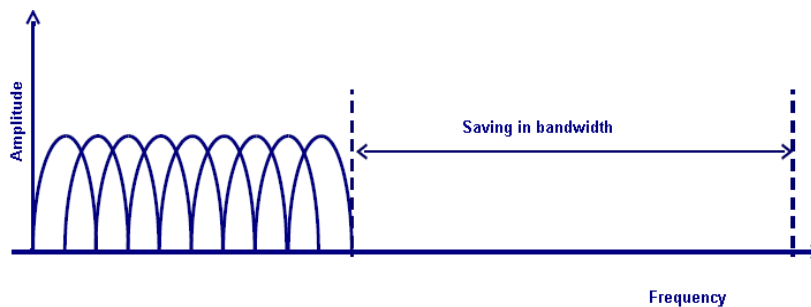


Figure 1.2 Orthogonal frequency division multiplexing.

If the FDM system as discussed above had been able to use a set of subcarriers that were orthogonal to each other, a higher level of spectral efficiency could have been achieved. The guard bands that were necessary to allow individual demodulation of subcarriers in an FDM system would no longer be necessary. The use of orthogonal subcarriers would allow the subcarrier's spectra to overlap, thus increasing the spectral efficiency. As long as orthogonality is maintained, it is still possible to recover the individual subcarrier's signals despite their overlapping spectrums. If the dot product of two deterministic signals is equal to zero, these signals are said to be orthogonal to each other. OFDM is improved form of FDM, in which subcarrier are orthogonal to each other as shown in Figure 1.2. The peak of one subcarrier coincides with the nulls of the other subcarriers. Due to the orthogonality, there is no

interference from other subcarriers at the peak of a desired subcarrier even though the subcarrier spectrums overlap [5-9]. Using OFDM system, huge amount of bandwidth can be saved in comparison to conventional FDM technique as shown Figure 1.1. The orthogonality among subcarriers can be viewed in time domain as shown Figure 1.3(a). OFDM achieves orthogonality by allocating integer number cycles per symbol duration. The mathematical representation of two orthogonal functions is shown below. Let us consider a set of function $g_1(t), g_2(t), \ldots, g_n(t), \ldots$ defined over the interval $t_1 \leq t < t_2$ and which are related to one another in such a way that any two functions of the set satisfy the condition:

$$\int_{t_1}^{t_2} g_m(t) g_n^*(t) \, dt = \begin{cases} 0 & m \neq n \\ 1 & m = n \end{cases} \tag{1.1}$$

A set of functions which has this property is called orthogonal from the interval $t_1$ to $t_2$. In case of OFDM, carrier frequencies are chosen so that all of them are orthogonal. The time and frequency domain representation of orthogonal signals are shown below in Figure 1.3(a) and Figure 1.3(b), respectively. The Figure 1.4 shows a simple representation of the OFDM communication system.

In this chapter, we have reviewed the OFDM communication system and its implementation in practice by using the discrete Fourier transform (DFT). From the signals and systems theory, the sinusoids of the DFT form an orthogonal basis set and a signal in the vector space of the DFT can be represented as a linear combination of the orthogonal sinusoids. If the input signal has some energy at a certain frequency, there will be a peak in the correlation of the input signal and the basis sinusoid that is at that corresponding frequency. This transform is used at the OFDM transmitter to map an input signal onto a set of orthogonal subcarriers that is the orthogonal basis functions of the DFT. Similarly, the transform is used again at the OFDM receiver to process the received subcarriers. The signals from the subcarriers are then combined to form an estimate of the source signal from the transmitter. The orthogonal and uncorrelated nature of the subcarriers is exploited in OFDM systems. Since the basis functions of the DFT are uncorrelated, the correlation performed in the DFT for a given subcarrier only sees energy for that corresponding subcarrier. The energy from other subcarriers does not contribute because it is uncorrelated. Because of the

separation of signal energy, the OFDM subcarrier's spectrums can overlap without causing interference. The idea behind the analog implementation of OFDM can be extended to the digital domain by using the discrete Fourier transform (DFT) and its counterpart, the inverse discrete Fourier transform (IDFT). These mathematical operations are widely used for transforming data between the time-domain and frequency-domain. These transforms are interesting from the OFDM perspective because they can be viewed as mapping data onto orthogonal subcarriers. For example, the IDFT is used to convert frequency-domain data into time-domain data. In order to perform that operation, the IDFT correlates the frequency-domain input data with its orthogonal basis functions, which are sinusoids at certain frequencies. This correlation is equivalent to mapping the input data onto the sinusoidal basis functions. In practice, OFDM systems are implemented by using a combination of fast Fourier transform (FFT) and inverse fast Fourier transform (IFFT) blocks that are mathematically equivalent versions of the DFT and IDFT, respectively, but are more efficient to implement. The IFFT takes in $N$ symbols at a time where $N$ is the number of subcarriers in the system. Each of these $N$ input symbols has a symbol period of $T$ seconds. The basis functions for an IFFT are $N$ orthogonal sinusoids. Each sinusoid has a different frequency and the lowest frequency is DC. Each input symbol acts like a complex weight for the corresponding sinusoidal basis function. Since the input symbols are complex, the value of the symbol determines both the amplitude and phase of the sinusoid for that subcarrier. The IFFT output is the summation of all $N$ sinusoids. Thus, the IFFT block provides a simple way to modulate data onto $N$ orthogonal subcarriers. The block of $N$ output samples from the IFFT make up a single OFDM symbol. The length of the OFDM symbol is $NT$ where $T$ is the IFFT input symbol period as mentioned above. After some additional processing, the time-domain signal that results from the IFFT is transmitted across the channel.

At the receiver, an FFT block is used to process the received signal and bring it into the frequency-domain. Ideally, the FFT output will be the original symbols that were sent to the IFFT at the transmitter. When plotted in the complex plane, the FFT output samples will form a constellation, however, there is no notion of a constellation for the time-domain signal. When plotted on the complex plane, the time-domain signal forms a scatter plot with no regular shape. Thus, any receiver

processing that uses the concept of a constellation (such as symbol slicing) must occur in the frequency-domain.



(a)



(b)
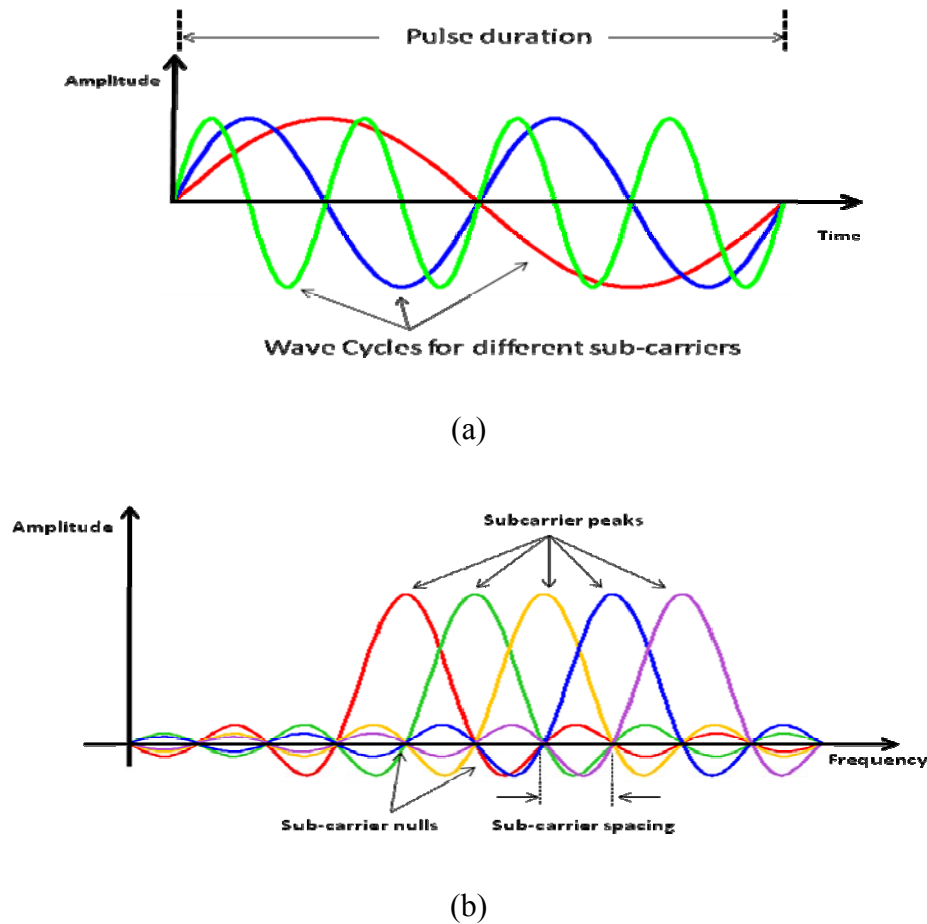
Figure 1.3 The signal waveforms to show the orthogonality among subcarriers in (a) time-domain and (b) frequency domain representation.

## 1.2 OFDM TRANSMITTER AND RECEIVER

Figure 1.4 shows the block diagram of a typical OFDM system [2, 9]. The transmitter comprises of serial–to-parallel convertor, signal mapper, IFFT, guard interval insertion, and parallel-to-serial convertor. The input data to be transmitted is mapped by modulation technique to get the appropriate subcarrier amplitude and phase. The mapped data is converted into the time domain using an IFFT. The IFFT takes in $N$ symbols at a time where $N$ is the number of subcarriers in the system. The IFFT perform subcarrier modulation and multiplexing in one step. At receiver end the one OFDM symbol is overlapped with the other due to multipath distortion. To eliminate

the problem of inter symbol interference (ISI), a guard time inserted between two symbol, duration of guard interval should be greater than maximum delay spread. The guard time consists no signal at all, in that case problem of inter-carrier interference (ICI) would arise because orthogonality among the carrier is disturbed. To overcome the problem of ICI OFDM symbol is cyclically extended in guard time interval means last part of OFDM symbol is copied in front. This ensures that delayed OFDM symbol have always integer number of cycle in given FFT interval, as long as delay is smaller than the guard time. The cyclic prefix allows linear convolution of a frequency selective multipath channel to be modelled as circular convolution and ensures the orthogonality between the subcarriers, which provides multipath immunity as well as symbol time synchronization tolerance. The receiver performs inverse action of transmitter as shown in Figure 1.4.
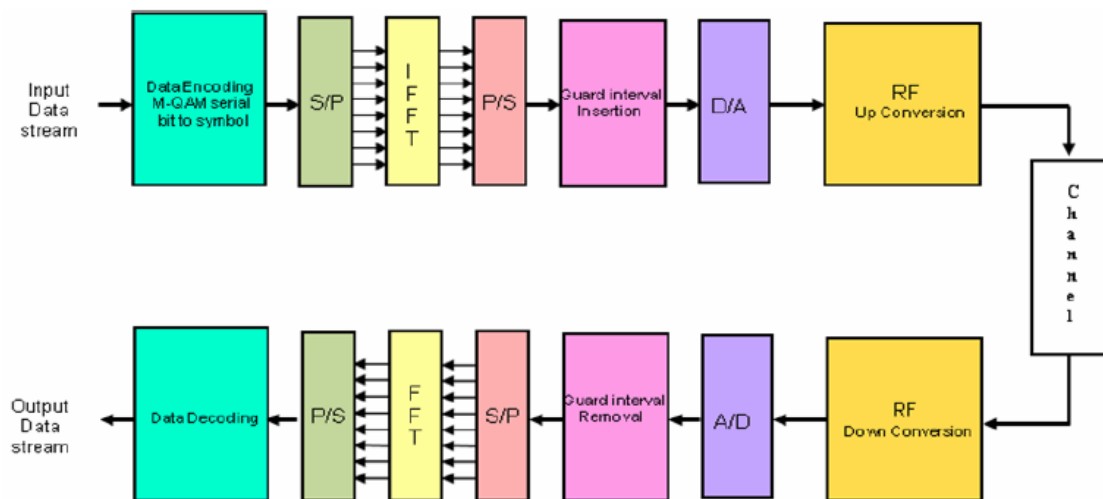


Figure 1.4 Schematic of OFDM transceiver systems.

The receiver converts the RF signal to base band for processing, then using a FFT to analyze the signal in the frequency domain. The amplitude and phase of the subcarriers is then picked out and converted back to digital data. The IFFT and the FFT are complementary function and the most appropriate term depends on whether the signal is being received or generated.

A major problem in most of the wireless systems is the presence of a multipath channel. In a multipath environment, the transmitted signal reflects off several

objects. As a result, multiple delayed versions of the transmitted signal arrive at the receiver. The multiple delayed versions of the signal cause the received signal to be distorted. Many wired systems also have a similar problem where multiple reflections occur due to impedance mismatches in the transmission line. A multipath channel will cause two problems for an OFDM system. The first problem is inter-symbol interference, which occurs when the received OFDM symbol is distorted by the previously transmitted OFDM symbol. The effect is similar to the inter-symbol interference that occurs in a single-carrier system. However, in such systems, the interference is typically due to several other symbols instead of just the previous symbol. Symbol period in single carrier systems is typically much shorter than the time span of the channel, whereas the typical OFDM symbol period is much longer than the time span of the channel. The second problem is unique to multicarrier systems and is called intra-symbol interference. It is the result of interference amongst a given OFDM symbol's own subcarriers. Assume that the time span of the channel is $L_C$ samples long, instead of a single carrier with a data rate of $R$ symbols/second. OFDM system has $N$ subcarriers, each with a data rate of $R/N$ symbols/second. Since the data rate is reduced by a factor of $N$, the OFDM symbol period is increased by a factor of $N$. By choosing an appropriate value for $N$, the length of the OFDM symbol becomes longer than the time span of the channel. Due to this configuration, the effect of inter-symbol interference is the distortion of the first $L_C$ samples of the received OFDM symbol and only the first few samples of the symbol are distorted. One can consider the use of a guard interval to remove the effect of inter-symbol interference. The guard interval could be a section of all zero samples transmitted in front of each OFDM symbol. Since it does not contain any useful information, the guard interval would be discarded at the receiver. If the length of the guard interval is properly chosen such that it is longer than the time span of the channel, the OFDM symbol itself will not be distorted.

The guard interval is not used in practical systems because it does not prevent an OFDM symbol from interfering with itself. This type of interference is called intra-symbol interference. The solution to the problem of intra-symbol interference involves a discrete-time property. In the continuous-time, a convolution in time is equivalent to a multiplication in the frequency-domain. This property is true in

discrete-time only if the signals are of infinite length or if at least one of the signals is periodic over the range of the convolution. It is not practical to have an infinite-length OFDM symbol, however, it is possible to make the OFDM symbol appear periodic. This periodic form is achieved by replacing the guard interval with cyclic prefix of length $L_P$ samples [2, 9]. The cyclic prefix is a replica of the last $L_P$ samples of the OFDM symbol where $L_P > L_C$. Since it contains redundant information, the cyclic prefix is discarded at the receiver. Like the case of the guard interval, this step removes the effects of inter-symbol interference. Because of the way in which the cyclic prefix was formed, the cyclically-extended OFDM symbol now appears periodic when convolved with the channel. An important result is that the effect of the channel becomes multiplicative. In a digital communications system, the symbols that arrive at the receiver have been convolved with the time-domain channel impulse response of samples of length $L_C$. Thus, the effect of the channel is convolution. In order to undo the effects of the channel, another convolution must be performed at the receiver using a time-domain filter known as an equalizer. The length of the equalizer needs to be of the order of the time span of the channel. The equalizer processes symbols in order to adapt its response in an attempt to remove the effects of the channel. Such an equalizer can be expensive to implement in hardware and often requires a large number of symbols in order to adapt its response in a desired manner.

The operational principle of OFDM systems is that the original bandwidth is divided into a high number of narrow sub-bands which are called subcarriers, so that mobile/wireless channels can be considered non-dispersive and are capable of operating without classic channel equalizers. Moreover, OFDM transmits data in parallel by modulating a set of orthogonal sub-carriers. OFDM is attractive because it provides relatively easy solutions to some difficult challenges that are encountered when using single-carrier modulation schemes on wireless channels. Simplified frequency domain equalization is often touted as a primary advantage of OFDM over single-carrier modulation with conventional time-domain equalization. However, frequency domain equalization can be applied just as easily to single-carrier modulation techniques as it can be applied to OFDM. OFDM is advantageous [5-10] because the modulation of closely-spaced orthogonal subcarriers partitions the available bandwidth into a collection of narrow sub-bands. One such possibility is

to use adaptive bit loading techniques, where the modulation alphabet size on each subcarrier is adjusted according to channel conditions. A larger signal constellation is used on subcarriers where the received signal-to-noise ratio is large and vice-versa. OFDM waveforms are resilient to timing errors, yet highly sensitive to frequency offsets and phase noise in the transmitter and sampling clock oscillators. These characteristics are opposite those of single-carrier modulation, which is more sensitive to timing errors and less sensitive to frequency offsets. This is a manifestation of the long OFDM modulated symbol duration and the closely-spaced orthogonal subcarriers. Hence, OFDM has its own set of unique implementation challenges that are not present in single-carrier systems.

In OFDM, the time-domain signal is still convolved with the channel response. However, the data will ultimately be transformed back into the frequency-domain by the FFT in the receiver. Because of the periodic nature of the cyclically-extended OFDM symbol, this time-domain convolution will result in the multiplication of the spectrum of the OFDM signal with the frequency response of the channel. The result is that each subcarrier's symbol will be multiplied by a complex number equal to the channel's frequency response at that subcarrier's frequency. Each received subcarrier experiences a complex gain due to the channel. In order to undo these effects, a frequency-domain equalizer is employed and such an equalizer is much simpler than a time-domain equalizer. The frequency-domain equalizer consists of a single complex multiplication for each subcarrier. For the simple case of no noise, the ideal value of the equalizer's response is the inverse of the channel's frequency response.

The effects of non-idealities in an OFDM system has been discussed, which include impairments and receiver offsets. Since the Fourier transform is a fundamental operation in OFDM, the effects of several offsets can be intuitively understood by applying Fourier transform theory. At start-up, the local oscillator frequency at the receiver is typically different from the local oscillator frequency at the transmitter. A carrier tracking loop is used to adjust the receiver's local oscillator frequency in order to match the transmitter's local oscillator frequency as closely as possible. The effect of having a local oscillator frequency offset can be explained by Fourier transform theory. The local oscillator offset can be expressed mathematically by multiplying the received time-domain signal by a complex exponential whose

frequency is equal to the local oscillator offset amount. From Fourier transform theory that multiplication by a complex exponential in time is equivalent to a shift in frequency. The local oscillator offset results in a frequency shift of the received signal spectrum. This shift causes a condition called "loss of orthogonality" to occur. The frequency shift causes the OFDM subcarriers to no longer be orthogonal. The orthogonality of the subcarriers is lost because the bins of the FFT will no longer line up with the peaks of the received signals pulses. The result is a distortion called inter-bin interference (IBI), which occurs when the energy from one bin spills over into adjacent bins and this energy distorts the affected subcarriers. In Fourier transform theory this effect is called DFT leakage. For the purpose of clarity, only one non-zero subcarrier was transmitted and this subcarrier is not interfering with its adjacent subcarriers. The spectrum of the non-zero subcarrier actually extends over the entire range of the FFT, however, due to the orthogonal nature of the signal, the zero-crossings of the spectrum exactly line up with the other FFT bins which shows the received spectrum of the same signal with one non-zero subcarrier. In this case, there is a local oscillator offset. This offset has resulted in a loss of orthogonality and the zero-crossings of the non-zero subcarrier's spectrum no longer line up with the FFT bins. The result is that energy from the non-zero subcarrier is spread out among all of the other subcarriers, with those subcarriers closest to the non-zero subcarrier receiving the most interference. In a practical system, almost all of the subcarriers would be actively used for transmitting data. A given subcarrier would experience IBI due to energy from all of the other active subcarriers in the system. The central limit theorem states that the sum of a large number of random processes will result in a signal that has a Gaussian distribution because of this property, the IBI will manifest itself as the additive Gaussian noise, thus lowering the effective SNR of the system.

The effect of a local oscillator frequency offset can be corrected by multiplying the signal by a correction factor. The correction factor would be a sinusoid with a frequency that is ideally equal to the amount of the local oscillator frequency offset. Various carrier tracking algorithms exist that can adaptively determine the frequency which will correct the offset. It is also possible to have a local oscillator phase offset, separate from local oscillator frequency offset. The two offsets can occur in conjunction or one or the other can be present by itself. As the name suggests, a local

oscillator phase offset occurs when there is a difference between the phase of the local oscillator output and the phase of the received signal. This effect can be represented mathematically by multiplying the time-domain signal by a complex exponential with a constant phase. The result is a constant phase rotation for all of the subcarriers in the frequency-domain. The constellation points for each subcarrier experience the same degree of rotation. If the phase rotation is small, the frequency-domain equalizer can correct this effect. Each filter coefficient in a frequency-domain equalizer multiplies its corresponding subcarrier by a complex gain that is amplitude scaling and phase rotation. The equalizer's coefficients can be used to correct for a small phase rotation as long as the rotation does not cause the constellation points to rotate beyond the symbol decision regions. Larger phase rotations are corrected by a carrier tracking loop.

Additive white Gaussian noise (AWGN) is the most common impairment encountered in a communications system. In a wireless medium, the noise source is typically considered to be thermal noise that is Gaussian and uniform across the frequency range. Additional noise sources include atmospheric sources and solar radiation. In a contained media, such as a coaxial cable system, thermal noise will be present, but the system may also have other sources that can increase the noise in the system. The effect of AWGN on an OFDM system is similar to its effect on a single carrier system. The signal-to-noise ratio is a function of the total signal power over the total noise power across the received channel. The uniform noise contributes to the SNR of each subcarrier in the OFDM system and the net result is equivalent to the effect on single channel systems. Noise in a communications channel can often be shaped, or "colored", by various effects. These effects can include transmit signal imperfections, transmission channel characteristics, or receiver frequency shaping. The implications of these effects for an OFDM system can be different compared to its single-carrier counterpart. The modulation of the OFDM system can be tailored for the noise characteristics. A method involves sending the same data on several subcarriers, or sending data that is having lower priority. In extreme cases, the subcarriers can transmit no data, essentially turning them off. Impulse noise is a common impairment in a communications system arising from motors or lightning, which is typically characterized as a short time-domain burst of energy. The burst

may be repetitive or may be a single event. In either case, the frequency spectrum from this energy burst is wideband, typically much wider than the channel, but is present for only a short time period. While OFDM transmission over mobile/wireless channels can alleviate the problem of multipath propagation, recent research efforts have focused on solving a set of inherent difficulties regarding OFDM, namely the peak-to-mean power ratio [11-13], time and frequency synchronisation, and on mitigating the effects of the frequency selective fading channel [7].

## 1.3 WIRELESS CHANNELS

In wireless channels, the electromagnetic waves experience different effects like diffraction, scattering, reflection, and absorption because of interaction with surface irregularities which create a continuum of scattered partial waves [14-22]. Reflections caused when the electromagnetic waves impinge upon surface having dimensions much larger than the wavelength of the impinging wave [15]. Diffractions caused due to the effects of sharp edges in the path of the radio waves between the transmitter and the receiver. Scattering is caused when the electromagnetic waves encounter objects of dimension much smaller than the wave in the propagation medium [15]. The amplitudes and phases variations of these partially refracted, scattered and reflected waves depend on the physical properties of the surfaces such as geometrical proportions and electromagnetic reflection properties. These partial waves create irregular electromagnetic field after interfering with each other and with the direct wave. On the other hand, the transmitted signal power decreases with the travelled distance and because of existence of large number of scattering objects between transmitter and receivers introduces random variations of the local mean of the envelope or equivalently the local mean power. Therefore, to statistically model the wireless channels [20], it is a very common practice to consider two independent propagation models, the small-scale propagation model for random amplitude and phase variations and large-scale propagation model for power (shadowing and path loss) variation as shown Figure 1.5. Small-scale fading is due to the superposition of the received multipath signals, which are due to the processes of reflection, diffraction and scattering. So, within a scale that is comparable to the carrier wavelength, the superposition of the multipath signals may add constructively (in-phase) or

destructively (out-of-phase) causing the phenomenon of small-scale fading. To derive statistical characteristics of the received wave-field that is due to the superposition of partial waves, the complex phasor of the received signal can be expressed as [23-25].

$$\overline{E}(t) = \sum_{n=1}^{N} A_n \delta(t - \tau_n) \exp(-j\varphi_n) \tag{1.2}$$

The channel impulse response can be characterized by $N$ time-delayed impulses, each represented by an attenuated and phase-shifted version of the original transmitted impulse. Here, $A_n$, $\tau_n$ and $\varphi_n$ are the attenuation, delay in time of arrival, and phase, corresponding to path $n$, respectively. The magnitude of the complex phasor in Equation (1.2) is defined as [23].

$$r = \left| \sum_{n=1}^{N} A_n \delta(t - \tau_n) \exp(-j\varphi_n) \right| \tag{1.3}$$

According to the central limit theorem, the received electromagnetic field can be expressed as a complex Gaussian random variable whose real and imaginary components are zero-mean Gaussian random variables with equal variance of 1/2, their magnitudes are Rayleigh distributed whose probability density function (PDF) can be as [26]:

$$p(r) = \frac{r}{\sigma^2} \exp\left( -\frac{r^2}{2\sigma^2} \right) \tag{1.4}$$

If a line-of-sight (LOS) is present (with a non-zero mean, $A_0$), the magnitude of the received signal has a Rician distribution [27]:

$$p(r) = \frac{r}{\sigma^2} \exp\left[ -\frac{(r^2 + A_o^2)}{2\sigma^2} \right] I_o\left( \frac{A_o r}{\sigma^2} \right) \tag{1.5}$$

where $I_0 (\cdot)$ denotes the modified Bessel function of the first kind with zero order. Another PDF that is versatile enough to include the Rayleigh PDF as a special case and approximate the Rician distribution is the Nakagami distribution [28]:

$$p(r) = \frac{2}{\Gamma(m)} \left( \frac{m}{\Omega} \right)^m r^{2m-1} \exp\left( -\frac{m r^2}{\Omega} \right) \tag{1.6}$$

where $\Gamma[\cdot]$ is the Gamma function, $\Omega = E(r^2)$, and *m* is the multipath fading parameter that varies from *m* = 1/2 for one-sided Gaussian PDF, to m = 1 for Rayleigh PDF, and m = ∞ for the non-fading scenario.

A channel is said to exhibit frequency-selective fading when the delay spread is greater than the symbol period [29-30]. This condition occurs whenever the received multipath components of a symbol extend beyond the time duration of the symbols. Such multipath dispersion of the signal yields a kind of inter-symbol interference called channel-induced ISI. On the other hand, if the signal bandwidth is greater than coherence bandwidth ($B_s > B_C$) then the channel amplitude values at frequencies separated by more than the coherence bandwidth are roughly independent. Thus, the channel amplitude varies widely across the signal bandwidth. In this case the fading is called frequency selective [29-30].
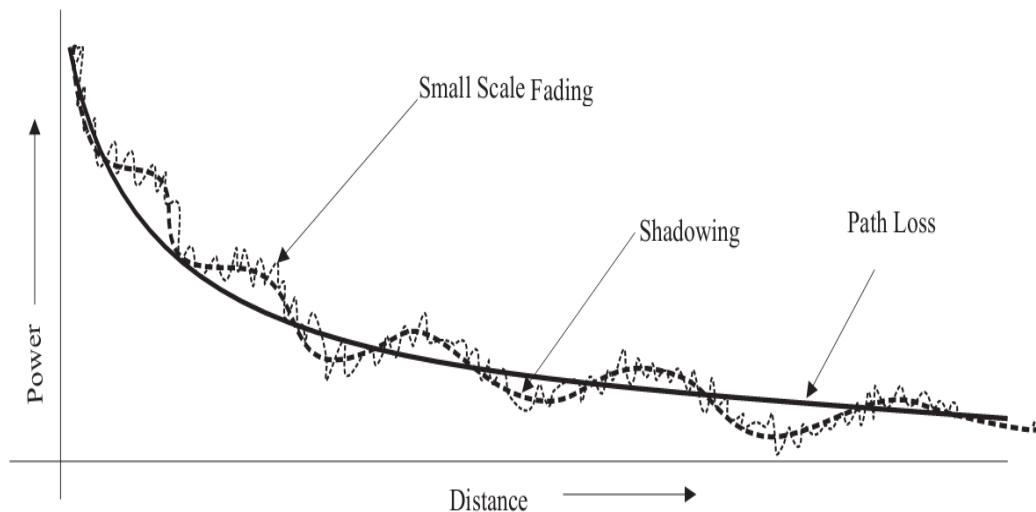


Figure 1.5 Small and large-scale propagation model versus distance.

When the delay spread is less than the symbol period, a channel is said to exhibit flat fading, or if we are transmitting a narrowband signal with bandwidth $B_s \ll B_C$, then fading across the entire signal bandwidth is highly correlated; that is, the fading is roughly equal across the entire signal bandwidth. This is usually referred to as flat fading [29-30]. Fast fading and slow fading are classified [29-30] on the basis of how rapidly the transmitted baseband signal changes, compared to the rate of the electrical-parameter changes of the channel. If the channel impulse response changes at a rate much faster than the trans-mitted signal, the channel may he

assumed to be a fast-fading channel otherwise, it is assumed to be a slow-fading channel. It is important to note that the velocity of the mobile unit or the velocity of objects using the channel through a baseband signal determines whether a signal undergoes fast fading or slow fading. Due to the scattering caused by obstacles, the local mean received power in a wireless channel varies, which is referred as shadowing. These variations are usually modelled by a lognormal random variable [31-33].

$$p(x) = \frac{1}{\ln 10/10\sqrt{2\pi}\sigma x} \exp\left[ -\frac{(10\log(x)-\mu_s)^2}{2\sigma_s^2} \right]$$
(1.7)

where $\mu_s$ is called the area mean and is determined by the propagation path loss, however, we may treat the path loss independently so that we may set $\mu_s = 0dB$. The standard deviation $\sigma_s^2$ varies with the propagation environment. Simplified model for path loss as a function of distance (d) over wireless channels is given by [30, 34].

$$P_r = P_t A \left[ \frac{d_o}{d} \right]^\gamma$$
(1.8)

where A is a unit-less constant that depends on the antenna characteristics and the average channel attenuation, $d_o$ is a reference distance for the antenna far field, and $\gamma$ is the path-loss exponent. The data user in wireless domain is growing faster these days than ever before [35-42].

## 1.4 PROBLEM DEFINITION

Orthogonal frequency division multiplexing (OFDM) is a multi-carrier modulation technique, which is widely used in various communication systems and standards due to its high data rate, high spectral efficiency and robustness to the frequency selective channels [51-75]. However, the OFDM has following problems:

1) The main problems in OFDM is its sensitivity to carrier frequency offset, which destroys the orthogonality between the subcarriers and causes inter-carrier interference [51-75] which degrades the performance of an OFDM system.

2) The phase noise arises predominantly due to imperfections of the local oscillator in the transceiver, which represents a time-varying drift of the local oscillator phase from its reference, and

3) The timing offset arises because of multi path delay spread [76-82].

The above mentioned problems causes number of impairments including disrupting the orthogonality among subcarriers, ISI because of timing offset only and introduces inter-carrier interference (ICI) that would significantly degrade the system performance. However, ICI induced by phase noise and timing offset, can be completely compensated or corrected. Since the Doppler spread or frequency shift is random, so we can only mitigate its impact [83]. Currently, several approaches for reducing the ICI have been developed including: ICI self-cancellation [54], frequency-domain equalization [51], time-domain windowing scheme [52], frequency offset estimation and compensation techniques [56, 67, 68], correlative coding [55], [62-15] and the conjugate cancellation scheme [61, 69].

Frequency domain equalization [51] is an extremely simple process for ICI cancellation, but the above method can only reduce the ICI caused by multipath fading distortion, which is not the major source of ICI. Li et al [52] has proposed a time-domain windowing approach for ICI mitigation that can reduce sensitivity of time offset. Zhao et al [55] have proposed the correlative coding between the signals modulated on subsequent subcarriers in binary phase-shift keying OFDM, but this scheme does not improves carrier-to-interference ratio (CIR) significantly. Yeh et al [61] have discussed the ICI mitigation using conjugate-cancellation, in this scheme, two sequences are transmitted in each data symbol. First sequence is original received sequence and another sequence is conjugate of the original sequence. Thus the two sequences are conjugate of each other rather than adjacent subcarriers with opposite polarities in order to cancel the ICI but they have not provided mathematical analysis for the cancelation of ICI. Dwivedi et al in [69] have been extended the work in Ref. [61]; they have also some mathematical using conjugate-cancellation scheme. A simple and most effective method, known as self-cancellation scheme has been proposed by Zhao and Haggman [54], which significantly reduces the ICI with little additional computational complexity. This scheme significantly reduces the ICI at the cost of reducing the transmission rate. Besides its little additional computational

complexity, it has a very important advantage, as this technique can also mitigate ICI created by spread of frequency shifts in the signal, such as a Doppler spread resulting from a time variable channel.

Physical limitations of the communication over wireless channel are still a big issue for researchers. These include multi-path fading, limited spectrum resources, multiple access interference and limited battery life of the devices. The multipath fading degrades the performance of wireless communication systems. Recently, Nakagami-*m* fading channel model has received considerable attention due to its great flexibility and accuracy [84]. In studying the performance of wireless communication system, it is usually assumed that two signals are independent of one another. However, there are number of real-life scenario in which this assumption is not valid, for example, insufficient antenna spacing in small-size mobile units equipped with space and polarization antenna diversity, the effect of correlated fading on the performance of a diversity combining receiver has received a great deal of research interest. The diversity combining [85-94] is an effective technique for mitigating detrimental effects of multipath fading and shadowing in wireless mobile channels. In the literature, on the performance of a maximal-ratio combiner (MRC) in the correlated Nakagami fading environment concentrated either on dual-branch diversity [95] or on arbitrary diversity order with simple correlation models. Bandjur et al [96] have been studied the performance of a dual-branch switch and stay combining diversity receiver with the switching decision based on the signal-to-interference ratio operating over the correlated Ricean fading channels in the presence of the correlated Nakagami-m distributed co-channel interference. Rui et al [97] have considered the diversity at transmitter and receiver both without correlation between them but when antennas are closely spaced then signal are correlated. In [98], Alao et al have been analyzed the performance over correlated Nakagami fading channel using PDF based approach but the above approach is mathematically much more complex. In the wireless environment, in addition to multipath fading, the quality of signal is also affected due to shadowing from various obstacles in propagation path. The Nakagami-*m* and Rayleigh-lognormal (Suzuki) are well known composite statistical distribution to model the multipath fading and shadowing but these models do not provide the close form solution. A generalized K- fading model has been proposed in literature to

approximate the Nakagami-m and Rayleigh-lognormal, which provides a close form solution [99]. In the past, few contributions dealing with $K_G$ and K-distribution with diversity combining have been published [99-101]. In [99], the performance analysis of diversity combining over generalized-K fading has been analyzed but the closed-form expression for the bit error rate (BER) is not discussed. In [100], the performance of generalized selection combing (GSC) receivers over K-fading is presented. In same reference marginal moment generating function (MGF) is derived but this marginal MGF is not used to obtain BER for M-array phase shift keying (MPSK). In [101], the outage probability performance is evaluated and further MGF based approach and Pade approximants method are used for the performance analysis. Bithas et al in [102] have provided a closed form expression for the symbol-error-rate (SER) and bit-error rate (BER) of various coherent and non-coherent digital modulations and the average channel capacity. Conti et al in [103] have analyzed effect of diversity on the outage probability over shadowing environment. All the above methods evaluate BER expression using either by using probability density function (PDF) based approach or by numerical methods, the above approaches are much more difficult. Recently, it has been recognized that the moment generating function (MGF) is a powerful tools for simplifying the analysis of diversity communication systems and to evaluate the performance over various fading channels.

In general, the capacity in fading channel is a complex expression in terms of the channel variation in time and/or frequency depending also upon the transmitter and/or receiver knowledge of the channel side information. For the various channel side information assumptions that have been proposed, several definitions of the channel capacity have been provided. These definitions depend on the different employed power and rate adaptation policies and the existence, or not, an outage probability [22]. Earlier, the capacity has been studied by various researchers for several fading environment [104-114]. All above methods are PDF based method for channel capacity analysis, results difficult expression and analysis becomes much more difficult in case of correlated Nakagami and K-fading channel. In [115], the moment generating function (MGF) based approach is proposed for computation of the channel capacity only for $C_{ora}$ scheme, by using numerical techniques. In [116], a

novel MGF based approach is developed for evaluation of channel capacity various rate adaptation and transmit power. In [116] integral is evaluated by using mainly two type of numerical technique, both the numerical techniques are lengthy, approximation and much more complex.

## 1.5 ORGANIZATION OF THE THESIS

This thesis is organized as follows. The Chapter 2 presents a novel method for ICI cancellation using IFFT and FFT at the transmitter and FFT and IFFT at the receiver. A novel mathematical expression for analysis of BER is derived and compared with other reported literature. In Chapter 3, we have discussed about carrier to interference ratio (CIR) of OFDM systems. For improvement CIR, repeated correlative coding has been proposed. An expression for the ICI power of OFDM systems using repeated correlative coding as a function of the frequency offset is derived and further evaluated the CIR power. The average CIR of proposed method is compared with other existing methods. Chapter 4 contains the performance analysis of OFDM systems over correlated Nakagami fading channel. A novel formula for BER and SER analysis for BPSK and M-QAM OFDM system respectively, using moment generating function (MGF) has been derived. In this chapter, effect of correlation and effect of diversity combiner (M) on performance of OFDM system has been also analyzed. An expression outage probability has been evaluated in the later part of this chapter. In Chapter 5, we present the marginal moment generating (MMGF) based channel capacity analysis over correlated Nakagami-$m$ fading channel with M-branch maximal-ratio combining (MRC). The main contribution of this chapter consists in the evaluation the MMGF function and the derived MMGF function is used to evaluate a closed-form expression for the channel capacity under optimal rate adaptation (ORA), channel capacity with optimal rate adaptation ($C_{ORA}$), channel inversion with fixed rate (CIFR) and Truncated CIFR is approach ($C_{TCIFR}$). The derived results are obtained in the terms of well known Meijer G function and other special functions. In Chapter 6, we have investigated the MGF based performance analysis for various modulation scheme over the generalized-K fading channel with M-branch MRC diversity at receiver. The main contribution of this paper consists with the evaluation of MGF function and the derived MGF function is used to

evaluate closed-form expressions for average bit-error-rate (BER) and average symbol-error-rate (SER). The derived results are obtained in the terms of well known Hypergeometric function and Meijer's G function. Chapter 7 explores the MMGF based channel capacity analysis over the generalized-K fading channel with M-branch MRC diversity at receiver. We have derived a general formula for channel capacity under different adaptive transmission schemes. The derived results are compared with the other reported literature to support the analysis. Finally, Chapter 8 concludes the thesis and recommended the possible future directions.

# ANALYSIS OF INTER-CARRIER-INTERFERENCE REDUCTION METHOD IN OFDM COMMUNICATION SYSTEMS

## 2.1 INTRODUCTION

Orthogonal frequency division multiplexing (OFDM) is a multicarrier modulation technique, which is widely used in various communication systems and standards due to its high data rate, high spectral efficiency and robustness to the frequency selective channels [51-68]. However, it is susceptible to the phase-noise and multicarrier frequency offset between the transmitter and receiver's local oscillator, which causes several impairments including disrupting the orthogonality among subcarriers and introduces inter-carrier interference (ICI) that would significantly degrade the system performance [53-59,117-125]. The ICI is introduced by carrier frequency offset, phase noise, and timing offset. The carrier frequency offset is caused by the mismatch of frequencies between the oscillators at the transmitter and receiver, or from the Doppler spread due to the relative movement between the transmitter and receiver [83]. The phase noise arises predominantly due to the imperfections of the local oscillator in the transceiver. Essentially, it represents a time-varying drift of the local oscillator phase from its reference [53]. The timing offset arises due to the multipath delay spread and because of timing offset not only inter-symbol interference (caused by the next symbol), but ICI also occur [83]. However, ICI induced by phase noise and timing offset can completely compensated or corrected. Since the Doppler spread or frequency shift is random, hence we can only mitigate the impact of the ICI induced by it [83].

A simple and most effective method that is called the self-cancellation scheme has been proposed by Zhao and Haggman [54], which significantly reduces the ICI with little additional computational complexity. This scheme significantly reduces the ICI at cost of reducing the transmission rate. Besides its low computational complexity, another very important advantage of the self-cancellation scheme is that it can also be

useful to mitigate the ICI created by a spread of frequency shifts in the signal such as Doppler spread resulting from a time variable channel. The main idea of this scheme is to modulate the input data symbol onto a group of subcarriers with predefined coefficients such that the generated ICI signals within that group cancel each other, hence the name is self-cancellation. In this ICI mitigation technique, the bandwidth efficiency becomes half, which is the major drawback of this technique. Ahn et al [51] has proposed the frequency domain equalization for ICI cancellation, which is very simple process [36]. After demodulation in OFDM receiver, the subcarriers will be subjected to different losses and phase shifts but there will be no interaction among them. The frequency domain equalization therefore consists solely of separate adjustments of subcarrier gain and phase or equivalently of adjusting the individual decision regions. For the case where the constellations consist of equal amplitude points, as in PSK (phase shift keying), this equalization becomes even simpler in that only phase need be corrected for each subcarrier because amplitude has no significant effect on decisions. This technique can reduce the ICI caused by multipath fading distortion only, which is not the major source of ICI that is the main drawback of this technique. The major source of ICI is due to the frequency mismatch between the transmitter and receiver and Doppler shift. Again it is only suitable for flat fading channels but in mobile communication the channels are frequency selective fading in nature because of multipath components and also the most commonly used ICI counter measure methods are frequency-domain equalization [51], which uses training symbol that is one of the most commonly used methods. However, the use of training symbol or redundant subcarriers reduces the bandwidth efficiency. Li et al [52] have proposed a time-domain windowing approach for ICI mitigation.

However, the time domain windowing should be implemented after cyclic extension of the frame, so that the windowed frame is not cyclically extended. The potential solution to this problem is to extend each frame to $2N$ points at the receiver and implement a $2N$ FFT. Practically, it requires a $2N$ IFFT block at the transmitter and $2N$ FFT at the receiver [36]. However, by using the partial FFT techniques, we can reduce the computation by calculating only the required frequency bins. It can only reduce sensitivity of only time offset, which is not the major source of ICI and also reduces bandwidth efficiency. The frequency offset estimation and compensation

techniques [56-68], correlative coding [55, 62-65] and the conjugate cancellation scheme [61, 19] are others techniques that is used to cancel ICI. Zhao et al [55] have proposed the correlative coding between the signals modulated on subsequent subcarriers in binary phase-shift keying OFDM but this scheme does not improves carrier-to-interference ratio (CIR) significantly. In the conjugate cancellation scheme, which is proposed in [61, 69], two sequences are transmitted in each data symbol. First sequence is original received sequence and another sequence is conjugate of the original sequence. Thus the two sequences are conjugate of each other rather than adjacent subcarriers with opposite polarities in order to cancel the ICI. Yeh et al [69] have discussed the ICI mitigation technique using conjugate-cancellation but they have not provided any mathematical analysis for the calculation of ICI. In [126], the upper bound of the bit-error-rate (BER) of the OFDM system is analyzed without ICI self-cancellation where as in [127], it is analyzed by using self-cancellation technique but this method is less accurate.

In this chapter, we have presented the BER analysis and improved ICI cancellation technique for the OFDM communication system. In the proposed technique, at the transmitter, IFFT is performed for first part of the data and FFT for the second part of data. At the receiver, FFT is performed for the first part of the data and IFFT for the second part of the data. These combined operation forms an ICI cancellation scheme for the OFDM communication system.

## 2. 2 SYSTEM MODEL

Figure 2.1 shows a typical discrete-time base band equivalent model of the OFDM digital communication systems. The input binary serial data stream is encoded by using suitable modulation technique (*M*-QAM, BPSK, and QPSK) as shown in Figure 2.1. Further, the symbols are transferred to the serial-to-parallel (S/P) converter and in this stage, duration of bits is increased. At the transmitter, the parallel bit stream is subjected to IFFT block and second part is subjected to FFT block. The modulated symbols are serialized using a parallel-to-serial (P/S) converter. Now, the guard band addition is performed because at the receiver, one OFDM symbol is overlapped with the other symbol due to the multipath distortion. To eliminate the problem of inter symbol interference a guard time inserted between two symbols and duration of the guard interval should be greater than the maximum delay spread. In the next block

digital signal is converted to analog via the digital-to-analog (D/A) converter before send down to the channel. At the receiver side, the guard interval is removed and the received symbol is converted from analog-to-digital by using the analog-to-digital (A/D) converter. In the next process, the data is transferred to the serial-to-parallel (S/P) converter and then data is sent in IFFT and FFT block. After FFT and IFFT block data is sent for parallel-to-serial conversion and then for demodulation. The ICI cancellation is performed after demodulation by using the diversity combiner.
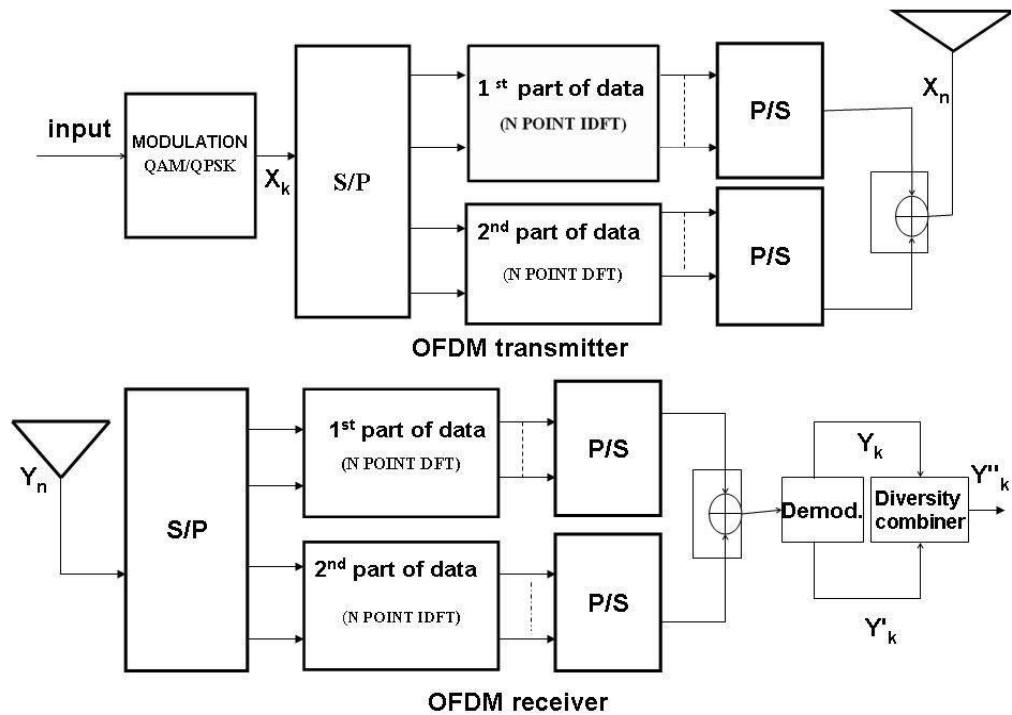


**Figure 2.1** The system model for the OFDM digital communication systems.


## 2.3 PROPOSED ICI CANCELLATION SCHEME

The input data bits are encoded by using the suitable modulation technique like (QPSK or QAM) and the output of this block is $X_k$. The IFFT output at transmitter is [56]:

$$x_n = \frac{1}{N} \sum_{k=0}^{N-1} X_k \, e^{2\pi j n k / N} \tag{2.1}$$

$n = 0, 1, 2\text{-----------}N\text{-}1.$

where $N \geq 2k + 1$, and $k$ is the number of subcarriers and $N$ is the period of IFFT. The frequency offset arises due to the frequency mismatch of oscillator of the transmitter and receiver as discussed in detail in [56]. At the received sequence after passing through the channel can be expressed as:

$$y_n = e^{\left( j2\pi\varepsilon n/N \right)}[x_n * h_n] + W_n \tag{2.2}$$

where $h_n$ is channel impulse response, $W_n$ is additive white Gaussian noise (AWGN) and $\varepsilon$ is normalized frequency offset. The normalized frequency offset is constant over the one IFFT period as discussed in [56, 117-118]. There are two deleterious effects caused by frequency offset: 1) is the reduction of signal amplitude in the output of the filters matched to each carrier and 2) is introduction of ICI [56]. The performance of OFDM communication systems degrade significantly because of ICI. After some mathematical manipulation the Equation (2.2), can be expressed as:

$$y_n = \frac{1}{N}\left[ \sum_{k=0}^{N-1} X_k H_k e^{2\pi j n(k+\varepsilon)/N} \right] + W_n \tag{2.3}$$

where $H_k$ is the channel transfer function at the frequency of $k^{\text{th}}$ subcarrier. Most types of the noise present in radio communication systems can be modeled accurately by using AWGN. This noise has a uniform spectral density (making it white) and Gaussian distribution in amplitude. Thermal and electrical noise from amplification, primarily have white Gaussian noise properties allowing them to be modeled accurately with AWGN. Also most other noise sources have AWGN properties due to transmission being OFDM and its signals have a flat spectral density and Gaussian amplitude distribution provided that numbers of carriers are large. The output of DFT demodulator can be expressed as:

$$Y_k = \sum_{n=0}^{N-1}\left\{ \frac{1}{N}\left[ \sum_{k=0}^{N-1} H_k X_k e^{2\pi j n(k+\varepsilon)/N} \right] + W_n \right\} e^{-2\pi j k n/N}$$

$$Y_k = (X_k H_k)\left\{ \frac{sin\,\pi\varepsilon}{N(\pi\varepsilon/N)} \right\} e^{j\pi(N-1)/N} + I_k \tag{2.4}$$

The first component on the right-hand side of Equation (2.4) is the modulation value $X_k$ which is modified by the channel transfer function. This component experiences an amplitude reduction and phase shift due to the frequency offset. The second term is the ICI term, which arises due to the frequency mismatch of the oscillator transmitter and receiver. So the ICI can be expressed as:

$$I_k = \sum_{l=0}^{N-1} \frac{1}{N} X_l H_l \sum_{n=0}^{N-1} e^{2\pi jn(l+\varepsilon-k)/N} \Bigg|_{l \neq k} \tag{2.5}$$

The summation term in Equation (2.5) is the geometric progression of total $N$ terms with common factor $\exp(2\pi(l+\varepsilon-k))$. The expansion of summation factor is as below:

$$I_k = \sum_{l=0}^{N-1} \frac{1}{N} X_l H_l \left[ 1 + e^{2\pi j\left((l+\varepsilon-k)/N\right)} + e^{4\pi j\left((l+\varepsilon-k)/N\right)} + \cdots + e^{2\pi j(N-1)\left((l+\varepsilon-k)/N\right)} \right]$$

After addition of the above geometric progression, we get:

$$I_k = \sum_{l=0}^{N-1} \frac{1}{N} X_l H_l \underbrace{\left[ \frac{1 - e^{2\pi j(l+\varepsilon-k)}}{1 - e^{2\pi j\left((l+\varepsilon-k)/N\right)}} \right]}_{P}$$

Bracketed term is taken as $P$ for simplicity and simplified as:

$$P = \left( \frac{1 - e^{2\pi j\left((l+\varepsilon-k)\right)}}{1 - e^{2\pi j\left((l+\varepsilon-k)/N\right)}} \right) \times \left( \frac{e^{-\pi j(l+\varepsilon-k)}}{e^{-\pi j\left((l+\varepsilon-k)/N\right)}} \times \frac{e^{-\pi j\left((l+\varepsilon-k)/N\right)}}{e^{-\pi j(l+\varepsilon-k)}} \right)$$

or

$$P = \left( \frac{\sin \pi(l+\varepsilon-k)}{\sin \pi\left((l+\varepsilon-k)/N\right)} \right) \times \left( \frac{e^{-\pi j\left((l+\varepsilon-k)/N\right)}}{e^{-\pi j(l+\varepsilon-k)}} \right)$$

So now Equation (2.5) can be written as:

$$I_k = \sum_{\substack{l=0 \\ l \neq k}}^{N-1} \frac{1}{N} X_l H_l \left[ \frac{\sin \pi(l+\varepsilon-k)}{\sin \pi\left(\frac{l+\varepsilon-k}{N}\right)} \right] e^{j\pi(N-1)\left(\frac{l+\varepsilon-k}{N}\right)} \tag{2.6}$$

The sequence $S(l-k)$ is defined as the ICI coefficient between $l^{th}$ and $k^{th}$ sub-carriers, which can be expressed as:

$$S(l-k) = \frac{sin(\pi(l-k+\varepsilon))}{N\,sin\left(\frac{\pi(l-k+\varepsilon)}{N}\right)}\; exp\left[j\pi\left(1-\frac{1}{N}\right)(l-k+\varepsilon)\right] \tag{2.7}$$

The first term in the right-hand side of Equation (2.4) represent the desired signal. Without the frequency error ($\varepsilon = 0$) and $S(0)$ takes its maximum value $S(0) = 1$. The second term is ICI component. As we know, if $\varepsilon$ becomes larger, the desired part $|S(0)|$ decreases and the undesired part $|S(l-k)|$ increases. $S''(l-k)$ is ICI coefficient of the self-cancellation technique and given by Equation (10) of [54]. $S'(l-k)$ is the proposed ICI coefficient. $W_n$ is additive white Gaussian noise it is assumed to be zero without loss in generality as given in [61]. Considering the FFT of same data $X_k$ at the transmitter ($2^{nd}$ part of the data) from Figure 2.1 the data duplication is necessary for the ICI cancellation as discussed in [54, 57, 61]. The bandwidth efficiency is reduced due to duplication of data but it is comparable with the other ICI cancellation techniques as in [54, 61, 69, 125-130].

$$x'_k = \sum_{n=0}^{N-1} X_k e^{-(2\pi jnk/N)} \tag{2.8}$$

and

$$y''_k = \left[\sum_{n=0}^{N-1} X_k H_k e^{2\pi jn(-k+\varepsilon)/N}\right] + W'_n \tag{2.9}$$

$$k = 0, 1, 2 \ldots\ldots\ldots N\text{-}1.$$

The output of the IDFT demodulator can be expressed as:

$$Y'_k = \frac{1}{N}\sum_{k=0}^{N-1}\left\{\left[\sum_{n=0}^{N-1} H_k X_k e^{2\pi jn(-k+\varepsilon)/N}\right] + W'_n\right\} e^{2\pi jkn/N}$$

$$Y'_k = \underbrace{(X_k H_k)\left\{\frac{(\sin\pi\varepsilon)}{N\sin(\pi\varepsilon/N)}\right\}\; e^{j\pi\varepsilon(N-1)/N}}_{\text{I}} + \underbrace{I'_k}_{\text{II}} \tag{2.10}$$

The first component in the Equation (2.10) is the modulation value $X_k$ is modified by channel transfer function. This component experiences an amplitude reduction and phase-shift due to the frequency offset. The second term is the ICI term, which arises due to frequency mismatch of oscillator transmitter and receiver. So ICI can be expressed as:

$$I'_k = \sum_{l=0}^{N-1} \frac{1}{N} X_l H_l \sum_{n=0}^{N-1} e^{2\pi j n((k+\varepsilon-l)/N)} \bigg|_{l\neq k}$$

(2.11)

Above summation term is in geometric progression of total $N$ terms of common factor are $\exp(2\pi(l-\varepsilon-k))$ and expand summation factor as below:

$$I'_k = \sum_{l=0}^{N-1} \frac{1}{N} X_l H_l \left[ 1 + e^{2\pi j((-l+\varepsilon+k)/N)} + e^{4\pi j((-l+\varepsilon+k)/N)} + \cdots + e^{2\pi j(N-1)((-l+\varepsilon+k)/N)} \right]$$

or

$$I'_k = \sum_{l=0}^{N-1} \frac{1}{N} X_l H_l \underbrace{\left[ \frac{1-e^{2\pi j(-l+\varepsilon+k)}}{1-e^{2\pi j((-l+\varepsilon+k)/N)}} \right]}_{P'}$$

Bracketed term is taken as $P'$ and it can be simplified as:

$$P' = \left( \frac{1-e^{2\pi j((k+\varepsilon-l)}}{1-e^{2\pi j((k+\varepsilon-l)/N)}} \right) \times \left( \frac{e^{-\pi j(k+\varepsilon-l)}}{e^{-\pi j((k+\varepsilon-l)/N)}} \times \frac{e^{-\pi j((k+\varepsilon-l)/N)}}{e^{-\pi j(k+\varepsilon-l)}} \right)$$

$$P' = \left( \frac{\sin \pi(k+\varepsilon-l)}{\sin \pi((k+\varepsilon-l)/N)} \right) \times \left( \frac{e^{-\pi j((k+\varepsilon-l)/N)}}{e^{-\pi j(k+\varepsilon-l)}} \right)$$

$$I'_k = \sum_{\substack{l=0 \\ l\neq k}}^{N-1} \frac{1}{N} X_l H_l \left[ \frac{\sin \pi(k+\varepsilon-l)}{\sin \pi\left(\frac{k+\varepsilon-l}{N}\right)} \right] e^{j\pi(N-1)\left(\frac{l+\varepsilon-k}{N}\right)}$$

(2.12)

$W'_n$ is also the additive white Gaussian noise. It is assumed to be zero without loss in generality in above discussion as shown in [61]. The ICI term at the output of the receiver is:

$$I''_k = \frac{I_k + I'_k}{2} \tag{2.13}$$

By substituting the value from Equation (2.6) and (2.12) in Equation (2.13), we get:

$$I''_k = \frac{1}{2} \sum_{l=0}^{N-1} e^{j\pi(N-1)((l+\varepsilon-k)/N)} X_l H_l \left\{ \left( \frac{\sin\pi(l+\varepsilon-k)}{\pi(l+\varepsilon-k)} \right) + \left( \frac{\sin\pi(k+\varepsilon-l)}{\pi(k+\varepsilon-l)} \right) \right\} \tag{2.14}$$

Now, we have considered following two cases:

**Case 1:** If $l - k =$ even numbers, then

$$I''_k = \frac{1}{2} \sum_{l=0}^{N-1} e^{j\pi(N-1)((l+\varepsilon-k)/N)} X_l H_l \frac{\sin\pi\varepsilon}{\pi} \left\{ \left( \frac{1}{(l+\varepsilon-k)} \right) - \left( \frac{1}{(l-\varepsilon-k)} \right) \right\}$$

$$= -\frac{1}{2} \sum_{l=0}^{N-1} e^{j\pi(N-1)((l+\varepsilon-k)/N)} X_l H_l \frac{\sin\pi\varepsilon}{\pi} \left\{ \frac{2\varepsilon}{(l-k)^2 - \varepsilon^2} \right\}$$

Since $(l - k) \rangle \varepsilon$ so $\varepsilon^2$ can be neglected in compression of $(l-k)^2$.

$$\approx -\sum_{l=0}^{N-1} e^{j\pi(N-1)((l+\varepsilon-k)/N)} X_l H_l \frac{\sin\pi\varepsilon}{\pi} \left\{ \frac{\varepsilon}{(l-k)^2} \right\}$$

$$= -\sum_{l=1}^{N-1} e^{j\pi(N-1)((l+\varepsilon-k)/N)} X_l H_l \frac{\sin\pi\varepsilon}{\pi} \left\{ \frac{\varepsilon}{(l)^2} \right\} \bigg|_{l\neq 0}$$

In order to evaluate the statistical properties of ICI after conjugate cancellation, assume $\mathrm{E}(I''_k) = 0$ and assuming average channel gain $\mathrm{E}\left[|H_l|^2\right] = |H|^2$ is constant and $\mathrm{E}\left[|X_l|^2\right] = |X|^2$. Now, we will find variance of ICI:

$$E\left[|I''_k|^2\right] = |X|^2 \sum_{l=1}^{N-1} E\left\{|H_l|^2 \left( \frac{\sin\pi\varepsilon\times\varepsilon}{\pi} \right)^2 \left\{ \frac{1}{(l)^2} \right\}^2 \right. \tag{2.15}$$

Here, $l = 1 \ldots\ldots$N-1, and $N \geq 2K + 1$, so we can write $-K \langle l \langle K$. Also $l^4$ is even function, Equation (2.15) can be written as:

$$E\left[|I''_k|^2\right] = |X|^2 \sum_{l=-K}^{K} E\left\{|H_l|^2 \left( \frac{\sin\pi\varepsilon\times\varepsilon}{\pi} \right)^2 \left\{ \frac{1}{(l)^2} \right\}^2 \right.$$

$$\leq |X|^2 |H|^2 \left( \frac{sin\, \pi \varepsilon \times \varepsilon}{\pi} \right)^2 2 \sum_{l=1}^{\infty} \left\{ \frac{1}{(l)^2} \right\}^2$$

The variance of ICI is:

$$\sigma_{ICI}^2 = |X|^2 |H|^2 \left( sin\, \pi \varepsilon \times \varepsilon \right)^2 \times 0.2195 \tag{2.16}$$

**Case 2:** If $l - k =$ odd numbers, then the Equation (2.14) can be written as:

$$I''_k = -\frac{1}{2} \sum_{l=0}^{N-1} e^{j\pi(N-1)((l+\varepsilon-k)/N)} X_l H_l \frac{\sin \pi \varepsilon}{\pi} \left\{ \left( \frac{1}{(l+\varepsilon-k)} \right) + \left( \frac{1}{(k+\varepsilon-l)} \right) \right\}$$

$$= -\frac{1}{2} \sum_{l=0}^{N-1} e^{j\pi(N-1)((l+\varepsilon-k)/N)} X_l H_l \frac{\sin \pi \varepsilon}{\pi} \left\{ \left( \frac{1}{(l+\varepsilon-k)} \right) - \left( \frac{1}{(l-\varepsilon-k)} \right) \right\}$$

$$= \frac{1}{2} \sum_{l=0}^{N-1} e^{j\pi(N-1)((l+\varepsilon-k)/N)} X_l H_l \frac{\sin \pi \varepsilon}{\pi} \left\{ \left( \frac{2\varepsilon}{(l-k)^2 - \varepsilon^2} \right) \right\}$$

Since, $l - k \gg \varepsilon$ so $\varepsilon^2$ can be neglected in compression of $(l-k)^2$, so the above Equation can be expressed as:

$$\approx \sum_{l=0}^{N-1} e^{j\pi(N-1)((l+\varepsilon-k)/N)} X_l H_l \frac{\sin \pi \varepsilon}{\pi} \left\{ \left( \frac{\varepsilon}{(l-k)^2} \right) \right\}$$

$$\approx \sum_{l=0}^{N-1} e^{j\pi(N-1)((l+\varepsilon-k)/N)} X_l H_l \frac{\sin \pi \varepsilon}{\pi} \left\{ \left( \frac{\varepsilon}{(l-k)^2} \right) \right\}$$

$$= \sum_{l=1}^{N-1} e^{j\pi(N-1)((l+\varepsilon-k)/N)} X_l H_l \frac{\sin \pi \varepsilon \times \varepsilon}{\pi} \left\{ \frac{1}{(l)^2} \right\} \Big|_{l \neq 0}$$

Now, we find the variance of the ICI as:

$$E\left[ |I''_k|^2 \right] = |X|^2 \sum_{l=1}^{N-1} E\left\{ |H_l|^2 \right\} \left( \frac{\sin \pi \varepsilon \times \varepsilon}{\pi} \right)^2 \left\{ \frac{1}{(l)^2} \right\}^2 \tag{2.17}$$

$$= |X|^2 \sum_{l=-K}^{K} E\left\{ |H_l|^2 \right\} \left( \frac{\sin \pi \varepsilon \times \varepsilon}{\pi} \right)^2 \left\{ \frac{1}{(l)^2} \right\}^2$$

Here, $l = 1$ …………$N$-1 and $N \geq 2K + 1$, so we can write $-K \langle l \langle K$. Also $l^4$ is even function the Equation (2.17) can be written as:

$$E\left[\left|I''_k\right|^2\right] = 2|X|^2 \sum_{l=1}^{K} E\left\{|H_l|^2\right\}\left(\frac{\sin \pi\varepsilon \times \varepsilon}{\pi}\right)^2 \left\{\frac{1}{(l)^2}\right\}^2$$

$$\leq 2|X|^2 \sum_{l=1}^{\infty} E\left\{|H_l|^2\right\}\left(\frac{\sin \pi\varepsilon \times \varepsilon}{\pi}\right)^2 \left\{\frac{1}{(l)^2}\right\}^2$$

$$= |X|^2|H|^2\left(\frac{\sin \pi\varepsilon \times \varepsilon}{\pi}\right)^2 2\sum_{l=1}^{\infty}\left\{\frac{1}{(l)^4}\right\}$$

The variance of the ICI is

$$\sigma_{ICI}^2 = |X|^2|H|^2\left(\frac{\sin \pi\varepsilon \times \varepsilon}{\pi}\right)^2 2 \times 1.083$$

$$\sigma_{ICI}^2 = |X|^2|H|^2\left(\sin \pi\varepsilon \times \varepsilon\right)^2 \times 0.2195 \tag{2.18}$$

The bit-error rate of QPSK modulated OFDM system is given in [131]:

$$\text{BER} = 1/2 * Q\left(\sqrt{E_s / N_0}\right) \tag{2.19}$$

where $Q(\bullet)$ is Gaussian Q function and $E_S$ is symbol energy. The BER of QPSK OFDM system after ICI cancellation as given by:

$$\text{BER} \leq 1/2 * Q\sqrt{|X|^2|H|^2\left\{(\sin \pi\varepsilon)/\pi\varepsilon\right\}^2 / (N_o + |X|^2|H|^2\left(\sin \pi\varepsilon \times \varepsilon\right)^2 \times .2195)}$$

$$= 1/2 * Q\sqrt{\frac{|X|^2|H|^2}{N_o}\left\{(\sin \pi\varepsilon)/\pi\varepsilon\right\}^2 / (1 + \frac{|X|^2|H|^2}{N_o}\left(\sin \pi\varepsilon \times \varepsilon\right)^2 \times .2195)}$$

$$\text{BER} = 1/2 * Q\sqrt{\frac{E_b}{N_o}\left\{(\sin \pi\varepsilon)/\pi\varepsilon\right\}^2 / (1 + \frac{E_b}{N_o}\left(\sin \pi\varepsilon \times \varepsilon\right)^2 \times .2195)} \tag{2.20}$$

where $E_b$ is the bit energy. This is an expression for the BER calculation for the proposed method.

## 2.4 RESULTS AND DISCUSSION

For the simulation of the proposed system model as shown in Figure 2.1, we have considered the number of subcarrier is $N = 64$ and guard interval seven for QPSK modulation scheme. Figure 2.2 shows the comparison of BER between the self-cancellation method and proposed improved method for the normalized frequency offset $\varepsilon = 0.1$ and 0.2. The main concept of self-cancellation scheme is to modulate one data symbol onto to the next subcarrier with predefined inversed weighting coefficients "-1". With this concept, the ICI signal generated within a group can be self-cancelled each other as discussed in [54]. By using the self-cancellation method at frequency offset 0.2, the obtained BER is greater than $10^{-1}$ at SNR = 0dB and less than $10^{-4}$ at SNR = 10dB. For the proposed method BER is $10^{-1}$ for 0dB SNR and it is just less than $10^{-5}$ at 10dB SNR, but for the normalized frequency offset 0.1 for self-cancellation method BER at 0dB SNR is greater than $10^{-1}$ as well as less than $10^{-5}$ at 10dB SNR whereas for proposed improved cancellation method BER $10^{-1}$ at 0dB SNR and greater than $10^{-5}$ at 10dB SNR. Hence, the proposed improved cancellation scheme is better than that of the ICI self-cancellation as discussed in detail in [127].
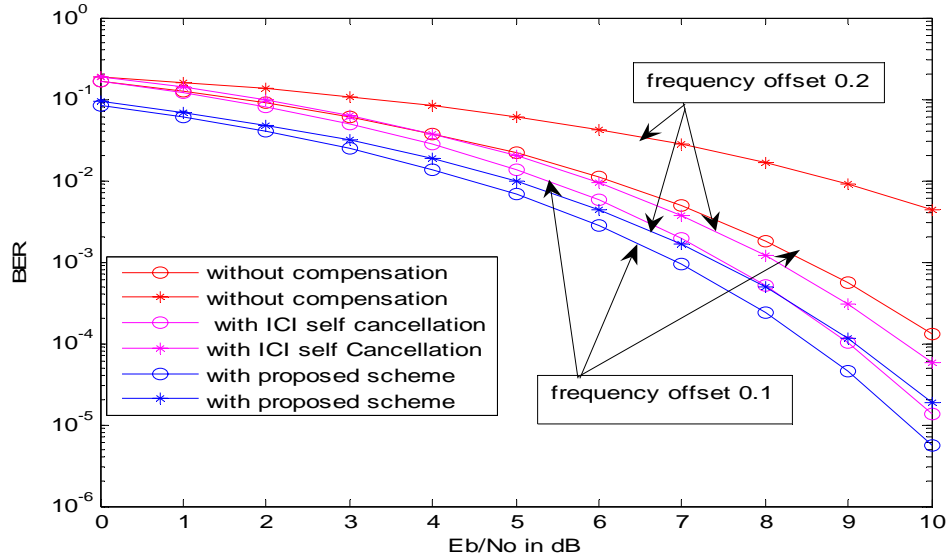


**Figure** 2.2 Comparison between the proposed improved ICI cancellation schemes with the self-cancellation scheme for BPSK OFDM system.

Figure 2.3 depicts the comparison of BER for higher alphabet size (16-QAM OFDM system) at $N = 64$ for normalized frequency 0.2, which reveals that proposed method is better that that of the self-cancellation at higher values of the signal-to-noise ratio..

Figure 2.4 shows the compression of the carrier-to-interference ratio (CIR) among several methods like [54], standard OFDM system, and proposed scheme for normalized frequency offset 0.5 our proposed result is comparable with [129].
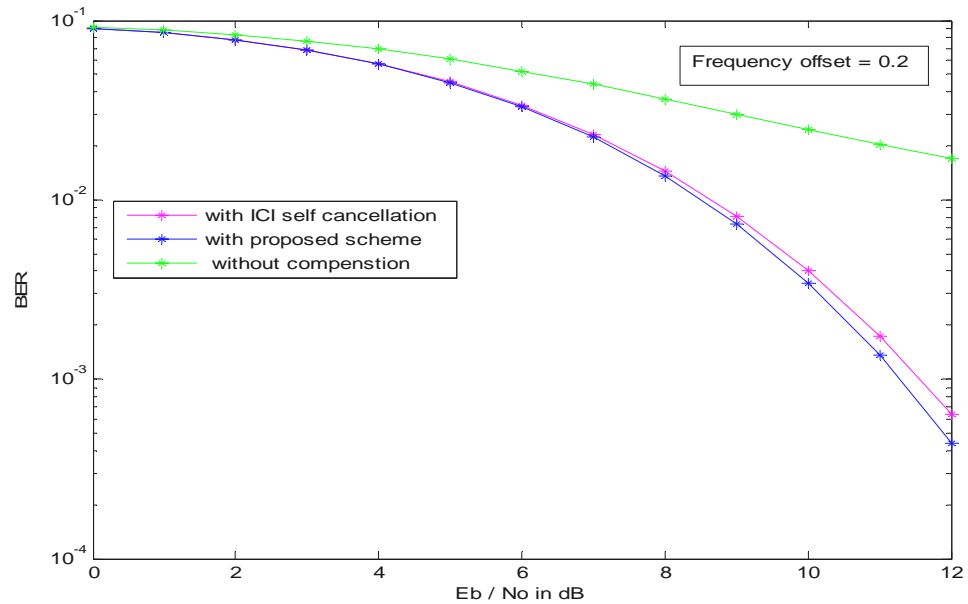


**Figure 2.3** Comparison of the BER characteristics of the proposed conjugate ICI cancellation schemes with self-cancellation scheme for 16-QAM OFDM system.
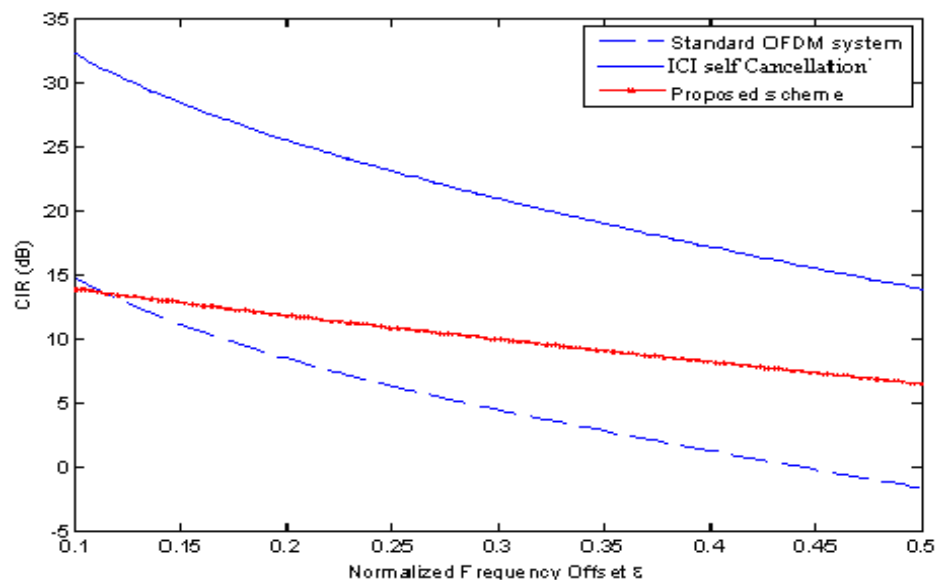


**Figure 2.4** Comparison of the carrier-to-interference ratios (CIR) characteristics with normalized frequency offset of the proposed scheme with standard OFDM as well as ICI-self cancellation scheme.

The ICI power level of the communication system can be evaluated by using the carrier-to-interference ratio [56]. The carrier-to-interference ratio of the proposed scheme is comparable to that of the conventional OFDM systems at smaller values of the normalized frequency offset as shown in the Figure 2.4. There are three types of ICI coefficients such as $S(l-k)$ for the standard OFDM system, $S^{'}(l-k)$ for ICI canceling modulation which is proposed in this chapter and $S^{''}(l-k)$ for combined ICI canceling modulation and demodulation. This combined ICI canceling modulation and demodulation methods is called the ICI self-cancellation scheme. Figure 2.5 shows comparison of ICI coefficient before and after cancellation of ICI.
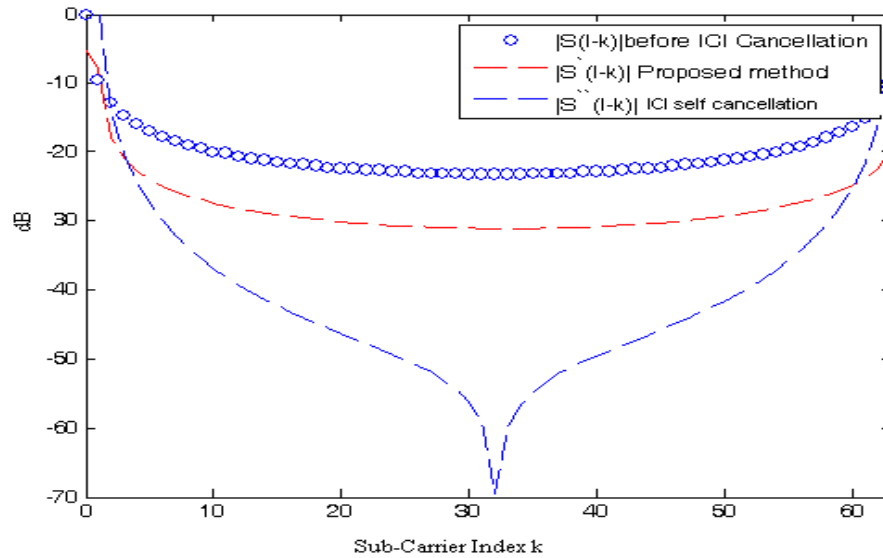


**Figure 2.5** Comparison of the ICI coefficient before and after cancellation of ICI.

## 2.5. CONCLUSION

In this chapter, we have explored a simple and improved ICI cancellation scheme to reduce the frequency offset sensitivity of the OFDM communication systems. The proposed scheme employs DFT at the transmitter and IDFT at the receiver. The regular OFDM samples, which are generated by the IDFT, are transmitted as the 1st block and the DFT output is transmitted as the 2nd block. At the receiver, a result of the 1st output generated by the DFT is combined with the 2nd output generated by the IDFT. This combined operation forms a parallel inter-carrier-interference cancellation scheme for mitigating frequency offset of OFDM communication system. The proposed method provides better BER characteristics of the OFDM communication system than that reported in [54].

# REPEATED CORRELATIVE CODING BASED ICI CANCELLATION TECHNIQUE

## 3.1 INTRODCTION

Future wireless communication systems are expected to offer extremely high data rates with appropriate link quality over poor transmission environments. One efficient way to achieve this is by using OFDM communication technique because of its sufficient robustness to handle the radio channel impairments and its bandwidth efficiency due to overlapping orthogonal subcarriers. Despite its benefits, its major disadvantage is its sensitivity to frequency offset. The frequency offset results from a Doppler shift due to a mobile environment as well as from carrier frequency synchronization error. Such a frequency offset causes the loss of carrier's orthogonality, therefore ICI occurs. Currently, several approaches have been suggested for ICI cancellation such as frequency-domain equalization [51], time-domain windowing scheme [52], ICI self-cancellation [54], conjugate cancellation scheme [61, 69], and correlative coding [55]. The most commonly used ICI counter measure methods are frequency-domain equalization [51], which uses training signal. Another most commonly used method is time-domain windowing [52], which uses redundant subcarrier. However, the use of training symbol or redundant subcarriers reduces the bandwidth efficiency. The self-cancellation scheme proposed in [54] requires to modulate one data symbol on to the next subcarrier with predefined inversed weighting coefficients "-1". This concept of predefined weighting coefficients makes the ICI component in the received signal to cancel among them and bandwidth efficiency for this technique becomes half. The scheme proposed in [61, 69] requires data to be sent on two paths. The first path employs a regular OFDM algorithm and the second path uses the conjugate transmission of the first path. Due to the duplication, the bandwidth efficiency becomes half for conjugate cancellation

scheme is also. Most of the techniques discussed in [51, 52, 54, 61, 69, 130] for ICI cancellation, are bandwidth inefficient, but correlative coding based ICI cancellation technique [55] is bandwidth efficient. However, the main problem of this technique is its very low value of carrier-to-interference ratio, which is important parameter for the performance analysis of OFDM communication system.

In this Chapter, we have discussed about one of the important issues of OFDM system that is carrier-to-interference ratio. For improvement of the carrier-to-interference ratio, we have proposed repeated correlative coding scheme in this chapter. An expression for the ICI power of OFDM systems using repeated correlative coding as a function of the frequency offset is derived and further, evaluated the carrier-to-interference ratio power. The average carrier-to-interference ratio power is used as the ICI level indicators and theoretical carrier-to-interference ratio expression is derived for the proposed scheme. The carrier-to-interference ratio performance of the proposed system is compared with that of ICI self-cancellation scheme [54], correlative coding scheme [55], and standard OFDM system. The BER of the proposed scheme is also compared with the ICI self-cancellation scheme [54] and correlative coding scheme [55], which shows that the CIR obtained by using repeated correlative coding scheme is significantly enhanced.

## 3.2 REPEATED CORRELATIVE CODING SCHEME FOR MITIGATION OF ICI IN OFDM SYSTEM

### 3.2.1 SYSTEM MODEL

Figure 3.1 shows a simplified block diagram of the binary phase-shift keying (BPSK) OFDM system using repeated correlative coding scheme. The binary signal sequence after BPSK modulation is expressed as $m_k$, where $k$ is subcarriers index. $m_k$ can take values of $\pm 1$ that fulfill the zero mean and independence condition. The symbols on two adjacent subcarriers have an $180^0$ phase difference between them such that $m_1 = -m_0, m_3 = -m_2, - - - -, m_{N-1} = -m_{N-2}$ [54]. The correlative coding is performed using F (D) = (1-D) [55], where D denotes the unit delay, which generates new sequence.

$$g_k = m_k - m_{k-1} \qquad (3.1)$$

Then the coded symbols $g_k$, k $\in$ [0, $N$/2-1] are modulated on $N$/2 subcarriers. The Equation (3.1) introduces correlation between the adjacent symbols ($g_k$, $g_{k-1}$), which implies that the independence condition is no longer maintained. The error propagation in decoding procedure can be avoided by using pre-coding technique [130]. The standard OFDM system can be achieved by removing the repeated code, correlative code and decoding blocks from the Figure 3.1.
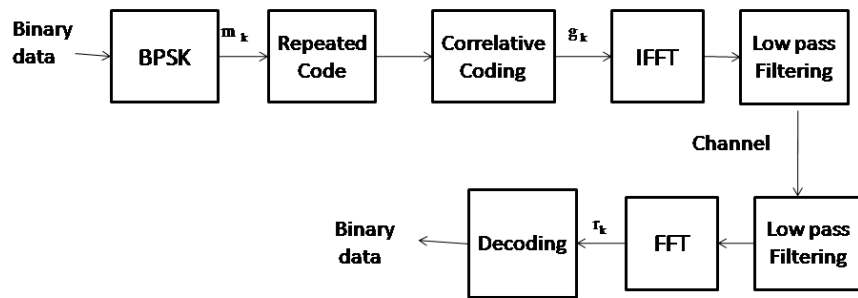


**Figure 3.1** Block diagram of the repeated correlative coding OFDM communication system.

**3.2.2 ICI MECHANISM**

In the OFDM communication system, the received signal on subcarrier $k$ is written as [54]:

$$Y_k = m_k S_0 + \sum_{l=0, l \neq k}^{N-1} m_l S_l + n_k \tag{3.2}$$

$k$ = 0, 1,………………., $N$-1

where $N$ is the total number of subcarriers and $n_k$ is an additive white Gaussian noise. The first term in the right hand side of Equation (3.2) represents the desired signal and second term is the ICI components. The sequence $S_k$ is defined as the ICI coefficient between $l^{th}$ and $k^{th}$ subcarriers, which can be expressed as [56]:

$$S_k = \frac{\sin \pi (k + \varepsilon)}{N \sin \frac{\pi}{N}(k + \varepsilon)} \exp(j\pi (1 - \frac{1}{N})(k + \varepsilon)) \tag{3.3}$$

The variable $\varepsilon$ is normalized frequency offset (ratio of the actual frequency offset to inter carrier spacing). The desired signal power on the $k^{th}$ subcarrier can be represented as:

$$E\left(\left|C_k\right|^2\right) = E\left(\left|m_k s_\circ\right|^2\right)$$

and the ICI power is:

$$E\left(\left|I_k\right|^2\right) = E\left(\left|\sum_{l=0,l\neq k}^{N-1} m_l \, S_l\right|^2\right)$$

It is assumed that the transmitted data have zero-mean and statistically independent, therefore, the expression for carrier-to-interference ratio for BPSK OFDM system without self-cancellation for subcarriers $0 \leq k \leq N-1$ can be derived as [54]:

$$CIR = \frac{|S_0|^2}{\sum_{l=1}^{N-1} |S_l|^2} \tag{3.4}$$

### 3.2.3 CIR IMPROVEMENT BY USING REPEATED CORRELATIVE CODING

The average carrier-to-interference ratio (CIR) power is used as the ICI level indicator [57]. The CIR is defined as the desired received signal power on the $k^{th}$ subcarrier divided by ICI power to other subcarriers. The impact of ICI power on OFDM system can be evaluated by computing the CIR. The received signal at the receiver can be expressed as given by Equation (3.2).

$$r_k = Y_k - Y_{k+1}$$

$$k = 0, 1....N-1$$

For the proposed OFDM system with repeated correlative coding, if the channel frequency offset normalized to the subcarrier separation is denoted by $\varepsilon$, then the received signal on subcarrier $k$ can be expressed as given in [66]:

$$r_k = (2S_0 - S_{-1} - S_1)g_k + \sum_{\substack{l=0 \\ l\neq k}}^{N/2-1} (2S_{2l} - S_{2l-1} - S_{2l+1})g_l + (n_{2k} - n_{2k+1})$$

The first term of the received signal is desired signal and the second term is the undesired ICI signal. In the following derivations, without loss of the generality an additive white Gaussian noise is assumed to be zero. The received signal $r_k$ can be written as:

$$r_k = C_k + I_k \tag{3.5}$$

where

$$C_k = (2S_0 - S_{-1} - S_1)g_k \tag{3.6}$$

and

$$I_k = \sum_{\substack{l=0 \\ l \neq k}}^{N/2-1} (2S_{2l} - S_{2l-1} - S_{2l+1})g_l \tag{3.7}$$

Since the $E[m_k] = 0$ for BPSK signals, which implies that the $E[g_k] = 0$ from Equation (3.1) which leads to $E[c_k] = 0$ and $E[I_k] = 0$. Since $m_k$ fulfils the independence condition, so we have:

$$E[m_k m_{k-1}] = \begin{cases} E[(m_k)^2], & k = l \\ 0 & k \neq l \end{cases} \tag{3.8}$$

Therefore, we have

$$E((g_k)^2) = E((m_k - m_{k-1})^2) = 2E((m_k)^2) \tag{3.9}$$

The average carrier power $E(|C_k|^2)$ can be derived as:

$$E\left(|C_k|^2\right) = 2(|2S_0 - S_{-1} - S_1|^2)(E(m_k)^2) \tag{3.10}$$

and the average ICI power $E(|I_k|^2)$ can be calculated as:

$$E(|I_k|^2) = E\left(\left|\sum_{l=0,l\neq k}^{N/2-1} (2S_{2l} - S_{2l-1} - S_{2l+1})g_l\right|^2\right)$$

$$= \sum_{\substack{l=0 \\ l\neq k}}^{N/2-1} \sum_{\substack{p=0 \\ p\neq k}}^{N/2-1} (2S_{2l} - S_{2l-1} - S_{2l+1})(2S_{2p}^* - S_{2p-1}^* - S_{2p+1}^*)E[g_l g_p] \tag{3.11}$$

Taking the correlation between $g_k$ and $g_{k\pm1}$ into account as given in [55]:

$$E(g_l g_p) = \begin{cases} 2E((m_k)^2), & l = p \\ E((m_l - m_{l-1})(m_p - m_{p-1})) = -E((m_k)^2) & p = l \pm 1 \\ 0, & \textit{Otherwise} \end{cases} \tag{3.12}$$

By using Equation (3.11) and (3.12), we get:

$$E(|I_k|^2) = \left( 2 \sum_{l=1}^{N/2-1} |2S_{2l} - S_{2l-1} - S_{2l+1}|^2 - \right.$$

$$\sum_{l=2}^{N/2-1} (2S_{2l} - S_{2l-1} - S_{2l+1})(2S_{2(l-1)}^* - S_{2(l-1)-1}^* - S_{2(l-1)+1}^*)$$

$$+ \left. (2S_{2(l-1)} - S_{2(l-1)-1} - S_{2(l-1)+1})(2S_{2l}^* - S_{2l-1}^* - S_{2l+1}^*) \right) E((m_k)^2) \tag{3.13}$$

Thus, the average CIR of the proposed repeated correlative coded OFDM system is obtained by using Equation (3.10) and (3.13).

$$CIR = \frac{(|2S_0 - S_{-1} - S_1|^2)}{\left\{ \sum_{l=1}^{N/2-1} |2S_{2l} - S_{2l-1} - S_{2l+1}|^2 - \right.}$$

$$(1/2)[\sum_{l=2}^{N/2-1} (2S_{2l} - S_{2l-1} - S_{2l+1})(2S_{2(l-1)}^* - S_{2(l-1)-1}^* - S_{2(l-1)+1}^*)$$

$$\left. + (2S_{2(l-1)} - S_{2(l-1)-1} - S_{2(l-1)+1})(2S_{2l}^* - S_{2l-1}^* - S_{2l+1}^*)] \right\} \tag{3.14}$$

## 3.3 RESULTS AND DISCUSSION

In order to minimize the ICI in the OFDM system, a novel repeated correlative coding method is proposed. The normalized frequency offset is introduced in order to analyze the performance of the system where subcarrier frequency offset is used to measure the IC1 in the system. The CIR power levels versus normalized frequency offset is computed by using Equation (3.4) and (3.14), for the ICI self-cancellation method [54] and proposed repeated correlative coding method are plotted for range of normalized frequency offset $(0 < \varepsilon < 0.5)$. This simulation has been performed for BPSK OFDM system by using repeated correlative coding for normalized frequency offset, where $N = 64$ and guard band is 7. Figure 3.2 shows the CIR as a function of the normalized frequency offset. The CIR values for BPSK OFDM system at $\varepsilon = 0.1$ for proposed repeated correlative coding is 35.7 dB, for ICI self cancellation scheme

is 35.2 dB, for correlative coding is 18.7 dB and for normal OFDM) system is 14.7 dB. For comparison, the CIR of the conventional scheme and proposed scheme is shown in Figure 3.2. Comparing with conventional scheme, the proposed scheme improves the CIR power remarkably. Although, the new $0 < \varepsilon < 0.5$ scheme is not in the range of ICI-self cancellation scheme because the number of ICI component reduces a half by using repeated symbols for adjacent subcarriers in frequency domain. Thus, it reveals that the new scheme is able to reduce ICI due to frequency offset and improve the performance of OFDM communication system.
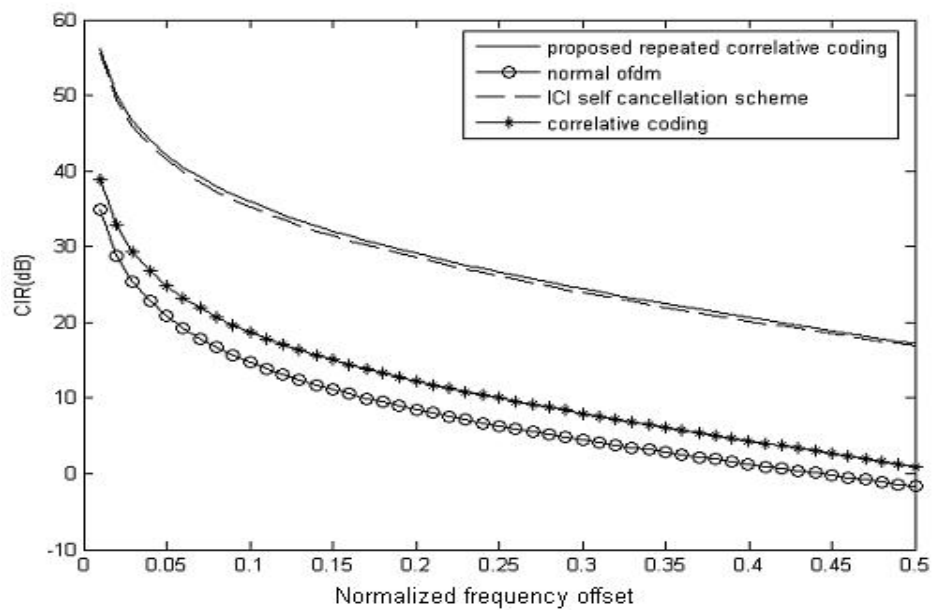


**Figure 3.2** The CIR characteristics of of the BPSK OFDM communication system with the normalized frequency offset.

The Equation (3.4) suggests that the CIR is a function of total number of subcarriers and frequency offset normalized by the subcarrier separation. However, the CIR power varies very small as a function of total number of subcarriers. Therefore, the CIR of the OFDM systems depends on the normalized frequency offset $\varepsilon$ approximately. Thus, it is not easy to reduce the ICI unless the normalized frequency offset $\varepsilon$ value is decreased [54]. For a certain channel frequency offset, smaller $\varepsilon$ values can be obtained by increasing the subcarriers separation. Thus, the bandwidth efficiency will be reduced and, therefore the guard interval will take a relatively larger portion of the useful signal. The spectral efficiency of the proposed method should be

taken into account when comparing bit-error-rate performance with the correlative coding scheme. Figure 3.3 shows the bit-error-rate comparison between the proposed repeated correlative coding scheme, ICI self-cancellation scheme [54], and correlative coding scheme [55]. With the ICI self-cancellation scheme, only the half subcarriers could be used to carry information symbols and the frequency spectral efficiency of the system will decrease to half. The bit-error-rate comparison of the proposed scheme with the ICI self-cancellation scheme for different normalized frequency offset ($\varepsilon = 0.05$, 0.1 and 0.15) at SNR = 6 dB is given in table 1. Here, the bit-error-rate of the proposed scheme is approximately same with that of the ICI self-cancellation scheme [54], but far better than correlative coding scheme in [55].
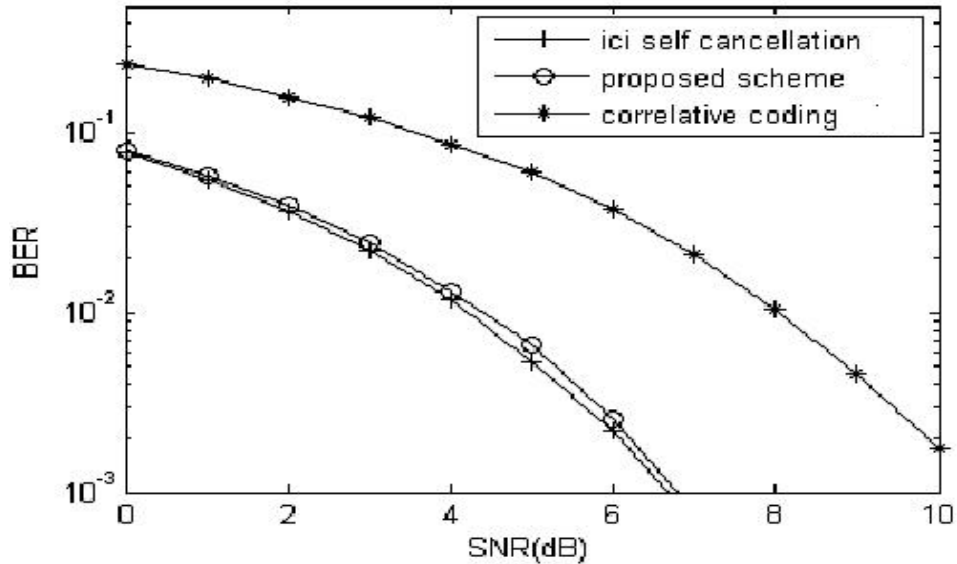


**Figure 3.3** BER comparisons for $\varepsilon = 0.05$ of proposed BPSK OFDM system with ICI-self-cancellation method and correlative coding scheme.

Table 3.1 Comparison of bit-error-rate for various normalized frequency offset with different ICI cancellation scheme.

| ICI Cancellation Scheme | BER for $\varepsilon = 0.05$ | BER for $\varepsilon = 0.1$ | BER for $\varepsilon = 0.15$ |
|---|---|---|---|
| ICI self-cancellation | 0.0059 | 0.0056 | 0.0055 |
| Correlative coding | 0.0597 | 0.0686 | 0.0836 |
| Repeated correlative coding | 0.0066 | 0.0079 | 0.0107 |

## 3.4 CONCLUSION

In this chapter, a novel solution for the ICI problem for OFDM communication systems is presented. The use of repeated correlative coding in BPSK OFDM system has been analyzed and compared with ICI self-cancellation scheme [54], correlative coding [55], and normal (un-coded) OFDM system. The proposed scheme enhances the CIR power with 0.45dB by ICI self-cancellation scheme, 16dB by correlative coding scheme, 20dB by normal OFDM system at frequency offset ($\varepsilon = 0.1$) without increasing system complexity, respectively. For $\varepsilon = 0.05$, the BER for both the repeated correlative coding and ICI self-cancellation scheme [54] is comparable. For $\varepsilon = 0.1$, there is a slight increase in the BER for the proposed scheme. This increment widens more for $\varepsilon = 0.15$. However, in all the cases, the bit-error-rate of the proposed scheme is comparable to that of the ICI self-cancellation scheme and is much improved from correlative coding scheme [55]. All the theoretical analysis and simulation results prove that the ICI caused by multicarrier frequency offset can be cancelled efficiently by proposed repeated correlative coding scheme for the OFDM communication system.

\

# CHAPTER – 4

# ERROR-RATE ANALYSIS OF OFDM FOR CORRELATED NAKAGAMI-M FADING CHANNEL BY USING MAXIMAL-RATIO COMBINING DIVERSITY

## 4.1 INTRODUCTION

OFDM is considered as an effective approach for the high-speed wireless multimedia communication systems due to its robustness against the multipath delay spread, feasibility in hardware implementation, flexibility in subcarrier allocation and adaptability in the subcarrier modulation [123,130]. The basic principle of OFDM communication system is to split the high-rate data stream into the number of lower-rate data streams, which are transmitted simultaneously over a number of subcarriers. Unfortunately, the integrity of digital communication in various mobile applications is subject to detrimental effects of multipath fading as an intrinsic characteristic of most wireless channels. Diversity combining is an effective technique for improving the performance of radio communication system in the multipath propagation environment. Therefore, the performance of diversity schemes has recently received considerable research efforts [85-97, 132-147]. The widely used signal processing techniques in diversity systems are the maximal ratio combining (MRC), equal gain combining (EGC) and selection combining (SC). The MRC diversity is always performing better than either SC or EGC because of its optimum combiner.

Moreover, all the branches are weighted by their respective instantaneous signal-to-noise ratios (SNRs) and then co-phased prior to summing in order to insure that all the branches are added in phase for maximum diversity gain. The summed signals are then used as the received signal and connected to the demodulator. The information on all channels is used with this technique to get a more reliable received signal. The study of maximal ratio combining diversity first addressed the case of dual diversity combining with correlated branches and Nakagami-m distributed SNR [133, 134]. The higher diversity orders with independent branches have been discussed in [95, 96]. Aalo et al [98] have been presented the error performance of multi-branch diversity with a special covariance matrix for the diversity branches for pre-detection MRC diversity. The first work on pre-detection MRC diversity with generally

correlated and unbalanced branches was presented by Lombardo et al. [135]. They used a closed-form expression of the multivariate gamma moment generating function (MGF) to derive the average error probability for pre-detection differentially coherent phase shift keying and non-coherent frequency shift keying.

Recently, the effect of correlated fading on the performance of a diversity combining receiver has received a great deal of research interest. In [136, 137], the Rayleigh distribution to model the fading statistics of the channel has been discussed in detail. However, there has been a continued interest in modeling various propagation channels with the Nakagami-m distribution [84], which includes Rayleigh as a special case with unit-fading parameters. It is also a very good approximation for Rice distribution when fading parameter is greater than unity [93]. In the literature, early studies on the performance of a maximal-ratio combiner in the correlated Nakagami fading environment concentrated either on dual-branch diversity [134] or on arbitrary diversity order with simple correlation models. The closed-form expressions for the error probability in Nakagami fading channels with a general branch correlations is discussed in [134], taking into account the average branch signal-to-noise ratio imbalance. Though the results are general for any diversity order and arbitrary branch correlation model, the effect of antenna spacing and the operating environment on BER performance cannot be evaluated by [134], due to the lack of general expression of the spatial cross-correlation coefficient. Currently, it has been recognized that the moment generating function (MGF) is a powerful tools for simplifying the analysis of diversity communication systems, which leads to simple expression to average BER and SER for wide variety of digital signal schemes on fading channels, including multichannel reception with correlated diversity [138]. The performance analysis of switch and stay combining diversity receivers operating over correlated Ricean fading satellite channels has been discussed in [138], where the performance is evaluated based on a bunch of novel analytical formulae for the outage probability, average symbol-error-probability, channel capacity, the amount of fading, and the average output SNR obtained in infinite series form. The similar performance analysis of the switched diversity receivers operating over the correlated Weibull fading channels in terms of outage probability, average symbol-error probability, moments, and MGF can be found in [139]. Bandjur et al [96] have studied the

performance of a dual-branch switch and stay combining diversity receiver with the switching decision based on signal-to-interference ratio operating over correlated Ricean fading channels in the presence of correlated Nakagami-*m* distributed co-channel interference. Earlier work presented in [140-143] has assumed that the frequency domain channel response samples are also the Nakagami-*m* distributed with the same fading parameters as the time domain channel. Kang et al [144] have shown that the magnitude of the frequency responses is well approximated by the Nakagami-*m* random variables with new parameters by considering only dual diversity at the receiver. Rui et al [97] have considered the diversity at transmitter and receiver both without correlation between them but when antennas are closely spaced then signal are correlated. Du et al [145,146] have analyzed the performance of OFDM system over frequency selective channel but they have not discussed the effect of correlation on the performance of OFDM system.

In this chapter, we have presented a novel method for the BER, SER and outage probability analysis of the correlated Nakagami-*m* fading channel by using MRC diversity. We consider the MRC diversity ($M \geq 2$) at the receiver and analyzed the OFDM performance for various modulation schemes. The performance of the communication system is much better than [144] and for M = 2 proposed result is similar with that of [144].

## 4.2 ANALYSIS

In this Section, we briefly summarize the OFDM transceiver and channel model for the wireless communication systems. A simplified schematic of the proposed OFDM transceiver is shown in Figure 1.4 [123].

### 4.2.1 BER ANALYSIS

Let $S_i(k)$ is the $k^{th}$ OFDM data block, which has to be transmitted with *N* subcarriers. The incoming serial bits are converted into parallel streams by using the serial-to-parallel converter block. There after these parallel streams are subjected to the inverse fast Fourier transform (IFFT) as shown in Figure 1.4. The IFFT block is used to modulate the input signal and after modulation, the signal can be represented as:

$$x_i(n) = \frac{1}{\sqrt{N}} \sum_{k=0}^{N-1} S_i(k) e^{j2\pi k/N}$$

(4.1)

$n = 0, 1, 2 \ldots \ldots \ldots N\text{-}1$

The cyclic prefix is inserted after the IFFT modulation, which will be removed before demodulation at the OFDM receiver. The resultant signal is up converted to RF before transmission and the receiver end it is down converted. The received signal after removal of the cyclic prefix is demodulated by using the FFT. The output of FFT is represented as:

$$R_i(k) = \frac{1}{\sqrt{N}} \sum_{n=0}^{N-1} r_i(n) e^{-j2\pi k/N} = H_i(k) S_i(k) + W_k$$

(4.2)

$k = 0, 1 \ldots N\text{-}1$

where $r_i(n)$ is received signal at the receiver. $W_k$ is an additive complex Gaussian noise with zero mean and $H_i(k)$ is frequency domain channel impulse response expressed as:

$$H_i(k) = \frac{1}{\sqrt{N}} \sum_{n=0}^{N-1} h_i(n) e^{-j2\pi k/N} = \frac{1}{\sqrt{N}} \left( e^H h_i(n) \right)$$

(4.3)

In the Equation (4.3), the $h_i(n)$ is the Nakagami-$m$ distributed random variable and

$$e = \left(1, \exp\left(-j2\pi n/N\right), ----, \exp\left(-j2\pi n(N-1)/N\right)\right)^T$$

where $T$ is the transpose of matrix. We consider that the average power signal as well as fading parameters in each $M$ channels of a maximal ratio combiner system is identical. The assumption of identical power is reasonable if the diversity channels are closely spaced and the gain of each channel is such that all noise power is equal [147]. The signal to noise ratio at the output of maximal ratio combining diversity is given by [148]:

$$\gamma_t = \frac{E_S}{\sigma^2} \sum_{i=1}^{M} |H_i|^2 = \frac{E_S}{\sigma^2} \sum_{i=1}^{M} (H_i)(H_i)^H = \sum_{i=1}^{M} \gamma_i$$

(4.4)

where $E_s$ is the symbol energy and $\sigma^2$ is the variance of zero mean complex mean Gaussian noise. When receiving antennas are closely spaced then receiving signal are also correlated then SNR of received signal $\gamma_1, \gamma_2 \ldots \gamma_M$ cannot be considered as independent random variable. The correlation coefficient between two receiving antenna are (by assuming equal correlation between antennas $\rho$ ) as given in [144].

$$\rho = E(h_i(k)h_j(k)) \Big/ \sqrt{E(h_i(k)h^*_i(k))\,E(h_j(k)h^*_j(k))}$$

The probability density function of $\gamma_t$ is given as [98].

$$P_\gamma(\gamma_t) = \frac{\left(\dfrac{\gamma_t\,m}{\overline{\gamma}_t}\right)^{M\,m-1} \exp\!\left(\dfrac{-\gamma_t m}{\overline{\gamma}_t\,(1-\rho)}\right)\,{}_1F_1\!\left(m,Mm,\dfrac{M\,m\,\rho\,\gamma_t}{\overline{\gamma}_t(1-\rho)(1-\rho+M\rho)}\right)}{\left(\dfrac{\overline{\gamma}_t}{m}\right)(1-\rho)^{m(M-1)}\,(1-\rho+M\rho)^m\,\Gamma(M\,m)}$$

(4.5)

where $m$ is fading parameter as defined in [144-146]. If $m \geq 1/2$, represent severity. The smaller value of the $m$ represent more fading in the channel and ${}_1F_1(\bullet)$ confluent hyper geometric function as discussed in [149]. On the other hand, recent advances on performance analysis of digital communication systems in fading channel has recognized the potential importance of the moment generating function (MGF) as a powerful tool for simplifying the analysis of diversity communication systems. This has led to simple expressions to average bit-error-rate and symbol-error-rate for variety of digital signaling schemes on fading channels, including multichannel reception with correlated diversity. The MGF is one of most important characteristics of any distribution function because it helps in the BER performance evaluation of the wireless communication systems. The MGF is defined as [150, 151]:

$$\psi(s) = \int\limits_0^\infty \exp(-s\gamma)\,P_\gamma(\gamma_t)\,d\gamma$$

(4.6)

The MGF given in Equation (4.6) is a versatile closed form measure, which can be used for the performance evaluation of various modulation schemes. It is also usable for both pre-detection and post-detection combining with varying ease of use. By substituting Equation (4.5) in (4.6) and by using the Equation [7.621.5] from [149], the MGF of Equation (4.5) is as follows.

$$\psi(s) = \left(1 - \frac{\overline{\gamma}_t(1-\rho+M\rho)\,s}{m}\right)^{-m}\left(1 - \frac{\overline{\gamma}_t(1-\rho)\,s}{m}\right)^{-m(M-1)}$$

(4.7)

If two independent diversity combiners are considered at receiver (M = 2), then

$$\psi(s) = \left(1 - \frac{\overline{\gamma}_t(1+\rho)\,s}{m}\right)^{-m}\left(1 - \frac{\overline{\gamma}_t(1-\rho)\,s}{m}\right)^{-m}$$

(4.8)

The Equation (4.8) is similar with Equation (9) of [144]. The conditional probability error function for coherent binary phase-shift keying (BPSK) and for coherent orthogonal binary frequency-shift keying (BFSK) is given by [151]:

$$P_e(\gamma_t) = Q\left(\sqrt{2\,g\gamma_t}\right)$$

(4.9)

where $g = 1/2$ for BFSK and $g = 1$ for BPSK and $g = 0.715$ for coherent BFSK with minimum correlation [150, 151], $Q(\bullet)$ is Gaussian $Q$ function defined by:

$$Q(x) = \left(1/\sqrt{2\pi}\right)\int_x^\infty \exp\left(-t^2/2\right) dt$$

(4.10)

The average bit error rate can be expressed as [151]:

$$\overline{P}_b = \int_0^\infty P_e(\gamma_t)\, p_e(\gamma_t)\, d\gamma_t$$

(4.11)

By putting the value of $P_e(\gamma_t)$ from Equation (4.9) to (4.11), we get:

$$\overline{P}_b = \int_0^\infty Q\left(\sqrt{2g}\,\gamma_t\right) p_e(\gamma_t)\, d\gamma_t$$

(4.12)

Another form to represent the Gaussian $Q$ function is:

$$Q(x) = \frac{1}{\pi}\int_0^{\frac{\pi}{2}} \exp(-x^2/2\sin^2\theta)\, d\theta$$

(4.13)

By putting the value $Q(x)$ in Equation (4.11), we get:

$$\overline{P}_b = \frac{1}{\pi}\int_0^\infty \int_0^{\frac{\pi}{2}} \exp(-g\gamma_t/\sin^2\theta)\, d\theta\, p_e(\gamma_t)\, d\gamma_t$$

$$\overline{P}_b = \frac{1}{\pi}\int_0^{\frac{\pi}{2}} \psi\left(-\frac{g}{\sin^2\theta}\right) d\theta$$

(4.14)

where

$$\psi(s) = E\left[e^{s\gamma_t}\right] = \int_0^\infty e^{s\gamma_t}\, p_e(\gamma_t)\, d\gamma_t$$

(4.14)

From Equation (4.15) and (4.7), we get:

$$\overline{P}_b = \frac{1}{\pi} \int_0^{\frac{\pi}{2}} \left(1 + \frac{\overline{\gamma}_t(1-\rho+M\rho)}{m}\frac{g}{sin^2\theta}\right)^{-m} \left(1 + \frac{\overline{\gamma}_t(1-\rho)}{m}\frac{g}{sin^2\theta}\right)^{-m(M-1)} d\theta \qquad (4.16)$$

By putting $t = cos^2(\theta)$ and after some mathematical manipulation, Equation (4.16) can be expressed as:

$$\overline{P}_b = \frac{\psi(-g)}{2\pi} \int_0^1 \left(1 - \frac{t}{1+\left(\frac{\overline{\gamma}_t(1-\rho+M\rho)g}{m}\right)}\right)^{-m} \left(1 - \frac{t}{1+\left(\frac{\overline{\gamma}_t(1-\rho)g}{m}\right)}\right)^{-m(M-1)} (1-t)^{mM-\frac{1}{2}} t^{-\frac{1}{2}} dt$$

$$(4.17)$$

From [149], the Equation (4.17) can be expressed as:

$$\overline{P}_b = \frac{\psi(-g)}{2\pi} \frac{\Gamma(1/2)\Gamma(mM+1/2)}{\Gamma(mM+1)} F_1\left(\frac{1}{2}, m, m(M-1), mM+1, \frac{1}{1+A}, \frac{1}{1+B}\right) \qquad (4.18)$$

where $F_1(\bullet)$ Appell hyper geometric function as given in [152],

$$A = \frac{\overline{\gamma}_t(1-\rho+M\rho)}{m},$$

$$B = \frac{\overline{\gamma}_t(1-\rho)g}{m}$$

$\overline{\gamma}_t$ = Signal to noise ratio and $\Gamma(\bullet)$ = is the Gamma function as given [149]. The total average BER of multiple received antenna OFDM system can be expressed as:

$$P_{etotal} = 1-(1-\overline{P}_b)^N \qquad (4.19)$$

## 4.2.2 SER ANALYSIS

The average SER for coherent square $M$-QAM signals is given by [151]:

$$\overline{P}_{QAM} = \frac{4q}{\pi}\underbrace{\int_0^{\pi/2}\psi\left(-\frac{g}{sin^2\theta}\right)d\theta}_{I_1} - \frac{4q^2}{\pi}\underbrace{\int_0^{\pi/4}\psi\left(-\frac{g}{sin^2\theta}\right)d\theta}_{I_2} \qquad (4.20)$$

where $q = 1-1/\sqrt{P}$, $g = 3/(2(P-1))$ and constellation size is given by $P = 2^v$ with $v$ is even number. The integral $I_1$ and $I_2$ are solved separately, by putting $s = -g/sin^2\theta$ in Equation (4.7). The Integrals $I_1$ and $I_2$ can be written as:

$$I_1 = \frac{1}{\pi} \int_0^{\frac{\pi}{2}} \psi\left(-\frac{g}{sin^2\theta}\right) d\theta \qquad (4.21)$$

and

$$I_2 = \frac{1}{\pi} \int_0^{\frac{\pi}{4}} \psi\left(-\frac{g}{sin^2\theta}\right) d\theta \qquad (4.22)$$

After some mathematical manipulation by using [149], the Equation (4.21) can be expressed as:

$$I_1 = \frac{\psi(-g)}{2\pi} \frac{\Gamma(1/2)\Gamma(mM+1/2)}{\Gamma(mM+1)} F_1\left(\frac{1}{2}, m, m(M-1), mM+1, \frac{1}{1+A}, \frac{1}{1+B}\right) \qquad (4.23)$$

$$I_2 = \frac{1}{\pi}(A)^{-m}(B)^{-m(M-1)} 2^{-(mM+1/2)} F_1\left(mM+1/2, m, m(M-1), mM+1, -\frac{1}{2A}, -\frac{1}{2B}\right) \qquad (4.24)$$

By putting $I_1$ and $I_2$ in the Equation (4.20), then the resultant average SER is:

$$\overline{P}_{QAM} = 2q \frac{\psi(-g)}{\pi} \frac{\Gamma(1/2)\Gamma(mM+1/2)}{\Gamma(mM+1)} F_1\left(\frac{1}{2}, m, m(M-1), mM+1, \frac{1}{1+A}, \frac{1}{1+B}\right)$$
$$- \frac{4q^2}{\pi}(A)^{-m}(B)^{-m(M-1)} 2^{-(mM+1/2)} F_1\left(mM+1/2, m, m(M-1), mM+1, -\frac{1}{2A}, -\frac{1}{2B}\right) \qquad (4.25)$$

The total average SER of multiple received antenna OFDM system can be expressed as:

$$P_{etotalQAM} = 1 - (1 - \overline{P}_{QAM})^N \qquad (4.26)$$

Depending on the particular application, the error probability can be bit-error rate or symbol error rate and if is consistent with the conditional error probability.

### 4.2.3 OUTAGE PROBABILITY

The outage probability is an important performance parameter that measures the probability that the instantaneous SNR falls below a specified threshold. In a fading radio channel, it is likely that a transmitted signal will be suffer deep fade that can lead a complete loss of the signal or outage of the signal. Outage probability is another standard performance criterion of the communication systems operating over fading channels. It is measure of the quality of the transmission in a mobile radio channel and defined as the probability that the instantaneous error rate exceeds a

specified value or equivalently that the (instantaneous) combined signal-to-noise ratio (SNR) falls below a certain specified threshold, $\gamma_0$ [22]. Hence, the outage probability,

$$P_{out} = \int_0^{\gamma_0} P_\gamma(\gamma_t) d\gamma_t \qquad (4.27)$$

By using Equation (4.5), we can evaluate the equation (4.27) as follows:

$$P_{out} = \int_0^{\gamma_0} \frac{\left(\dfrac{\gamma_t m}{\overline{\gamma}_t}\right)^{Mm-1} \exp\left(\dfrac{-\gamma_t m}{\overline{\gamma}_t(1-\rho)}\right) {}_1F_1\left(m, Mm, \dfrac{Mm\rho\gamma_t}{\overline{\gamma}_t(1-\rho)(1-\rho+M\rho)}\right)}{\left(\dfrac{\overline{\gamma}_t}{m}\right)(1-\rho)^{m(M-1)}(1-\rho+M\rho)^m \Gamma(Mm)} d\gamma_t \qquad (4.28)$$

By expanding ${}_1F_1(.)$ from the [149] and after some mathematical manipulation, the Equation (4.27) can be expressed as:

$$P_{out} = \sum_{k=0}^{\infty} C \frac{\Gamma(m+k)\,\Gamma(mM)}{\Gamma(m)\,\Gamma(mM+k)} \frac{(D)^k}{k!} I_3 \qquad (4.29)$$

where

$$C = \left(\frac{m}{\overline{\gamma}_t}\right)^{Mm} \frac{1}{(1-\rho)^{m(M-1)}(1-\rho+M\rho)^m \Gamma(Mm)}, \quad D = \frac{Mm\rho}{\overline{\gamma}_t(1-\rho)(1-\rho+M\rho)},$$

$$E = \frac{m}{\overline{\gamma}_t(1-\rho)} \quad \text{and}$$

$$I_3 = \int_0^{\gamma_0} (\gamma_t)^{mM+k-1} \exp(-E\gamma_t) d\gamma_t \qquad (4.30)$$

By expressing $\exp(-E\gamma_t) = G_{0\ \ 1}^{1\ \ 0}\left(E\gamma_t \Big|\begin{matrix}-\\0\end{matrix}\right)$ from [27] and again from [27], the Equation (4.30) can be expressed as:

$$I_3 = (\gamma_0)^{mM+k} G_{1\ \ 2}^{1\ \ 1}\left(E\gamma_0 \Big|\begin{matrix}1-(Mm+k)\\0 \quad -(Mm+k)\end{matrix}\right) \qquad (4.31)$$

By putting $I_3$ in the Equation (4.29), the outage probability ($P_{out}$) can be expressed as:

$$P_{out} = \sum_{k=0}^{\infty} C \frac{\Gamma(m+k)\,\Gamma(mM)}{\Gamma(m)\,\Gamma(mM+k)} \frac{(D)^k}{k!} (\gamma_0)^{mM+k} G_{1\ \ 2}^{1\ \ 1}\left(E\gamma_0 \Big|\begin{matrix}1-(Mm+k)\\0 \quad -(Mm+k)\end{matrix}\right) \qquad (4.32)$$

The expressions involve the Meijer G-function, which, although easy to evaluate by using the modern mathematical packages such as Mathematica and Maple.

## 4.3 RESULTS AND DISCUSSION

In general, it is well known that the performance of any communication system in terms of the bit-error-rate, symbol-error-rate, and signal outage probability is depending on the statistics of the signal-to-noise ratio (SNR). The bit-error-rate is an important property for all the digital communication systems, which provides a base line for the amount of information transferred and the design depends heavily on type of channel and type of modulation.



**Figure 4.1** The average BER performance of the BPSK OFDM system over correlated Nakagami-m fading for various values of the fading parameter.

The bit-error-rate computations depend fundamentally on the signal-to-noise ratio at the receiver. In this chapter, the bit-error-rate performance of the OFDM with received diversity over correlated Nakagami-$m$ fading channel is analyzed and simulated. When the antennas are closely spaced, the received signals are correlated. Figure 4.1 depicts the total average bit-error-rate characteristics with average signal-to-noise ratio for various values of the arbitrary fading parameter.
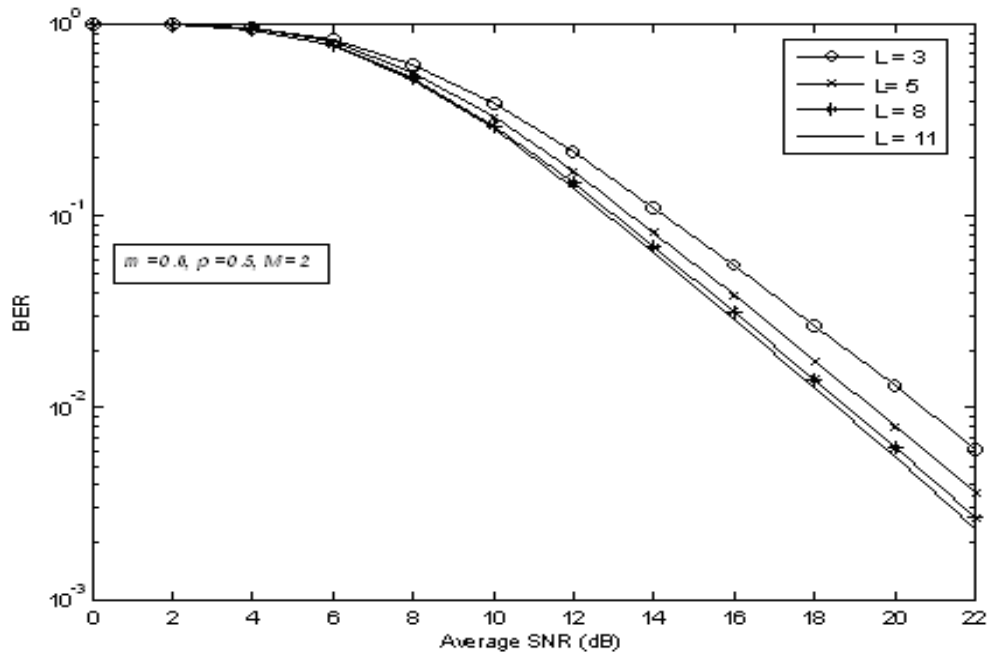
**Figure 4.2** The average BER performance of the BPSK OFDM system over correlated Nakagami-m fading for different values of the channel length.

As the value of fading parameter increases, the bit-error-rate performance of the BPSK OFDM system is improved for a given value of the SNR. The bit-error-rate performance of the system also improves with the increase of SNR after a certain value and this improvement is much better with the increase of the fading parameters. Figure 4.2 shows the effect of channel length [145-146] on the average BER performance, which is improved with the increase of the channel length for a given value of SNR and other system parameters but it is not much effective in comparison with the fading parameter. Figure 4.3 depicts the effect of diversity of receiver on the average bit-error-rate performance of the OFDM system. As the diversity receiver is increased, the average bit-error-rate performance of the OFDM system is improved significantly. Figure 4.4 shows the effect of correlation coefficients on the bit-error-rate performance of OFDM system, as correlation coefficient increases bit-error-rate performance of OFDM system decreases. Figure 4.5 shows the compression of the average bit-error-rate performance of the proposed OFDM system with Kang et al [144]. The moment generating function as given by the Equation (4.6) at the value of diversity receiver (M = 2) is same as that of the Kang et al [144].
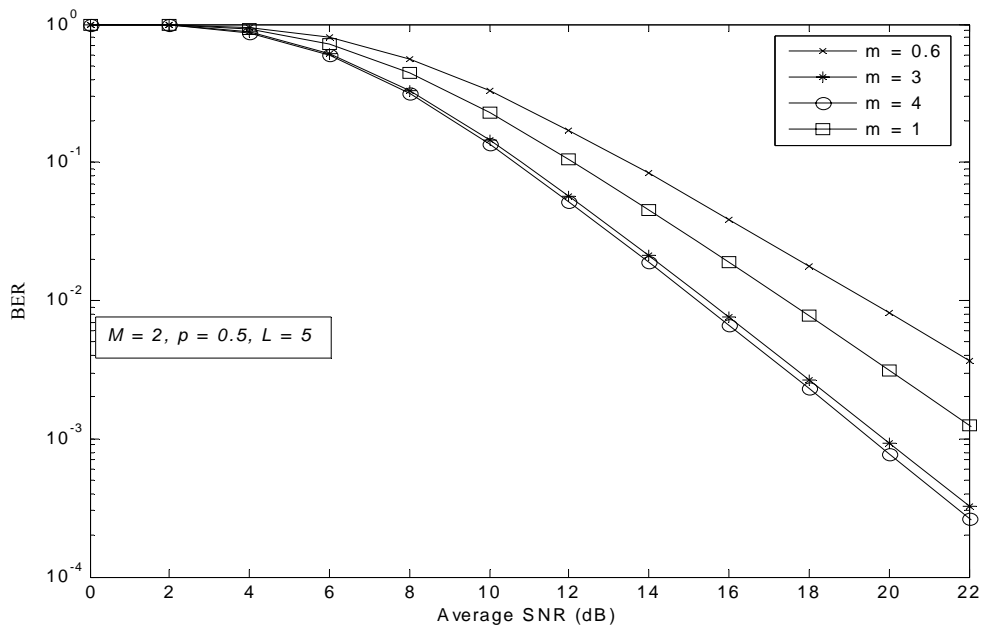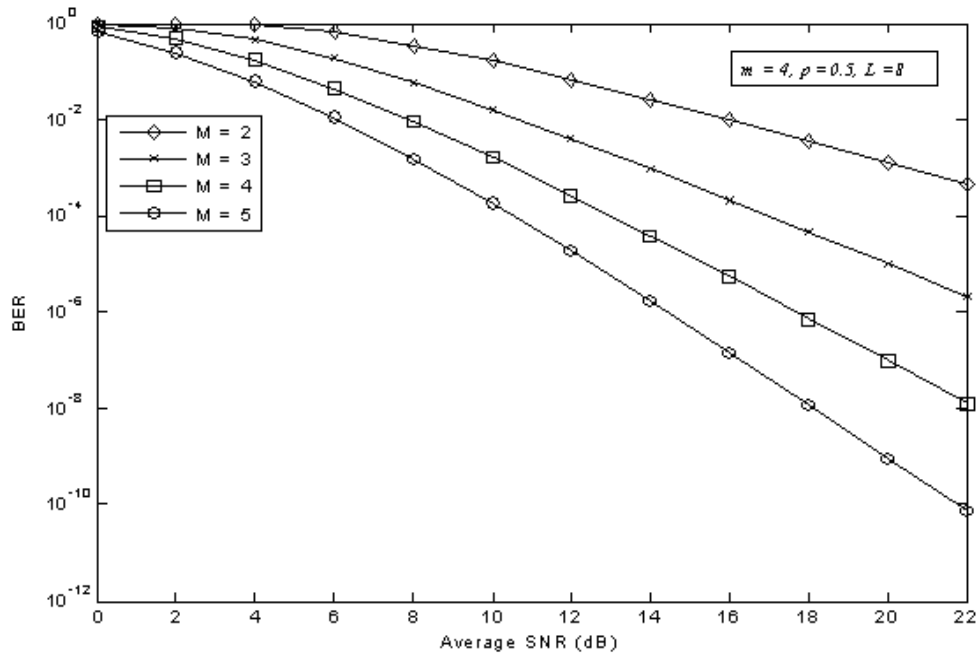
**Figure 4.3** The average BER performance of the BPSK OFDM system over correlated Nakagami-m fading for various values of the diversity receivers.

Thus, Equation (4.7) is a general expression for the moment generating function whereas the Kang et al [144] moment generating function is valid only for M = 2. As the value of receiver diversity is increases the average bit-error-rate performance of proposed method is improved significantly. Figure 4.6 shows the symbol-error-rate (SER) probability of MRC over the correlated Nakagami fading channel with 4-QAM modulation for different correlation parameter. At $\rho$ = 1 SER approaches $10^{-1}$ for 20dB SNR and $\rho$ = 0 SER approaches $10^{-3}$ for 20 dB SNR. As correlation increases SER performance of system is decreased. Figure 4.7 shows SER probability of MRC over the correlated Nakagami fading channel with 4-QAM modulation for different number combined M, the Nakagami fading parameter for $m$ = 4 and correlation coefficient $\rho$ = 0.5 for analysis. SER performance is improved as no diversity path is increased. Figure 4.8 shows the outage probability and average SNR plot for M = 4 and M = 6 at $\gamma_0$ = 10 dB. From figure it is clear that as M increases, outage probability improves significantly. Figure 4.9 and Figure 4.10 show the effect of correlation coefficient and the Nakagami fading parameter, on the outage probability for various values of the diversity.
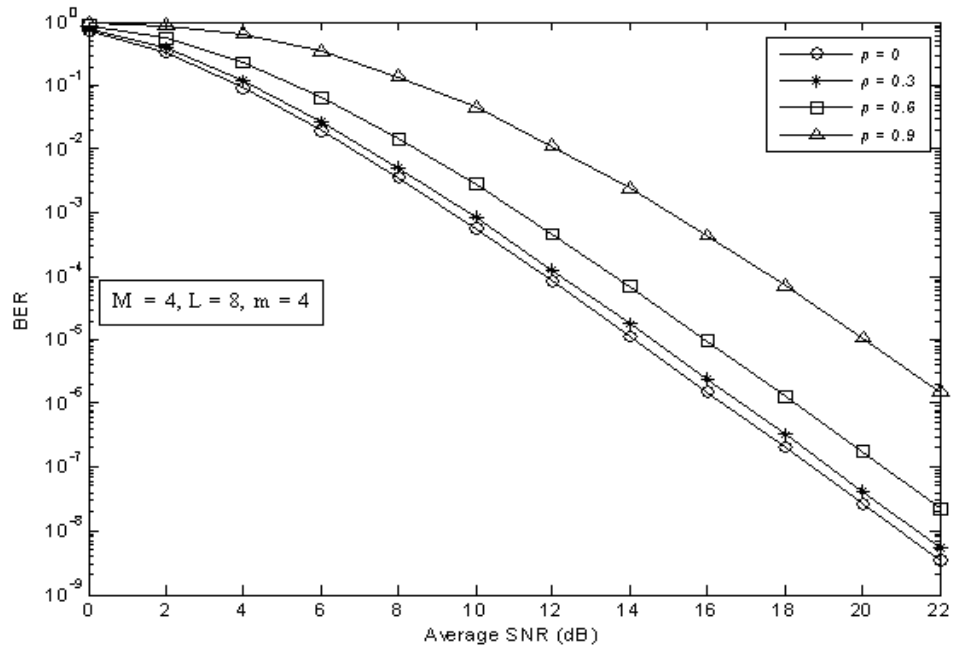
**Figure 4.4** The average BER performance of the BPSK OFDM system over correlated Nakagami-m fading for the various values of correlation coefficients.
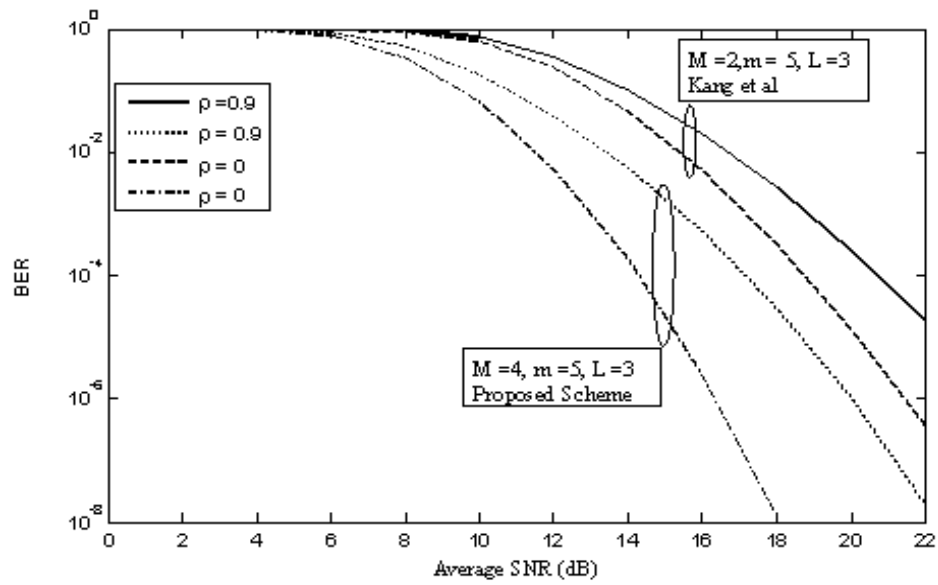


**Figure 4.5** The BER compression of the proposed BPSK OFDM system with Kang et.al [144] scheme.
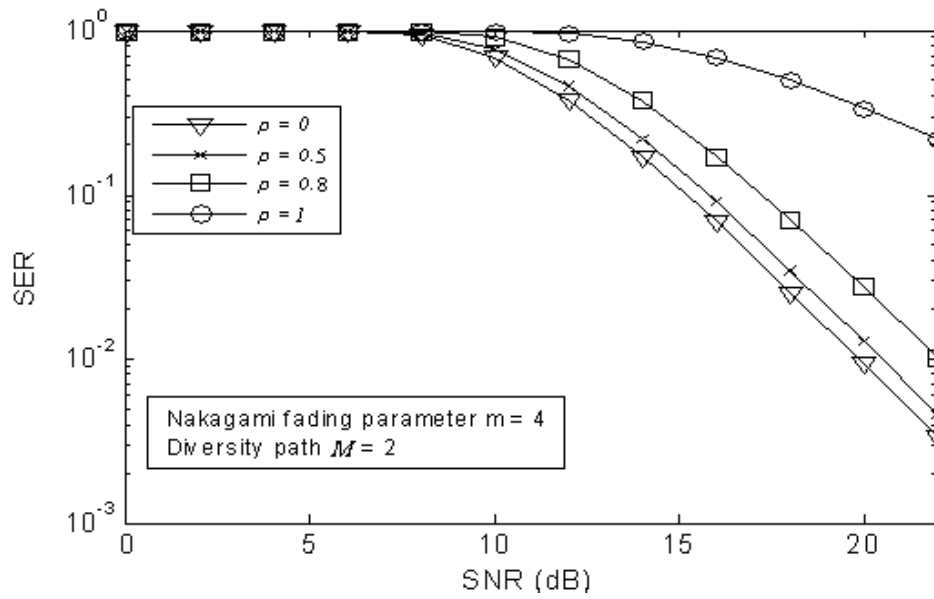
**Figure 4.6** The SER of MRC over correlated Nakagami-*m* fading for 4-QAM OFDM system with several correlation coefficients.
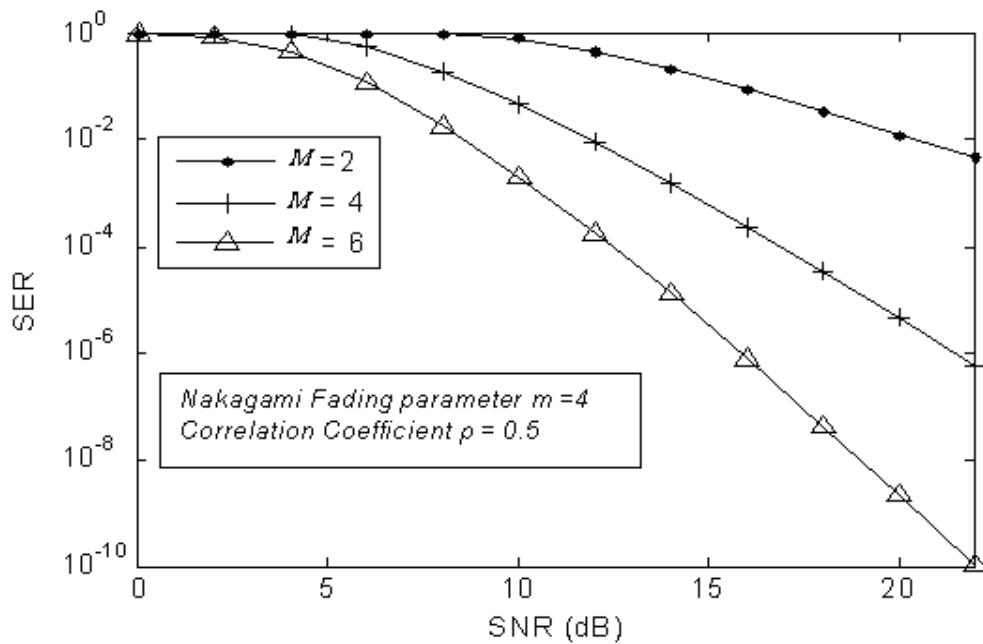


**Figure 4.7** The SER of MRC over correlated Nakagami-*m* fading for 4-QAM OFDM system for the various combined paths.

Form Figure 4.9 and Figure 4.10, it is clear that as the correlation coefficient increases, the outage probability decreases and it improves as fading parameter increases. In general, low correlation the infinite series converges quickly, and the truncation error is small.
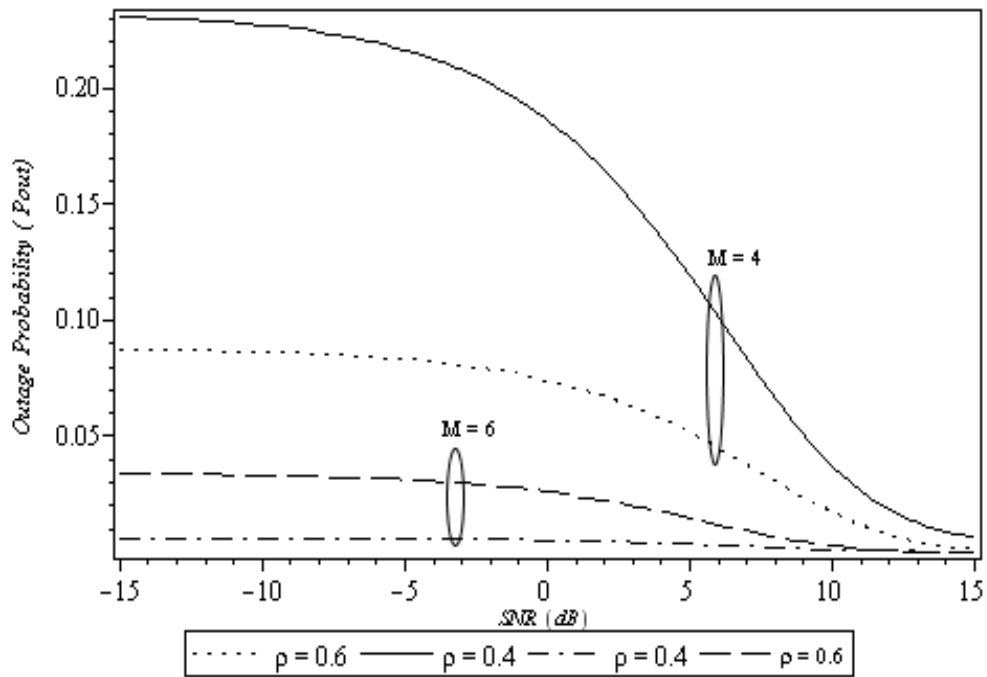
**Figure 4.8** The outage probability versus average SNR for the several values of correlation coefficients.
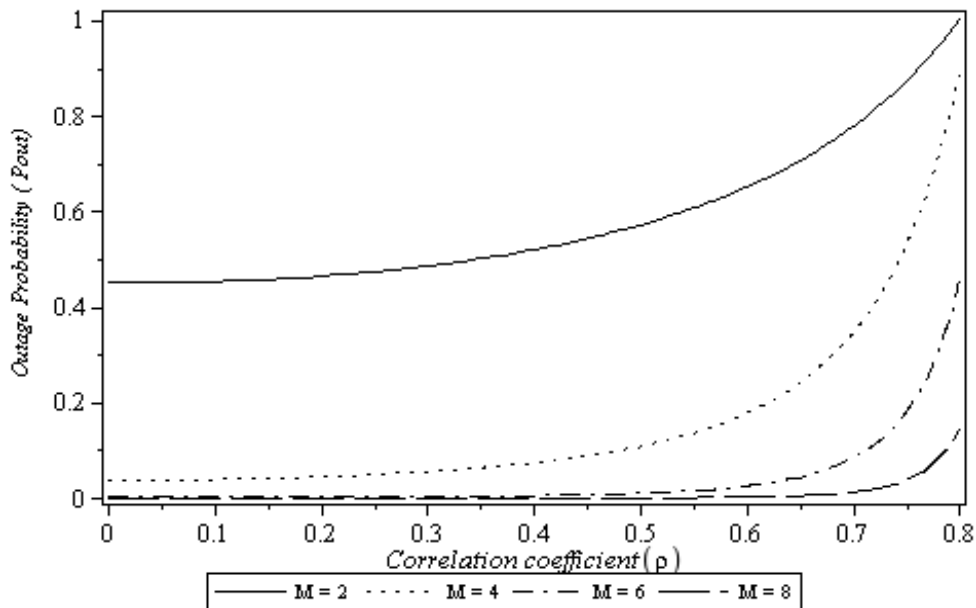


**Figure 4.9** The outage probability versus correlation coefficient for the various values of diversity.

The Nakagami fading parameters fading parameter determines the severity of fading channels. Two special values of $m$ are of particular interest. In the case of $m = 1$, the sum of independent zero-mean complex Gaussian random variables provide a zero-mean complex Gaussian random variables with its envelop following a Rayleigh

distribution exactly and thus the Nakagami-m fading specializes to the Reyleigh fading. In the limiting case, when $m = 0$, the Nakagami-m fading channel approaches a static channel.
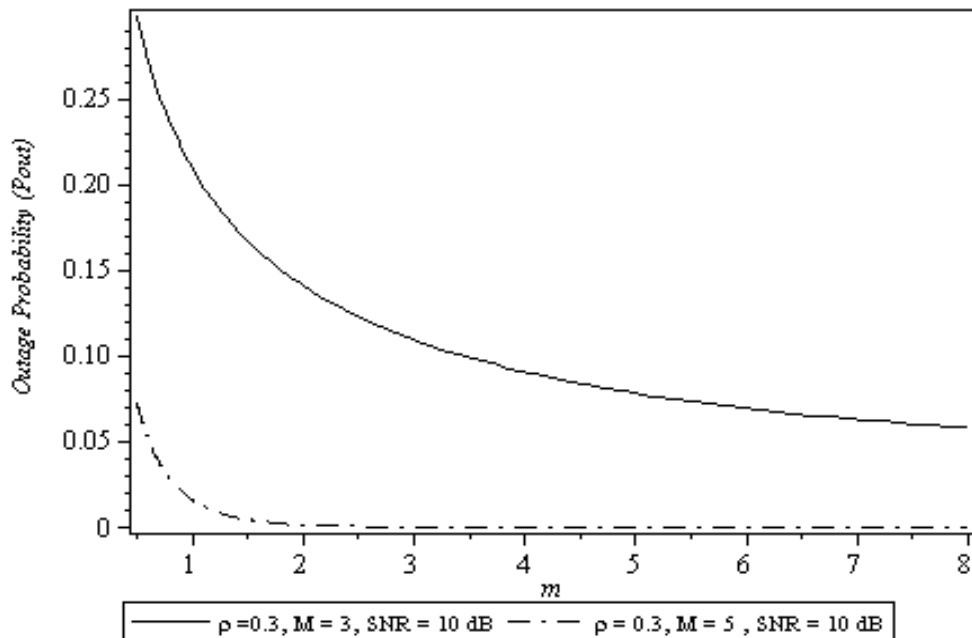


**Figure 4.10** Characteristics of the outage probability versus Nakagami-*m* fading parameter for the diversity at the receiver is M = 3 and M = 5.

## 4.4 CONCLUSION

In this Chapter, we have investigated the MGF based approach for the average bit-error-rate, symbol-error-rate and outage probability performance analysis of the OFDM communication system over the correlated Nakagami-*m* fading channel by using the maximal ratio combining diversity at the receiver. In this proposed method, a closed-form mathematical expression for the average BER for BPSK and SER for *M*-QAM is derived. In this analysis, we have considered the diversity path (M ≥ 2) greater than two at the receiver hence the average BER performance of the OFDM system is improved significantly. Moreover, we have also derived a mathematical expression for the outage probability. The proposed mathematical analysis is used to study various novel performance evaluation results with parameters of interest such as fading severity and correlation coefficients, which is very significant for the design consideration of the OFDM communication systems.

# A MARGINAL MGF BASED ANALYSIS OF CHANNEL CAPACITY OVER CORRELATED NAKAGAMI-M FADING WITH MAXIMAL-RATIO COMBINING DIVERSITY

## 5.1 INTRDUCTION

Recently, OFDM is considered as an effective approach for the high-speed wireless multimedia communication systems due to its robustness against the multipath delay spread, feasibility in hardware implementation, flexibility in subcarrier allocation and adaptability in the subcarrier modulation [2]. Unfortunately, the integrity of digital communication in various mobile applications is subject to detrimental effects of multipath fading as an intrinsic characteristic of the most wireless channels. The growing demand for wireless communication makes it important to determine the capacity limits of the underlying channels for the communication systems. In 1948, Shannon has provided a mathematical theory of communication underlying channel capacity. He defined that channel capacity is the maximum data rates that can be transmitted over wireless channels with small error probability, assuming no constraints on delay or complexity of the encoder and decoder. In the wireless communication systems, fading is an important phenomenon, as discussed in previous chapter. In this chapter, we have discussed the effect of multipath fading on the channel capacity.
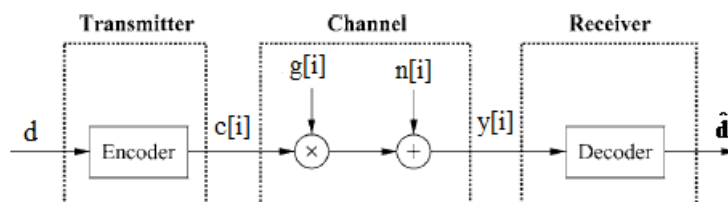


**Figure 5.1** System model for flat fading channel.

The system model for the flat fading is shown in Figure 5.1, where $d$ is an input signal that is sent from transmitter to receiver, $\hat{d}$ is an estimated signal of transmitted

signal *d.* If the transmitted message is coded into code word *c* and transmitted over time varying channel as c[i] at any time i. The channel gain g[i] is also called as channel side information (CSI), which changes during transmission of code word [30]. The channel capacity of any channel depends on that is known about g[i] at the transmitter and receiver [30]. On the basis of channel knowledge, three different scenarios are discussed below.

1. **Channel distribution information (CDI):** The distribution of g[i] is known to the transmitter and receiver.

2. **Receiver CSI:** The value of g[i] is known to the receiver at time *i*, and both the transmitter and receiver know the distribution of g[i].

3**. Transmitter and receiver CSI:** The value of g[i] is known to the transmitter and receiver.

In this Chapter mainly, three type of the channel capacity is discussed on the basis of channel side information at the transmitter and receiver. In general, the channel capacity in fading channel is a complex expression in terms of the channel variation in time and/or frequency depending also upon the transmitter and/or receiver knowledge of the channel side information. For the various channel side information assumptions that have been proposed, several definitions of the channel capacity have been provided. These definitions depend on the different employed power and rate adaptation policies and the existence, or not, an outage probability [22]. Earlier, the capacity has been studied by various researchers for several fading environment [104-116,153]. Goldsmith and Varaiya [104] have examined the channel capacity of the Rayleigh fading channels under different adaptive transmission techniques. Lee [105] has derived an expression for the channel capacity of a Rayleigh fading channel. Gunther [106] has extended the results presented in [105] by deriving the channel capacity of Rayleigh fading channels under diversity scheme. In [107], Alouini and Goldsmith have derived the channel capacity of Rayleigh fading channels under different diversity schemes and different rate adaptation and transmit power schemes. Other fading channels like Nakagami, Weibull, Rician, and Hoyt fading channels were studied in [108-109]. Khatalin and Fonseka [110] have been discussed the channel capacity for correlated Nakagami-m fading channel by using the dual diversity. In [111], the characteristics function (CF) is developed for computing the

ergodic channel capacity. In [153], the channel capacity under different diversity schemes and different rate adaptation and transmit power schemes for the correlated Rayleigh have been derived. In [112-115], the moment generating function based (MGF) approach is proposed for computation of channel capacity only for $C_{ora}$ scheme, by using the numerical techniques. In [116] a novel MGF based approach is developed for evaluation of channel capacity various rate adaptation and transmit power. In [116] the integral is evaluated by using mainly two type of numerical technique and both the numerical techniques are lengthy and much more complex. In [154] the channel capacity limit for fading channel is discussed.

In this Chapter, we have presented a marginal moment generating (MMGF) based channel capacity analysis over correlated Nakagami-m fading channel with M-branch maximal-ratio combining (MRC) diversity. This chapter consists of the evaluation the MMGF function and the derived MMGF function is used to evaluate a closed-form expression for the channel capacity under optimal rate adaptation $(C_{ORA})$, channel capacity with optimal simultaneous power and rate adaptation $(C_{OPRA})$, channel inversion with fixed rate $(C_{CIFR})$ and truncated CIFR is approach $(C_{TCIFR})$. The results obtained for these channel capacities are discussed in the terms of well known Meijer G function and other special functions, which can be easily implemented by using Maple or Mathematica software.

## 5.2. SYSTEM MODEL

We have considered the average power signal as well as fading parameters in each M-channels of a MRC system that is identical. The assumption of identical power is reasonable if the diversity channels are closely spaced and the gain of each channel is such that all the noise power is equal [148]. The signal-to-noise ratio at the output of MRC diversity is given by [148]. When receiving antennas are closely spaced then receiving signal are also correlated and SNR of received signal $\gamma_1, \gamma_2 \dots \gamma_M$ cannot be considered as independent random variable. The probability density function of $\gamma_t$ for correlated Nakagami-m fading as given by Equation (4.5) is:

$$P_\gamma(\gamma_t) = \frac{A}{D} e^{-B\gamma_t} {}_1F_1\big(m, Mm, C\gamma_t\big)(\gamma_t)^{Mm-1} \tag{5.1}$$

$$A = \left(\frac{m}{\bar{\gamma}_t}\right)^{Mm}, B = \frac{m}{\bar{\gamma}_t(1-\rho)}, C = \frac{M\,m\,\rho}{\bar{\gamma}_t(1-\rho)(1-\rho+M\rho)} \text{ and}$$

$$D = (1-\rho)^{m(M-1)}\big(1-\rho+M\rho\big)^m \Gamma(M\,m)$$

## 5.3 MARGINAL MOMENT EVALUATION

In this Section, MMGF is evaluated of the SNR of M-branch MRC diversity and further, it is used for the computation of channel capacity. The MMGF is defined as [155]:

$$\hat{M}(s,a) = \int_a^\infty e^{-s\gamma} f_\gamma(\gamma)\,d\gamma \tag{5.2}$$

By substituting the value of $f_\gamma(\gamma)$ from the Equation (5.1) in Equation (5.2), we get:

$$\hat{M}(s,a) = \frac{A}{D} \int_{\gamma_\circ}^\infty (\gamma_t)^{Mm-1} e^{-B\gamma_t} {}_1F_1\big(m, Mm, C\gamma_t\big) e^{-s\gamma_t}\,d\gamma_t \tag{5.3}$$

By expanding ${}_1F_1(\bullet)$ from [149 Equation (9.14.1)] and putting in Equation (5.3), we get:

$$\hat{M}(s,a) = \frac{A}{D} \sum_{k=0}^\infty \frac{\Gamma(k+m)\Gamma(Mm)}{\Gamma(m)\Gamma(k+Mm)} \frac{(C)^k}{k!} I_1 \tag{5.4}$$

where

$$I_1 = \int_a^\infty (\gamma_t)^{k+Mm-1} e^{-(s+B)\gamma_t}\,d\gamma_t \tag{5.5}$$

From [149 Equation (3.381.3)], the Equation (5.5) can be written as:

$$I_1 = (B+s)^{-(k+MM)} \Gamma(k+mM, a(B+s)) \tag{5.6}$$

By putting the result of $I_1$ from Equation (5.5) to Equation (5.4), we get:

$$\hat{M}(s,a) = \frac{A}{D} \sum_{k=0}^\infty \frac{\Gamma(k+m)\Gamma(Mm)}{\Gamma(m)\Gamma(k+Mm)} \frac{(C)^k}{k!} \frac{\Gamma(k+mM, a(B+s))}{(B+s)^{(k+mM)}} \tag{5.7}$$

By putting $a = 0$ in Equation (5.7), the marginal MGF changs to moment generating function(MGF) as:

$$M(s) = \frac{A}{D} \sum_{k=0}^{\infty} \frac{\Gamma(k+m)\Gamma(Mm)}{\Gamma(m)\Gamma(k+Mm)} \frac{(C)^k}{k!} \frac{\Gamma(k+mM,0)}{(B+s)^{(k+mM)}}$$

$$= \frac{A}{D} \frac{\Gamma(Mm)}{(B+s)^{(mM)}} \sum_{k=0}^{\infty} \frac{\Gamma(k+m)}{\Gamma(m)\Gamma(k+Mm)} \frac{1}{k!} \left(\frac{C}{B+s}\right)^k$$

$$M(s) = \frac{A}{D} \Gamma(Mm) \times \sum_{k=0}^{\infty} \frac{\Gamma(k+m)}{\Gamma(m)} \frac{1}{k!} (c)^k \frac{1}{(B+s)^{Mm+k}} \tag{5.8}$$

From [149 Equation (7.621.4)] table of integral, we get:

$$M(s) = \frac{A}{D} \frac{\Gamma(Mm)}{(B+s)^{Mm}} \,_2F_1\left(m, Mm; Mm; \frac{C}{B+s}\right) \tag{5.9}$$

From [156 Equation (15.1.8)], the Equation can be expressed as:

$$M(s) = \left(1 + \frac{\bar{\gamma}_t(1-\rho+M\rho)s}{m}\right)^{-m} \left(1 + \frac{\bar{\gamma}_t(1-\rho)s}{m}\right)^{-m(M-1)} \tag{5.10}$$

MGF in Equation (5.10) is further used to evaluate channel capacity under various adaptive schemes.

## 5.4 MARGINAL MGF BASED CHANNEL CAPACITY ANALYSIS
### 5.4.1 OPTIMAL RATE ADAPTATION

When the transmitter power remains constant, usually as a result of channel state information being available at receiver side, the channel capacity with optimal rate adaptation ($C_{ORA}$) in terms of the MGF based approach can be expressed as [157]:

$$C_{ORA} = \frac{1}{ln(2)} \int_0^{\infty} E_i(-s) M_\gamma^{(1)}(s) ds \tag{5.11}$$

where $E_i(\cdot)$ denotes the exponential integral function as defined in [156] and $M_\gamma^{(1)}(s)$ is the first derivative of the MGF. The integral in Equation (5.11) is called $E_i$-transform, as $E_i(\cdot)$ kernel function defines this integral transform. Moreover, in those scenarios where very complicated expressions of the MGF of the received SNR do not allow easily computing the aforementioned integral in closed form, the result in the Equation (5.11) can efficiently and easily obtained by using standard computing

environments, such as MAPLE and Wolfram MATHEMATICA. By differentiating Equation (5.8) with respect s we get

$$M^1(s) = -\frac{A}{D}\Gamma(Mm) \times \sum_{k=0}^{\infty} \frac{\Gamma(k+m)}{\Gamma(m)} \frac{1}{k!}(c)^k \frac{(Mm+k)}{(B+s)^{Mm+k+1}} \tag{5.12}$$

By putting the value of $M^1(s)$ in Equation (5.11) we get,

$$C_{ORA} = -\frac{1}{ln(2)}\frac{A}{D}\Gamma(Mm) \times \sum_{k=0}^{\infty} \frac{\Gamma(k+m)}{\Gamma(m)} \frac{(Mm+k)}{k!}(c)^k I_2 \tag{5.13}$$

where

$$I_2 = \int_0^{\infty} E_i(-s) \frac{1}{(B+s)^{Mm+k+1}} ds = \frac{1}{(B)^{Mm+k+1}} \int_0^{\infty} E_i(-s) \frac{1}{\left(1+\dfrac{s}{B}\right)^{Mm+k+1}} ds \tag{5.14}$$

By putting $\dfrac{s}{B} = t$ in Equation (5.14), and after some mathematical manipulation, we get:

$$I_2 = \frac{1}{(B)^{Mm+k}} \int_0^{\infty} \frac{E_i(-Bt)}{(1+t)^{Mm+k+1}} dt \tag{5.15}$$

From [157 Equation (8.4.2.7)] along with [157 Equation (8.4.11.1)], Equation (5.15) can be expressed as:

$$I_2 = -\frac{1}{(B)^{Mm+k}\Gamma(k+mM+1)} \int_0^{\infty} G_{1\ 1}^{1\ 1}\left[t\left|\begin{matrix} -(k+Mm) \\ 0 \end{matrix}\right.\right] G_{1\ 2}^{2\ 0}\left[Bt\left|\begin{matrix} 1 \\ 0\quad 0 \end{matrix}\right.\right] dt \tag{5.16}$$

From [157 Equation (2.24.1)], Equation (5.16) can be expressed as:

$$I_2 = -\frac{G_{2\ 3}^{3\ 1}\left[B\left|\begin{matrix} 0 \qquad\quad 1 \\ 0\quad 0\quad(k+mM) \end{matrix}\right.\right]}{(B)^{Mm+k}\Gamma(k+mM+1)} \tag{5.17}$$

By putting value of $I_2$ from Equation (5.17) to Equation (5.13), we get:

$$C_{ORA} = \frac{1}{ln(2)}\frac{A}{D}\Gamma(Mm) \times \sum_{k=0}^{\infty} \frac{\Gamma(k+m)}{\Gamma(m)} \frac{(Mm+k)}{k!}(c)^k \frac{G_{2\ 3}^{3\ 1}\left[B\left|\begin{matrix} 0 \qquad\quad 1 \\ 0\quad 0\quad(k+mM) \end{matrix}\right.\right]}{(B)^{Mm+k}\Gamma(k+mM+1)}$$

$$\tag{5.18}$$

where $G(\bullet)$ is Meijer's G function [149 Equation (9.301)]. Expression of $C_{ORA}$ in Equation (5.18) shows summation of infinite series but it diverges rapidly with the increase of number of terms and only few terms are required to get closed form expression of $C_{ORA}$.

### 5.4.2 OPTIMAL SIMULTANEOUS POWER AND RATE ADAPTATION

When both the transmitter and receiver having perfect channel information, then the channel capacity for optimal rate adaptation ($C_{OPRA}$) is given by [107]:

$$C_{OPRA} = B \int_{\gamma_\circ}^{\infty} log_2 \left( \frac{\gamma}{\gamma_\circ} \right) f_\gamma(\gamma) d\gamma \tag{5.19}$$

where $B$ is the channel bandwidth (in Hz) and $\gamma_\circ$ is optimal cut off SNR level below which no transmission takes place. This optimal cutoff must satisfy

$$\int_{\gamma_\circ}^{\infty} \left( \frac{1}{\gamma_\circ} - \frac{1}{\gamma} \right) f_\gamma(\gamma) d\gamma = 1 \tag{5.20}$$

to achieve the channel capacity by Equation (5.19), the amount of fading must be tracked at the transmitter and receiver both, transmitter adapts its power and data rate to the channel variations by allocating high-power levels and rates for good channel condition and low power levels and rates for bad channel condition [107]. Furthermore, this optimal policy suffers a probability of outage $P_{out}$, equal to probability of no transmission, given by:

$$P_{out} = \int_{0}^{\gamma_\circ} f_\gamma(\gamma) d\gamma \tag{5.21}$$

Now, an alternate method to evaluate the $C_{OPRA}$ by using the marginal MGF is discussed below. By substituting first substituting $\gamma = q + \gamma_\circ$ in the Equation (5.19) and then again substituting $q/\gamma_\circ = x$ in Equation (5.19), the equation (5.19) is reduces to:

$$C_{OPRA} = \frac{\gamma_0}{ln(2)} \int_{0}^{\infty} ln(1+x) f_\gamma(\gamma_\circ(1+x)) dx = \frac{\gamma_0}{ln(2)} \widehat{E}(ln(1+\gamma); \gamma_\circ) \tag{5.22}$$

Form [112 Equation (6)] by using

$$ln(1+x) = \int_0^\infty \left( \frac{1-e^{-xz}}{z} \right) e^{-z} dz \tag{5.23}$$

From (5.27) and (5.28), we get:

$$C_{OPRA} = \frac{\gamma_0}{ln(2)} \int_0^\infty \frac{\left[ 1 - \hat{E}\left[ e^{-xz} \right] \right] e^{-z}}{z} dz \tag{5.24}$$

where $\hat{E}\left[ e^{-xz} ; \gamma_0 \right] = \int_0^\infty e^{-xz} f_\gamma \left( \gamma_\circ (1+x) \right) dx$

$$I_3 = \int_0^\infty e^{-xz} f_\gamma \left( \gamma_\circ (1+x) \right) dx \tag{5.25}$$

By putting $\gamma_\circ (1+x) = g$ in Equation (5.25) and after some mathematical manipulation, the integral $I_3$ in Equation (5.25) can be expressed as:

$$I_3 = \frac{e^z}{\gamma_0} \int_{\gamma_0}^\infty e^{-\frac{zg}{\gamma_0}} f_\gamma(g) dg = \frac{e^z}{\gamma_0} \hat{M}\left( \frac{z}{\gamma_0}, \gamma_0 \right) \tag{5.26}$$

where $\hat{M}\left( \frac{z}{\gamma_0}, \gamma_0 \right)$ is a marginal MGF as given by Equation (5.2). By putting value of

$I_3$ from Equation (5.26) to Equation (5.24), we get:

$$C_{OPRA} = \frac{\gamma_0}{ln(2)} \left[ \int_0^\infty \frac{e^{-z}}{z} - \frac{1}{\gamma_0} \int_0^\infty \frac{\hat{M}\left( \frac{z}{\gamma_0}, \gamma_0 \right)}{z} \right] dz \tag{5.27}$$

For evaluation of $C_{OPRA}$ in Equation (5.27), first integral and second integral can be evaluated numerically by using standard software like Maple and Mathematica. To obtain the optimal cut-off SNR $\gamma_\circ$ in Equation (5.27), we need to solve the Equation (5.20), by using standard techniques as given in [107, 153]. Here, we are presenting MMGF based approach for optimization of cut-off SNR $\gamma_\circ$. By re-arranging the Equation (5.20), we get:

$$\frac{1}{\gamma_\circ} \int_{\gamma_\circ}^\infty f_\gamma(\gamma) d\gamma - \int_{\gamma_\circ}^\infty \frac{1}{\gamma} f_\gamma(\gamma) d\gamma = 1 \tag{5.28}$$

$$I_4 = \frac{1}{\gamma_\circ} \int\limits_{\gamma 0}^{\infty} f_\gamma(\gamma)d\gamma \tag{5.29}$$

$$I_5 = \int\limits_{\gamma 0}^{\infty} \frac{f_\gamma(\gamma)}{\gamma} d\gamma \tag{5.30}$$

By substituting s = 0 and $a = \gamma_\circ$ in Equation (5.2), we get:

$$\hat{M}(0,\gamma_\circ) = \int\limits_{\gamma 0}^{\infty} f_\gamma(\gamma)d\gamma \tag{5.31}$$

From Equation (5.29) and Equation (5.31), $I_4$ can be expressed as:

$$I_4 = \frac{\hat{M}(0,\gamma_\circ)}{\gamma_\circ} \tag{5.32}$$

By replacing $\dfrac{1}{\gamma} = \int\limits_{0}^{\infty} e^{-\gamma s} ds$ in the Equation (5.30) and by the changing the order of integration, we get:

$$I_5 = \int\limits_{0}^{\infty}\left( \int\limits_{\gamma 0}^{\infty} e^{-xt} f_\gamma(x)dx \right)dt = \int\limits_{0}^{\infty} \hat{M}(s,\gamma_0)ds \tag{5.33}$$

By substituting $I_4$ and $I_5$ in Equation (5.28), we get:

$$\frac{\hat{M}(0,\gamma_\circ)}{\gamma_\circ} - \int\limits_{0}^{\infty} \hat{M}(s,\gamma_\circ)ds = 1 \tag{5.34}$$

where $\hat{M}(s,\gamma_0)$ is the MMGF as given in Equation (5.2). From Equation (5.33) and Equation (5.7), Integral $I_5$ is evaluated as given below:

$$I_5 = \frac{A}{D} \sum\limits_{k=0}^{\infty} \frac{\Gamma(k+m)\Gamma(Mm)}{\Gamma(m)\Gamma(k+Mm)} \frac{(C)^k}{k!} I_6 \tag{5.35}$$

$$I_6 = \int\limits_{0}^{\infty} \frac{\Gamma(k+mM,\gamma_\circ(B+s))}{(B+s)^{(k+mM)}} ds \tag{5.36}$$

By substituting $B+s = t$ in the Equation (5.36) and after simplification, we get:

$$I_6 = \int\limits_{B}^{\infty} \frac{\Gamma(k+mM,t)}{(t)^{(k+mM)}} dt \tag{5.37}$$

From [157 Equation (8.4.16.2)], the Equation (5.37) can be expressed as:

$$I_6 = \int\limits_B^\infty (t)^{-(k+mM)} G_1^2 \,{}_2 \left[ \gamma_\circ t \, \Big|_0^1 \; {}_0 \right] dt \tag{5.38}$$

From [157 Equation (2.24.2.3)], the Equation (5.38) can be expressed as:

$$I_6 = (B)^{1-(k+mM)} G_2^3 \,{}_3 \left[ B\gamma_\circ \, \Big|_{(k+mM)-1}^{1} \; {}_0^{k+mM} \; {}_{(k+mM)} \right] \tag{5.39}$$

By putting result of $I_6$ from the Equation (5.39) in Equation (5.35), we get:

$$I_5 = \frac{A}{D} \sum_{k=0}^\infty \frac{\Gamma(k+m)\Gamma(Mm)}{\Gamma(m)\Gamma(k+Mm)} \frac{(C)^k}{k!} \frac{G_2^3 \,{}_3 \left[ B\gamma_\circ \, \Big|_{(k+mM)-1}^{1} \; {}_0^{k+mM} \; {}_{(k+mM)} \right]}{(B)^{(k+mM)-1}} \tag{5.40}$$

From Equation (5.2) Integral $I_4$ can be expressed as:

$$I_4 = \frac{\hat{M}(0,\gamma_\circ)}{\gamma_\circ} = \frac{A}{\gamma_\circ D} \sum_{k=0}^\infty \frac{\Gamma(k+m)\Gamma(Mm)}{\Gamma(m)\Gamma(k+Mm)} \frac{(C)^k}{k!} \frac{\Gamma(k+mM,\gamma_\circ)}{(B)^{(k+mM)}} \tag{5.41}$$

By substituting results of Equation (5.40) and (5.41) in Equation (5. 34), we get:

$$\left[ \left( \frac{A}{\gamma_\circ D} \sum_{k=0}^\infty \frac{\Gamma(k+m)\Gamma(Mm)}{\Gamma(m)\Gamma(k+Mm)} \frac{(C)^k}{k!} \frac{\Gamma(k+mM,\gamma_\circ)}{(B)^{(k+mM)}} \right) - \left( \frac{A}{D} \sum_{k=0}^\infty \frac{\Gamma(k+m)\Gamma(Mm)}{\Gamma(m)\Gamma(k+Mm)} \frac{(C)^k}{k!} \right. \right.$$

$$\left. \left. \times \frac{G_2^3 \,{}_3 \left[ B\gamma_\circ \, \Big|_{(k+mM)-1}^{1} \; {}_0^{k+mM} \; {}_{(k+mM)} \right]}{(B)^{(k+mM)-1}} \right) \right] = 1$$

$$\tag{5.42}$$

Although, the optimal cut-off SNR $\gamma_\circ$ cannot be obtained in close-form in Equation (5.42), so numerical evaluation is performed in order to get optimal cut-off SNR $\gamma_\circ$.

### 5.4.3 CHANNEL INVERSION WITH FIXED RATE

The channel capacity for channel inversion with fixed rate ($C_{CIFR}$) requires that the transmitter exploits the channel state information so that constant SNR is maintained at receiver. As this method inverts the channel fading at receiver therefore it provides a fixed transmission rate .The channel capacity with fixed channel inversion rate can be expressed as [107]:

$$C_{CIFR} = \log_2\left(1 + \frac{1}{\int_0^\infty \frac{f_\gamma(\gamma)}{\gamma}d\gamma}\right) \tag{5.43}$$

The Equation (5.43) can be expressed in the term of the MGF as:

$$I_7 = \int_0^\infty \frac{f_\gamma(\gamma)}{\gamma}d\gamma \tag{5.44}$$

By replacing $\dfrac{1}{\gamma} = \int_0^\infty e^{-\gamma s}ds$ in Equation (5.44), we get:

$$I_7 = \int_0^\infty f_\gamma(\gamma)\left(\int_0^\infty e^{-\gamma s}ds\right)d\gamma \tag{5.45}$$

By changing the order of integration in Equation (5.45), we get:

$$I_7 = \int_0^\infty \left(\int_0^\infty f_\gamma(\gamma)e^{-\gamma s}d\gamma\right)ds$$

So now

$$I_7 = \int_0^\infty M(s)ds \tag{5.46}$$

By putting the value of $I_4$ from the Equation (5.46) in Equation (5.43), we get:

$$C_{CIFR} = \log_2\left(1 + \frac{1}{\int_0^\infty M(s)\,ds}\right) \tag{5.47}$$

By putting the value of $M(s)$, from Equation (5.10) to Equation (5.47), we get:

$$I_7 = \int_0^\infty \left(1 + \frac{\bar{\gamma}_t(1 - \rho + M\rho)s}{m}\right)^{-m}\left(1 + \frac{\bar{\gamma}_t(1 - \rho)s}{m}\right)^{-m(M-1)}ds \tag{5.48}$$

By using [149 Equation (3.259.3)], Integral $I_7$ in Equation (5.47) can be expressed as:

$$I_7 = \frac{m\,B(1, mM-1)}{(1 + \rho(M-1))\bar{\gamma}_t}\,_2F_1\left(m(M-1), 1; mM\,; \frac{M\rho}{1 + \rho(M-1)}\right) \tag{5.49}$$

By putting the result in (5.49) in Equation (5.47), we get:

$$C_{CIFR} = \log_2\left(1 + \frac{(1 + \rho(M-1))\bar{\gamma}_t}{m\,B(1, mM-1)\,_2F_1\left(m(M-1), 1; mM; \frac{M\rho}{1 + \rho(M-1)}\right)}\right) \quad (5.50)$$

where $B(\bullet)$ is beta function [149 Equation (8.384.1)]. The above expression evaluates accurate value of channel capacity for channel inversion with fixed rate scheme for arbitrary value of fading parameter.

### 5.4.4 TRUNCATED CHANNEL INVERSION

The CIFR suffers from a large capacity penalty relative to the other techniques. The truncated CIFR is better approach than CIFR, where channel fading is inverted above a cut-off SNR $(\gamma_0)$. The capacity for truncated CIFR is defined as [107]:

$$C_{TCIFR} = \log_2\left(1 + \frac{1}{\int_{\gamma_0}^{\infty} \frac{f_{\gamma}(\gamma)}{\gamma} d\gamma}\right)(1 - P_{out}) \quad (5.51)$$

In the Equation (5.51), Integral $\int_{\gamma_0}^{\infty} \frac{f_{\gamma}(\gamma)}{\gamma} d\gamma$ is similar with Integral $I_5$ in the Equation (5.30) and it can be written in term of MMGF as given in Equation (5.33). The outage probability $P_{out}(\gamma_{\circ})$ in Equation (5.21) can be rewritten as:

$$P_{out}(\gamma_{\circ}) = 1 - \int_{\gamma_{\circ}}^{\infty} f_{\gamma}(\gamma) d\gamma \quad (5.51)$$

From Equation (5.31), the Equation (5.51) can be expressed as:

$$P_{out}(\gamma_{\circ}) = 1 - \hat{M}(0, \gamma_{\circ}) \quad (5.52)$$

By putting $a = \gamma_{\circ}$ and $s = 0$ in Equation (5.12), $P_{out}(\gamma_{\circ})$ can be expressed as:

$$P_{out}(\gamma_{\circ}) = 1 - \frac{A}{D} \sum_{k=0}^{\infty} \frac{\Gamma(k+m)\Gamma(Mm)}{\Gamma(m)\Gamma(k+Mm)} \frac{(C)^k}{k!} \frac{\Gamma(k+mM, \gamma_{\circ}B)}{(B)^{(k+mM)}} \quad (5.53)$$

$$C_{TCIFR} = \log_2\left(1 + \frac{1}{\int_0^{\infty} \hat{M}(t, \gamma_0) dt}\right)\left\{\hat{M}(0, \gamma_{\circ})\right\} \quad (5.54)$$

By substituting the result of $I_5$ from the Equation (5.40) and $P_{out}$, in Equation (5.54), we get:

$$C_{TCIFR} = \log_2 \left( 1 + \cfrac{1}{\left[ \cfrac{A}{D} \sum_{k=0}^{\infty} \cfrac{\Gamma(k+m)\Gamma(Mm)}{\Gamma(m)\Gamma(k+Mm)} \cfrac{(C)^k}{k!} \cfrac{G_{2\ 3}^{3\ 0}\left[ B\gamma_\circ \Big| \begin{matrix} 1 & & k+mM \\ (k+mM)-1 & 0 & (k+mM) \end{matrix} \right]}{(B)^{(k+mM)-1}} \right]} \left\{ \hat{M}(0,\gamma_\circ) \right\} \right) \tag{5.55}$$

By using Equation (5.55), the channel capacity for truncated CIFR scheme can be evaluated easily for arbitrary value of fading parameter.

## 5.5 RESULT AND DISCUSSION

In this section, we have presented numerical results for the channel capacity with MRC diversity over correlated Nakagami-$m$ fading channel. Figure 5.2 shows the channel capacity with optimal rate adaptation ($C_{ORA}$) versus SNR for various diversity receivers. As the number of diversity receiver increases, $C_{ORA}$ improves significantly. Figure 5.3 shows the effect of correlation coefficient on the channel capacity for optimal rate adaptation ($C_{ORA}$).
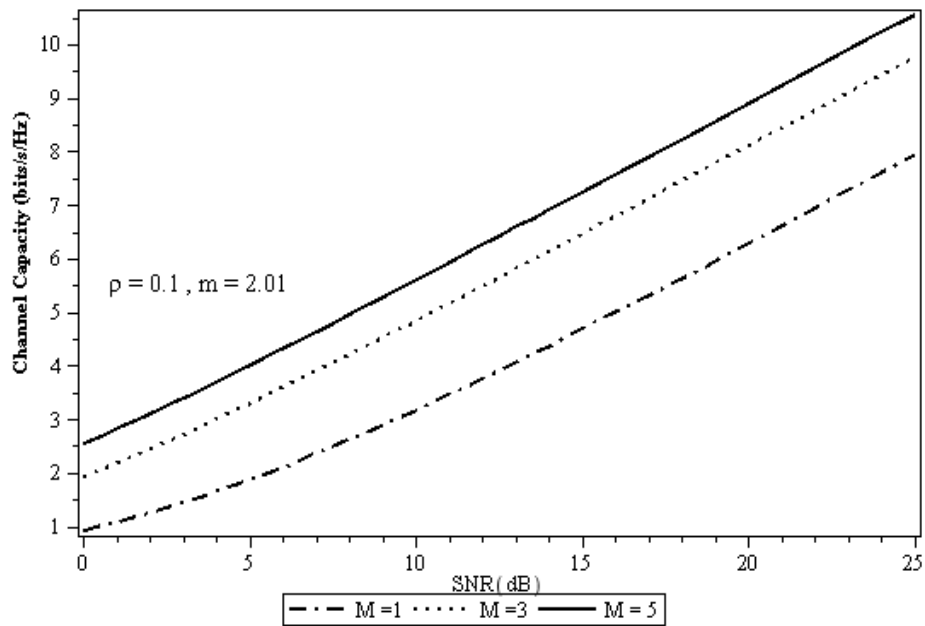


**Figure 5.2** The channel capacity with optimal rate adaptation ($C_{ORA}$) versus SNR for various diversity receivers.

As the correlation coefficient increases, $C_{ORA}$ decreases. Figure 5.4 depicts the channel capacity for optimal simultaneous power and rate adaptation $(C_{OPRA})$ versus SNR for various diversity receivers. As the number of diversity receivers increases, $C_{OPRA}$ improves, similarly as in Figure 5.2.
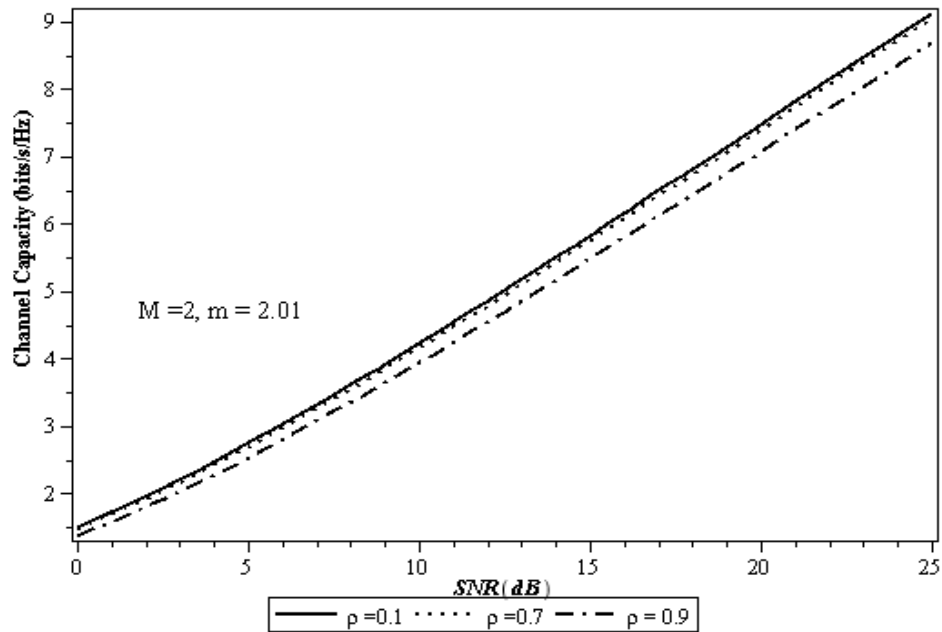
**Figure 5.3** The channel capacity with optimal rate adaptation ($C_{ORA}$) versus SNR for several correlation coefficients.
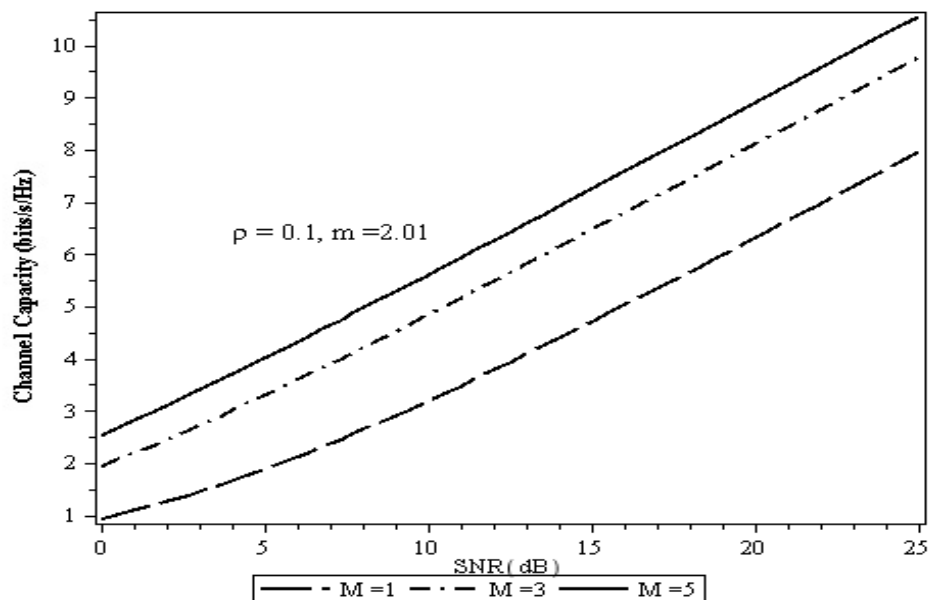
**Figure 5.4** The channel capacity for optimal rate adaptation $(C_{OPRA})$ versus SNR for various diversity receivers.

Figure 5.5 shows the channel capacity for $C_{OPRA}$ versus SNR for several correlation coefficients, similarly as in Figure 5.3. Figure 5.6 shows the characteristics of channel inversion with fixed rate ($C_{CIFR}$) versus SNR for various diversity receivers, in this $C_{CIFR}$ improves with the increase of diversity receiver.
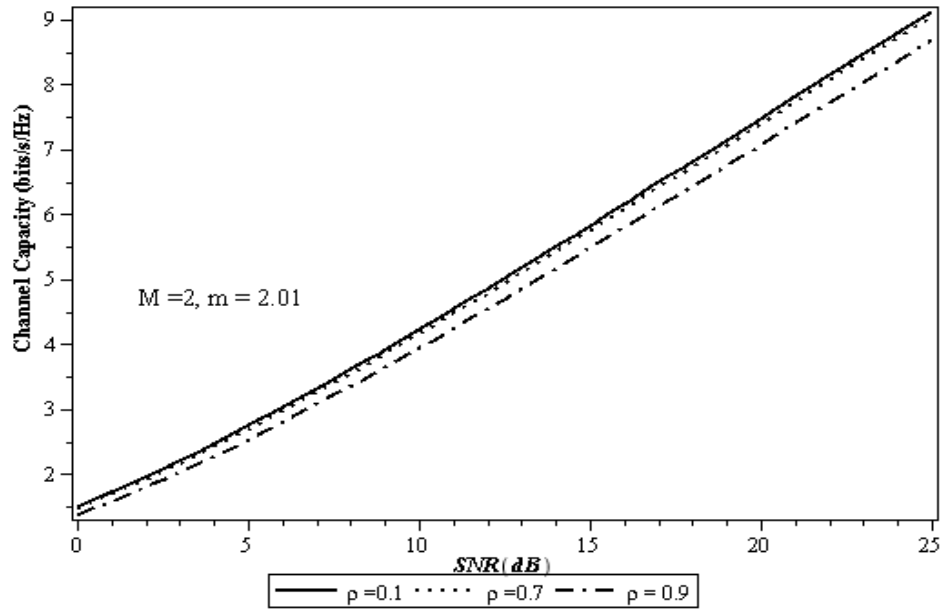


**Figure 5.5** The channel capacity for optimal rate adaptation $(C_{OPRA})$ versus SNR for several of correlation coefficients.
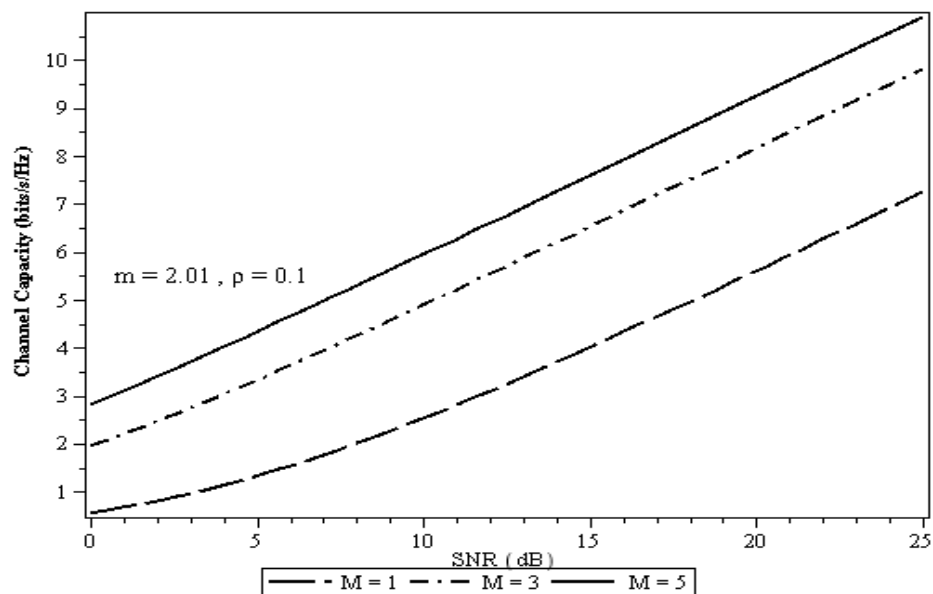


**Figure 5.6** The channel inversion with fixed rate (CIFR) versus SNR for various diversity receivers.
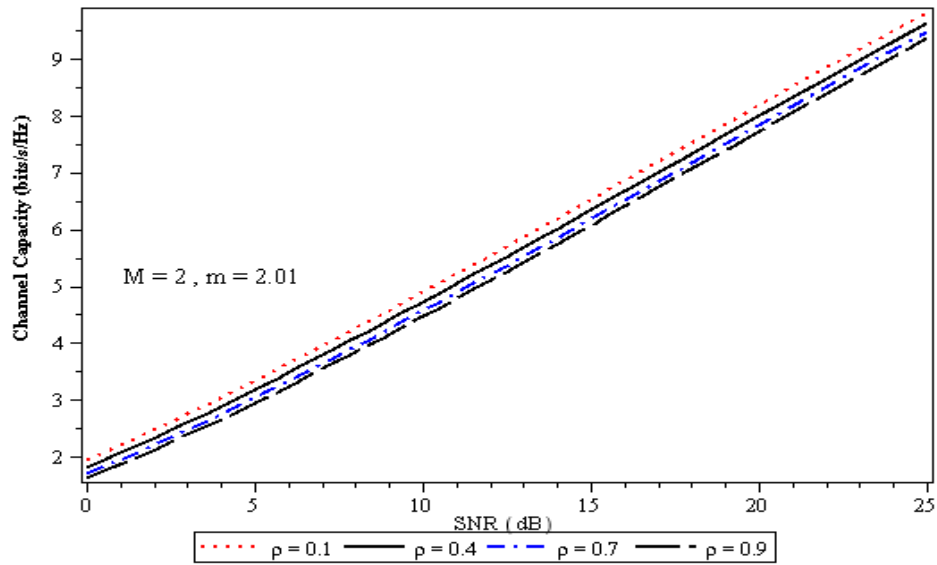
**Figure 5.7** The channel inversion with fixed rate (CIFR) versus SNR for various correlation coefficients.
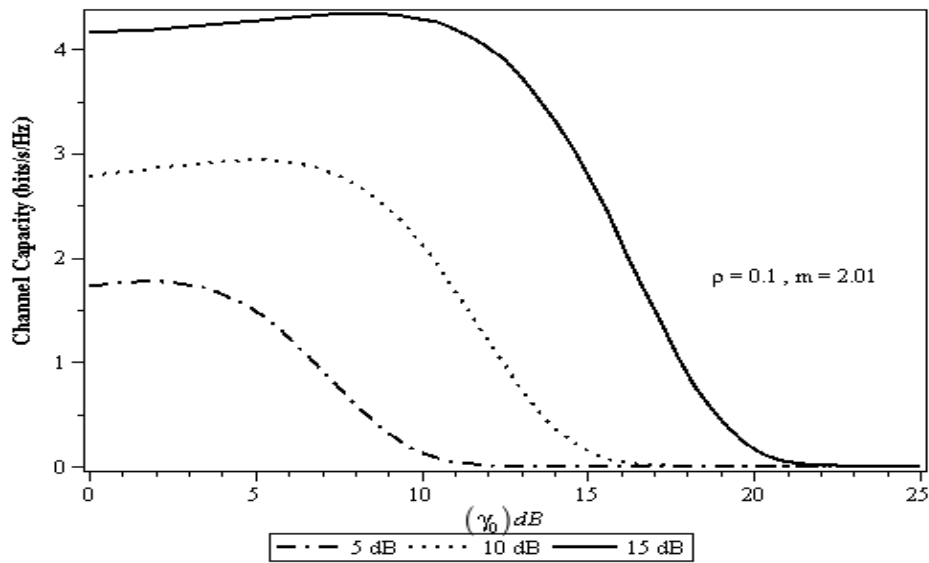


**Figure 5.8** The channel capacity with truncated channel inversion ($C_{TCIFR}$) versus cut-off SNR ($\gamma_0$) for various value of SNR.

Figure 5.7 shows effect of correlation coefficient on channel inversion with fixed rate ($C_{CIFR}$) versus SNR, as correlation coefficients increases, $C_{CIFR}$ decreases but decrement is less in comparison to that as shown in Figure 5.3 and Figure 5.5. Figure 5.8 shows the characteristics of channel capacity with truncated channel inversion ($C_{TCIFR}$) with cut-off SNR ($\gamma_0$) for various values of SNR. From Figure 5.8 it is clear that as SNR increase, the cut-off rate ($\gamma_0$) also increases. Figure 5.9 shows the channel

capacity with truncated channel inversion ($C_{TCIFR}$) versus MRC diversity, as the MRC diversity increases, the cut-off rate $(\gamma_0)$ increases significantly.
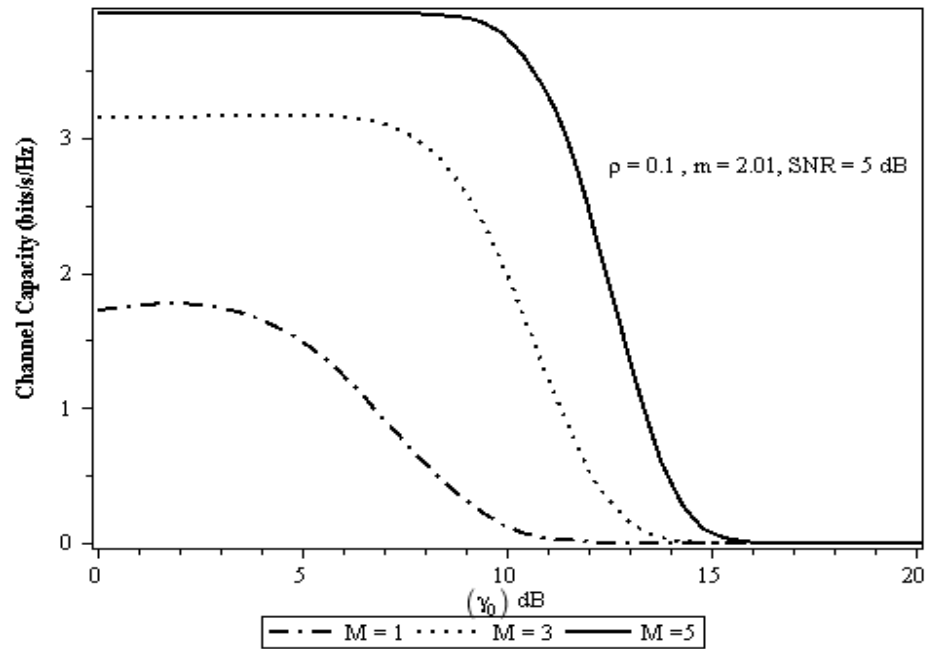


**Figure 5.9** The channel capacity with truncated channel inversion ($C_{TCIFR}$) versus MRC diversity.



**Figure 5.10** The channel capacity with truncated channel inversion ($C_{TCIFR}$) versus cut-off SNR $(\gamma_0)$ for the various values of correlation coefficient.
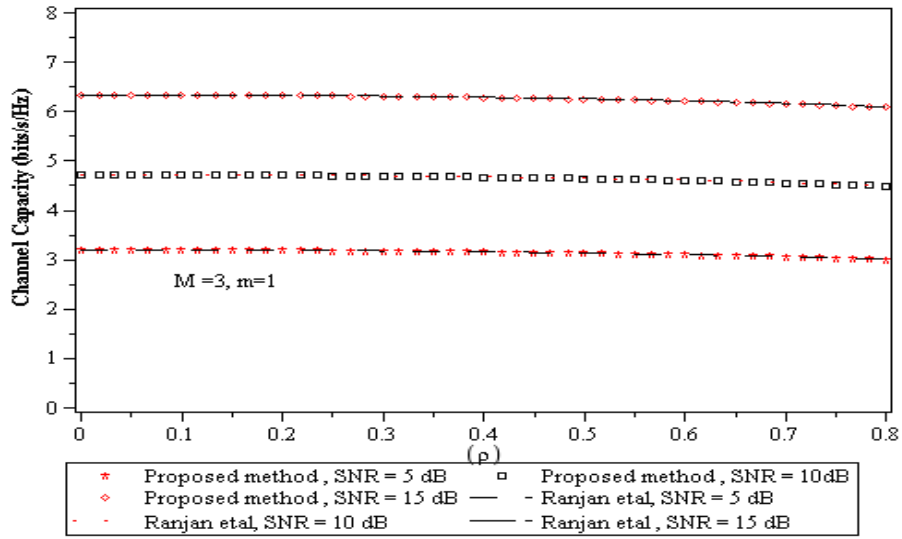
**Figure 5.11** Comparison of the channel capacity with optimal rate adaptation ($C_{ORA}$) versus correlation coefficient for diversity M = 3 for different values of SNR.

Figure 5.10 depicts the channel capacity with truncated channel inversion ($C_{TCIFR}$) with cut-off SNR ($\gamma_0$) for various values of correlation coefficient. As the correlation coefficient increases, the cut-off rate decreases slowly. Figure 5.11 to Figure 5.14 shows the comparison of channel capacity under various adaptive condition with the reported literature [153] for correlated Rayleigh fading channel ($m = 1$). The result of the proposed method is similar with that of [153].
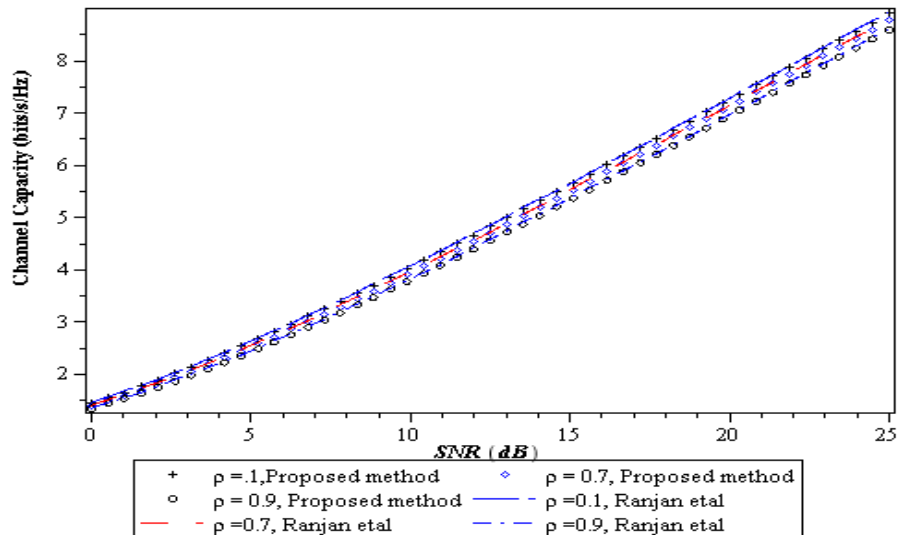


**Figure 5.12** Comparison of channel capacity for the optimal simultaneous power and rate adaptation ($C_{OPRA}$) versus SNR for various correlation coefficients of the proposed method with [153].
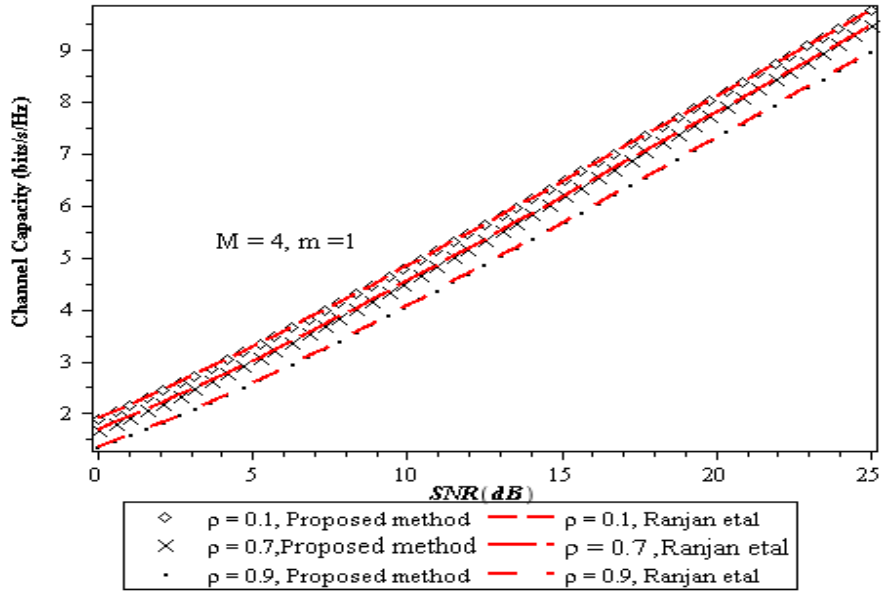
**Figure 5.13** Comparison of the channel capacity of channel inversion with fixed rate (CIFR) versus SNR for various correlation coefficients of the proposed method with [153].

In the Figure 5.11, the characteristic of the channel capacity for optimal rate adaptation with correlation coefficients of the proposed method has been compared with [153] by considering the Rayleigh fading channel ($m = 1$). The results of the proposed method are comparable with that of the [153]. In Figure 5.12 shows the comparison of the characteristics of channel capacity for optimal simultaneous power and rate adaptation with SNR for various correlation coefficients of the proposed method with [153] by considering the Rayleigh fading channel ($m = 1$).

The results of the proposed method are comparable with that of the [153]. In Figure 5.13 depicts the comparison of the characteristics of channel capacity of channel inversion with fixed rate with SNR for various correlation coefficients of the proposed method with [153] by considering the Rayleigh fading channel ($m = 1$). The results of the proposed method are comparable with that of the [153].

In Figure 5.14 explore the comparison of the characteristics of channel capacity of channel inversion with truncated channel inversion ($C_{TCIFR}$) versus cut-off SNR ($\gamma_0$) for various correlation coefficients of the proposed method with [153] by considering the Rayleigh fading channel ($m = 1$). The results of the proposed method are comparable with that of the [153].
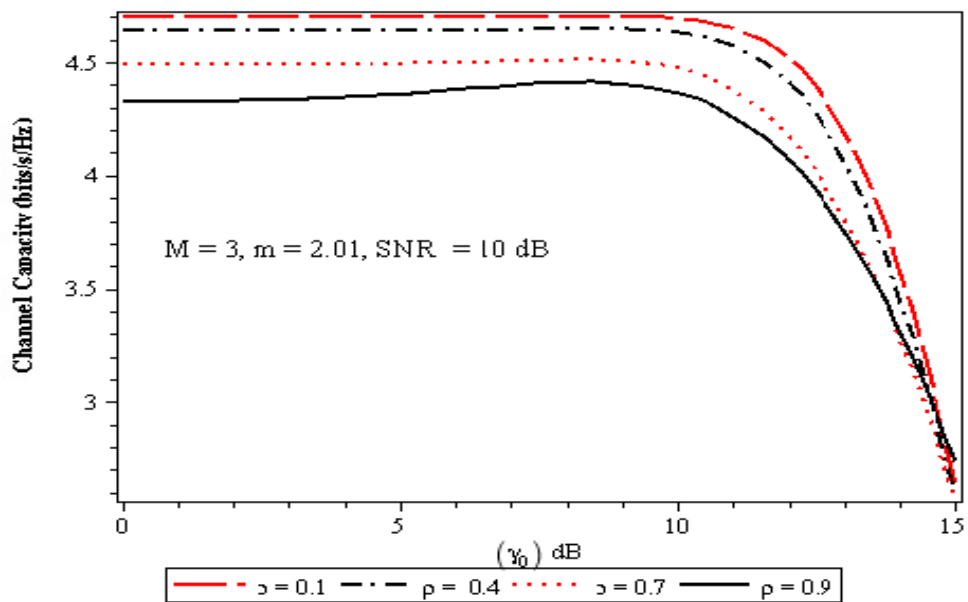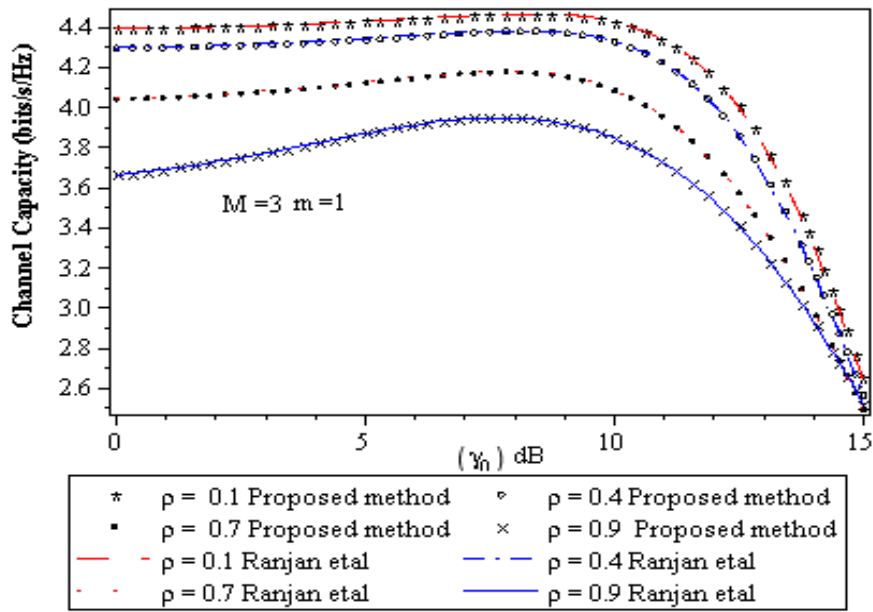
**Figure 5.14** The channel capacity with truncated channel inversion ($C_{TCIFR}$) versus cut-off SNR ($\gamma_0$) for various correlation coefficients of the proposed method with [153].

## 5.5 CONCLUSION

In this Chapter, we have obtained the marginal MGF for correlated Nakagami-*m* fading channel with MRC diversity. The obtained expression for marginal MGF function is used to evaluate the channel capacity under different adaptation policies. We have obtained the novel expression for various channel capacities for arbitrary value of *m*. We have also analyzed the effect of correlation coefficients on channel capacity. Due to the simple forms, these results offer a useful analytical tool for the accurate performance evaluation of various communication systems of practical interest.

# PERFORMANCE ANALYSIS OF GENERALZIED-K FADING MODEL

## 6.1 INTRODUCTION

The received signal in wireless communication systems are characterized by small-scale fading as well as large-scale fading. The large scale fading is due to the reflection, refraction and scattering caused by various obstacles in the medium. Thus, the local mean received power in wireless channel is varies which is referred to as shadowing. These variations of signal amplitude are modeled by lognormal distribution [31-32,158,159]. The PDF of lognormal distribution is given by:

$$f(x) = \frac{K}{x\sqrt{2\pi\sigma^2}} \exp\left[-\frac{(10\log(x)-\mu)^2}{2\sigma^2}\right]$$  (6.1)

where $K = \frac{10}{\ln(10)}$ and $\mu$ is the area mean since averaging over shadowing effect takes place over large area and it is determined by propagation path loss. The standard deviation $(\sigma^2)$ varies with propagation environment, which provides empirical justification for distribution in the urban and ionospheric environment propagation [31, 32]. A heuristic theoretical explanation for encountering this distribution is due to the multiple reflections in multipath environment. The multipath fading can be characterized as multiplicative process and multiplication of all the signal amplitude gives rise to a lognormal distribution [25]. Recently, Gamma distribution has been also adopted to model the shadowing [158, 159], which is given by:

$$f(x) = \left(\frac{x}{\Omega_\circ}\right)^k \frac{1}{x\,\Gamma(k)} \exp\left(-\frac{x}{\Omega_\circ}\right)$$  (6.2)

where $k$ and $\Omega_\circ$ are scaling and shaping parameters of Gamma distribution, respectively. For small values of $k$, the PDF has skewed exponential shape, which is symmetric for large values of $k$.

## 6.2 COMPOSITE FADING CHANNEL MODEL

The Nakagami-$m$ and Rayleigh-lognormal (Suzuki) are well known composite statistical distribution to model the multipath fading and shadowing [160-163]. Considering the envelope of the received signal due to the small-scale fading is modeled by the Nakagami-$m$ distribution (the PDF of the received power is $x$ and conditioned on mean power $\Omega$ which can be expressed as:

$$f_{x/\Omega}(x) = \frac{\left(\dfrac{m}{\Omega}\right)^m}{\Gamma(m)} x^{m-1} \exp\left(-\frac{mx}{\Omega}\right) \qquad x \geq 0, m \geq 0.5 \qquad (6.3)$$

In a shadowed fading channel, the probability density function $p_\lambda(x)$ is written as:

$$f_X(x) = \int_0^\infty f_{x/\Omega}(x) f(x) dx \qquad (6.4)$$

By substituting the values from Equation (6.1) and from Equation (6.3) in Equation (6.4), the Nakagami-m lognormal composite model can be expressed as [163]:

$$f_X(x) = \int_0^\infty \frac{\left(\dfrac{m}{\Omega}\right)^m}{\Gamma(m)} x^{m-1} \exp\left(-\frac{mx}{\Omega}\right) \frac{K}{\Omega\sqrt{2\pi\sigma^2}} \exp\left[-\frac{(10\log(\Omega)-\mu)^2}{2\sigma^2}\right] d\Omega \qquad (6.5)$$

The expression in Equation (6.5), for $m = 1$ reduces to the Rayleigh-lognormal (Suzuki) model.

## 6.3 GENELIZED K-FADING MODEL

The Nakagami-$m$ lognormal model as shown by Equation (6.5), do not lead to a closed form mathematical solution. The use of a Gamma PDF was proposed for shadowing instead of the lognormal based on the similarities between them as discussed in [161-163]. The resultant PDF is the so called generalized-K distribution ($K_G$) for the shadowed fading channel and the K-distribution when the short-term fading is modeled by using the Rayleigh instead of the Nakagami-$m$ PDF. So by substituting Equation (6.2) and (6.3) in Equation (6.4), we get the closed-form expression of composite fading model [103,160, 161] as:

$$f_X(x) = \frac{4x^{m+k-1}}{\Gamma(m)\Gamma(k)} \left(\frac{m}{\Omega_\circ}\right)^{\frac{k+M}{2}} K_{k-m}\left[2\left(\frac{m}{\Omega_\circ}\right)^{1/2} x\right] \qquad x > 0 \qquad (6.6)$$

where *k* and m are the shaping parameter of the distribution. $K_\nu(\cdot)$ is the modified Bessel function of order $\nu(\cdot)$ [13 Equation (8.432.1)]. $\Gamma(\cdot)$ is the Gamma function [149 Equation (8.310.1)]. In the Equation (6.6), $\Omega = E[X^2]/k$ is the mean power and $E[\cdot]$ denotes the expectation.

The diversity combining [22, 132] is an effective technique for mitigating detrimental effects of the multipath fading and shadowing in the wireless mobile channels. Recently, few contributions dealing with generalized-K and K-distribution with diversity combining have been reported in [155, 163, 164]. In [155], the performance of generalized selection combing (GSC) receivers over K-fading is presented. In same article marginal moment generating function (MMGF) is derived but this marginal MGF is not used to obtain bit-error-rate for M-array phase shift keying (MPSK). In [163], the performance analysis of diversity combining over generalized-K fading channel has been analyzed but the closed-form expression for the bit-error-rate is not discussed. In [164], the outage probability performance is evaluated and further MGF based approach and Pade approximants method are used for the performance analysis. Bithas et al [102] have provided a closed-form expression for the symbol-error-rate and bit-error-rate of various coherent and non-coherent digital modulations.

In this Chapter, we have investigated the MGF based performance analysis for various modulation scheme over the generalized-K fading channel with M-branch MRC diversity at receiver. The main contribution of this chapter consists with the evaluation of MGF function and the derived MGF function is used to evaluate closed-form expressions for average bit-error-rate and symbol-error-rate. The derived results are obtained in the terms of well known hypergeometric function and Meijer's G function, which can be easily implemented by using Maple or Mathematica simulation tool. The evaluation of symbol-error-rate for *M*-QAM modulation scheme is solved uniquely.

## 6.4 GENERALIZED-K FADING CHANNEL MODEL WITH MRC DIVERSITY

When the fading environment is such that the maximum delay spread of the channel is large compared to the symbol time that is the frequency selective fading, then there

exist multiple resolvable paths (the maximum number of which is determined by the ratio of the maximum delay spread to the symbol time) resulting in multiple channel reception. For the generic case of multi-channel reception, the diversity combining that practically depend on the characteristics of the modulation and their associated detection which can be employed at the receiver to improve the signal-to-noise ratio and thus average bit-error-rate performance. For coherent detection, the optimum form of diversity combining is MRC. Let us consider an M-branch MRC diversity receiver operating over the generalized-K fading channel, so replacing $m$ with mM and $\Omega_\circ$ by $M\Omega_\circ$ in Equation (6.6), then the PDF for M- branch MRC diversity can be expressed as:

$$f_X(x) = \frac{4\, x^{Mm+k-1}}{\Gamma(mM)\,\Gamma(k)}\left(\frac{m}{\Omega_\circ}\right)^{\frac{k+m\,M}{2}} K_{k-m\,M}\left[2\left(\frac{m}{\Omega_\circ}\right)^{1/2} x\right] \qquad x \geq 0 \qquad (6.7)$$

The instantaneous SNR per received symbol at the output of diversity branch is:

$$\gamma = X^2 E_S/N_0$$

where $E_S$ is the average symbol energy and $N_0$ is single-sided power spectral density of the additive white Gaussian noise. Assuming all the branches are identical and corresponding average SNR is given as $\bar{\gamma} = k\,\Omega\, E_S/N_0$. By changing the variables, the PDF of $\gamma$ from Equation (6.7) can be written as:

$$f_\gamma(\gamma) = \frac{2\,(\gamma)^{(\alpha-1)/2}}{\Gamma(mL)\Gamma(k)}(\Xi)^{(\alpha+1)/2} K_\beta\left[2\sqrt{\Xi\gamma}\right] \qquad \gamma \geq 0 \qquad (6.8)$$

where $\alpha = mM+k-1, \beta = k-mM$ and $\Xi = k\,m/\bar{\gamma}$. For the diversity technique consideration, it is assumed that the distance among the diversity branches is small. Furthermore, it is well known that the shadowing occurs in large geographical areas. Thus, it is reasonable to assume that the shadowing effects are not de-correlated so that shadowing parameters $k$ can be assumed equal for all the diversity branches.

## 6.5 PERFORMANCE ANALYSIS

The model corresponds to Nakagami-Gamma composite distribution and is controlled by two shaping parameters $m$ and $k$, where the parameter $m \geq 1/2$ inversely reflects the fading severity, and the positive parameter $k$ inversely reflects the shadowing

severity [163]. The K-distribution is derived as a special case of the generalized-K distribution by letting $m = 1$. The generalized-K distribution fading model characterizes the confined effect of fast and slow fading in the received signal by using two shaping parameters $m$ and $k$, where $m$ is the Nakagami fading parameters for the short term fading and $k$ is the parameter of the Gamma distribution for received average power due to the shadowing. Assuming that the fading environment is such that the signal envelop $X$ is the propagation path. Therefore, it is useful for wireless system designers to have a general statistical model that encompasses both of these random processes. The Rayleigh-Lognormal (R-L) is a well known composite statistical distribution when both multipath and shadowed components are present at receiver. However, the R-L distribution is not widely used because it does not have convenient mathematical form for evaluating the system performance. For this reason, the R-L distribution has been mixture of the Rayleigh and Gamma distribution that facilitates the derivation of analytical performance [163].

## 6.5.1 MOMENT GENERATING FUNCTION

The MGF function is one of most important characteristics of any distribution function because it helps in the bit-error-rate performance evaluation of the wireless communication systems. However, it is shown in [22] that MGF can be used to obtain the average bit-error-rate of the modulation (with and without diversity) either in closed-form or in the form of a simple finite range integral. The MGF is, therefore, a key tool that needs to be derived. MGF is defined as [22]:

$$M_\gamma(s) = \int_0^\infty \exp(-s\gamma) f_\gamma(\gamma) d\gamma \tag{6.9}$$

By substituting the Equation (6.8) in Equation (6.9), the MGF of Equation (6.8) can be evaluated as:

$$M_\gamma(s) = \frac{2(\Xi)^{(\alpha+1)/2}}{\Gamma(mM)\Gamma(k)} \int_0^\infty exp(-s\gamma)(\gamma)^{(\alpha-1)/2} K_\beta \left[2\sqrt{\Xi\gamma}\right] d\gamma$$

By expressing $K_\beta(\cdot)$ as [157 Equation (8.4.23.1)] and using [157 Equation (2.24.3.1)], the MGF can be expressed as:

$$M_\gamma(s) = \frac{(\Xi/s)^{\frac{\alpha+1}{2}}}{\Gamma(mM)\Gamma(k)} G_{1\;2}^{2\;1}\left[\frac{\Xi}{s}\middle|\begin{array}{cc}(1-\alpha)/2 & \\ \beta/2 & -\beta/2\end{array}\right] \tag{6.10}$$

where $G(\cdot)$ is Meijer's G function [149 Equation (9.301)], which can be easily evaluated by using the standard software like MAPLE and Mathmatica.

## 6.5.2 CALCULATION OF BER FOR VARIOUS MODULATION SCHEMES

The average bit-error-rate probability constitutes probably the most important performance measure of a digital communication system. Unfortunately, the average bit-error-rate probability is generally not easy to find in the closed form. The average bit-error-rate for BPSK/BFSK modulation scheme is [22]:

$$\overline{P}_b = \frac{1}{\pi}\int_0^{\frac{\pi}{2}} M_\gamma\left(\frac{g}{\sin^2\theta}\right)d\theta \tag{6.11}$$

where $g$ is a constant associated with modulation scheme, $g = 1$ for BPSK, $g = 1/2$ for coherent detection of BFSK and $g = 0.715$ for coherent detection of minimum shift keying. Let the integrand in Equation (6.11) is:

$$I_1 = \int_0^{\frac{\pi}{2}} M_\gamma\left(\frac{g}{\sin^2\theta}\right)d\theta \tag{6.12}$$

By using Equation (6.10) and (6.12), $I_1$ can be expressed as:

$$I_1 = \frac{(\Xi)^{\frac{\alpha+1}{2}}\,1}{\pi\,\Gamma(mL)\Gamma(k)}\int_0^{\frac{\pi}{2}}\left(\frac{g}{\sin^2\theta}\right)^{-\frac{(\alpha+1)}{2}} G_{1\;2}^{2\;1}\left[\frac{\Xi\sin^2\theta}{g}\middle|\begin{array}{cc}(1-\alpha)/2 & \\ \beta/2 & -\beta/2\end{array}\right]d\theta$$

By changing variable $t = \sin^2\theta$ and after some mathematical manipulation, the above integral can be expressed as:

$$I_1 = \frac{(\Xi/g)^{\frac{\alpha+1}{2}}}{2\pi\,\Gamma(mL)\Gamma(k)}\int_0^1 (t)^{\frac{(\alpha)}{2}}(1-t)^{-1/2} G_{1\;2}^{2\;1}\left[\frac{\Xi\,t}{g}\middle|\begin{array}{cc}(1-\alpha)/2 & \\ \beta/2 & -\beta/2\end{array}\right]dt$$

By using [157 Equation (2.24.2.2)], the integral $I_1$ can be expressed as:

$$I_1 = \frac{(\Xi/g)^{\frac{(1+\alpha)}{2}}\sqrt{\pi}}{2\,\Gamma(mL)\Gamma(k)} G_{2\;3}^{2\;2}\left[\frac{\Xi}{g}\middle|\begin{array}{ccc}-\alpha/2 & (1-\alpha)/2 & \\ \beta/2 & -\beta/2 & -(\alpha+1)/2\end{array}\right]$$

From Equation (6.11) and $I_1$, the average bit-error-rate for BPSK/ BFSK modulation scheme can be expressed as:

$$\overline{P}_b = \frac{(\Xi/g)^{\frac{(1+\alpha)}{2}}}{2\sqrt{\pi}\,\Gamma(mL)\Gamma(k)} G_{2\ 3}^{2\ 2}\left[\frac{\Xi}{g}\left|\begin{matrix} -\alpha/2 & (1-\alpha)/2 \\ \beta/2 & -\beta/2 & -(\alpha+1)/2 \end{matrix}\right.\right] \tag{6.13}$$

For M = 1 the Equation (6.13) is similar with the [102 Equation (8)]. The quadrature amplitude modulation (QAM) is a two-dimensional generalization of *M*-QAM which can be viewed as a combined amplitude/phase modulation [22] or more conveniently as a complex amplitude-modulated carrier. The signal constellation is a rectangular grid with points uniformly spaced along each axis by two units. Let *M* still denote the number of possible transmitted waveforms, the average SER for *M*-QAM modulation scheme by using the MGF based approach as given in [22].

$$\overline{P}_{qam} = \frac{4}{\pi}\left(1 - \frac{1}{\sqrt{M}}\right)\int_0^{\frac{\pi}{2}} M_\gamma\left(\frac{g_{QAM}}{\sin^2\theta}\right)d\theta - \frac{4}{\pi}\left(1 - \frac{1}{\sqrt{M}}\right)^2 \int_0^{\frac{\pi}{4}} M_\gamma\left(\frac{g_{QAM}}{\sin^2\theta}\right)d\theta \tag{6.14}$$

where $g_{QAM} = 3/2(M-1)$. The Equation 6.14 consists of two integrals:

$$I_2 = \int_0^{\frac{\pi}{2}} M_\gamma\left(\frac{g_{QAM}}{\sin^2\theta}\right)d\theta \tag{6.15}$$

and

$$I_3 = \int_0^{\frac{\pi}{4}} M_\gamma\left(\frac{g_{QAM}}{\sin^2\theta}\right)d\theta \tag{6.16}$$

Similarly, $I_2$ can be solved as $I_1$ and $I_3$ can be expressed as given below by using [149 Equation (6.643.3)] and Equation (6.10), the MGF of $I_3$ can be expressed as:

$$M_\gamma(s) = \left(\frac{\Xi}{s}\right)^{\alpha/2} \exp\left(\frac{\Xi}{2s}\right) W_{-\alpha/2,\beta/2}\left(\frac{\Xi}{s}\right) \tag{6.17}$$

where $W_{-\mu,\nu}(\cdot)$ is the Whittaker function as given by [149 Equation (9.220.4)]. From Equation (6.17), $I_3$ can be expressed as:

$$I_3 = \int_0^{\frac{\pi}{4}}\left(\frac{\Xi\sin^2\theta}{g_{QAM}}\right)^{\alpha/2}\exp\left(\frac{\Xi\sin^2\theta}{2g_{QAM}}\right) W_{-\alpha/2,\beta/2}\left(\frac{\Xi\sin^2\theta}{g_{QAM}}\right)d\theta$$

By applying the transformation $t = 2\sin^2\theta$ and after some mathematical manipulation the above integral $I_3$ can be expressed as:

$$I_3 = \frac{1}{2\sqrt{2}}\left(\frac{\Xi}{2g_{QAM}}\right)^{\alpha/2}\int_0^1 t^{(\alpha-1)/2}\left(1-t/2\right)^{-1/2}\exp\left(\frac{\Xi\, t}{4g_{QAM}}\right)W_{-\alpha/2,\beta/2}\left(\frac{\Xi\, t}{2g_{QAM}}\right)dt \quad (6.18)$$

By using [149 Equation (9.220.4)], [149 Equation (9.220.3)] and [149 Equation (9.220.2)] and after some mathematical manipulation, the Equation (6.18) can be expressed as:

$$I_3 = \frac{1}{2\sqrt{2}}\left(\frac{\Xi}{2g_{QAM}}\right)^{\alpha/2}\int_0^1 t^{(\alpha-1)/2}\left(1-t/2\right)^{-1/2}\left[\frac{\Gamma(-\beta)}{\Gamma(1/2-\beta/2+\alpha/2)}\left(\frac{\Xi\, t}{2g_{QAM}}\right)^{(\beta+1)/2}\right.$$
$$\left.\times 1F1\left(\frac{\alpha+\beta+1}{2},\beta+1,\frac{\Xi\, t}{2g_{QAM}}\right) + \frac{\Gamma(\beta)}{\Gamma(1/2+\beta/2+\alpha/2)}\left(\frac{\Xi\, t}{2g_{QAM}}\right)^{(-\beta+1)/2}\times 1F1\left(\frac{\alpha-\beta+1}{2},\beta+1,\frac{\Xi\, t}{2g_{QAM}}\right)\right]dt$$

where $_1F_1(\bullet)$ is confluent hypergeometric function as [13 Equation (9.210.1)]. By using [149 Equation (9.210.1)] and [149 Equation (9.111)], above integral $I_3$ can be expressed as:

$$I_3 = \frac{1}{2\sqrt{2}}\left[\frac{\Gamma(-\beta)}{\Gamma(1/2-\beta/2+\alpha/2)}\left(\frac{\Xi}{2g_{QAM}}\right)^{(\alpha+\beta+1)/2}I_4 + \frac{\Gamma(\beta)}{\Gamma(1/2+\beta/2+\alpha/2)}\left(\frac{\Xi}{2g_{QAM}}\right)^{(\alpha-\beta+1)/2}I_5\right] \quad (6.19)$$

where

$$I_4 = \sum_{n=0}^{\infty}\frac{1}{n!}\frac{\Gamma[(\alpha+\beta+1)/2+n]}{\Gamma[(\beta+\alpha+1)/2]}\frac{\Gamma(\beta+1)}{\Gamma(\beta+1+n)}\left(\frac{\Xi}{2g_{QAM}}\right)^n \times B\left(n+\frac{\alpha+\beta+2}{2},1\right)\times$$

$$F\left(1/2,n+(\alpha+\beta+2)/2,n+(\alpha+\beta+4)/2,1/2\right)$$

and

$$I_5 = \sum_{n=0}^{\infty}\frac{1}{n!}\frac{\Gamma[(\alpha-\beta+1)/2+n]}{\Gamma[(\alpha-\beta+1)/2]}\frac{\Gamma(\beta+1)}{\Gamma(\beta+1+n)}\left(\frac{\Xi}{2g_{QAM}}\right)^n \times B\left(n+\frac{\alpha-\beta+2}{2},1\right)\times$$
$$F\left(1/2,n+(\alpha-\beta+2)/2,n+(\alpha-\beta+4)/2,1/2\right)$$

where $F(\cdot)$ is hypergeometric function as given by [149 Equation (9.100)] and $B(\cdot)$ is beta function as given by [149 Equation (8.30.1)]. By substituting the value of $I_3$

from the Equation (6.19) and value $I_2$ in Equation (6.15) in Equation (6.14), the average SER of $M$- QAM can be expressed as:

$$\bar{P}_{qam} = \frac{2}{(\pi)^{3/2}}\left(1-\frac{1}{\sqrt{M}}\right)\frac{\left(\Xi/g_{QAM}\right)^{\frac{(1+\alpha)}{2}}}{\Gamma(mL)\Gamma(k)}G_2^2\,{}_3^2\left[\frac{\Xi}{g_{QAM}}\left|\begin{array}{ccc}-\alpha/2 & (1-\alpha)/2 \\ \beta/2 & -\beta/2 & -(\alpha+1)/2\end{array}\right.\right]-\frac{\sqrt{2}}{\pi}\left(1-\frac{1}{\sqrt{M}}\right)^2$$

$$\left[\frac{\Gamma(-\beta)}{\Gamma(1/2-\beta/2+\alpha/2)}\left(\frac{\Xi}{2g_{QAM}}\right)^{(\alpha+\beta+1)/2}\sum_{n=0}^{\infty}\frac{1}{n!}\frac{\Gamma[(\beta+\alpha+1)/2+n]}{\Gamma[(\beta+\alpha+1)/2]}\frac{\Gamma(\beta+1)}{\Gamma(\beta+1+n)}\left(\frac{\Xi}{2g_{QAM}}\right)^n\times\right.$$

$$B\left(n+\frac{\alpha+\beta+2}{2},1\right)\times F\left(1/2,n+(\alpha+\beta+2)/2,n+(\alpha+\beta+4)/2,1/2\right)+\frac{\Gamma(\beta)}{\Gamma(1/2+\beta/2+\alpha/2)}\left(\frac{\Xi}{2g_{QAM}}\right)^{(\alpha-\beta+1)/2}$$

$$\sum_{n=0}^{\infty}\frac{1}{n!}\frac{\Gamma[(\alpha-\beta+1)/2+n]}{\Gamma[(\alpha-\beta+1)/2]}\frac{\Gamma(\beta+1)}{\Gamma(\beta+1+n)}\left(\frac{\Xi}{2g_{QAM}}\right)^n\times B\left(n+\frac{\alpha-\beta+2}{2},1\right) \tag{6.20}$$

The average symbol-error-rate over the generalized-K fading channel with M-branch MRC diversity as given in Equation (6.20) is a novel expression.

### 6.5.3 OUTAGE PROBABILITY

The outage probability is another standard performance criterion of the communication systems operating over fading channels. It is defined as the probability that the instantaneous error-rate exceeds a specified value or equivalently combined signal-to-noise ratio reduced below a certain specified threshold, $\gamma_\circ$ as given in [22]. Hence, the outage probability,

$$P_{out} = \int_0^{\gamma_\circ} f(\gamma)d\gamma,$$

by using Equation (6.8), the outage probability can be written as:

$$P_{out} = \int_0^{\gamma_\circ}\frac{2(\gamma)^{(\alpha-1)/2}(\Xi)^{(\alpha+1)/2}}{\Gamma(mL)\Gamma(k)}K_\beta\left[2\sqrt{\Xi\gamma}\right]d\gamma$$

By using [149, Equation (6.561.8)], the outage probability can be written as:

$$P_{out} = 1-\frac{2(\Xi\gamma_\circ)^{(\alpha)/2}}{\Gamma(mL)\Gamma(k)}K_{\beta+1}\left[2\sqrt{\Xi\gamma_\circ}\right] \tag{6.21}$$

## 6.6 RESULT AND DISCUSSION

In this Section, we have presented performance evaluation results by using the preceding analysis on the error probability of digital modulation scheme and outage probability. We have presented some numerical results for the average bit-error-rate, average symbol-error-rate for different modulation schemes and outage probability. For the generalized-K fading, if $k > 8$ the probability density function of the SNR depends almost completely on fading parameter, $m$, making it a Nakagami-$m$ fading channel with little shadowing, when as low value of k and $m$ correspond to severe shadowing and fading, respectively [163]. We have used the Equation (6.13) and (6.20) to study the average bit-error-rate and average symbol-error-rate characteristics and Equation (6.21) is used to study the outage probability. Figure 6.1 depicts the average bit-error-rate versus the average SNR in generalized-K fading with MRC diversity scheme.
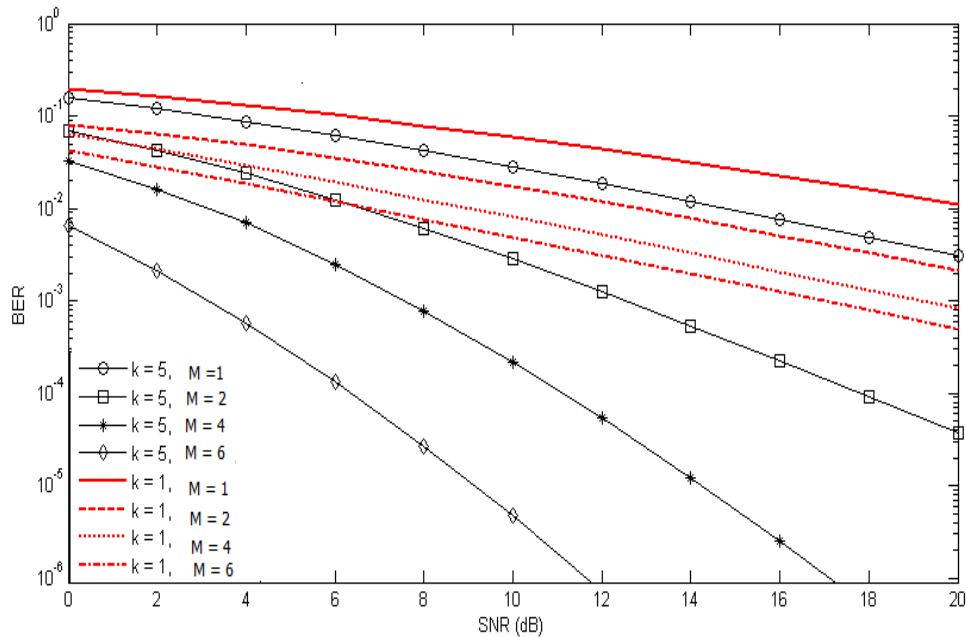


**Figure 6.1** Average BER versus SNR plot for BPSK modulation scheme over generalized-K fading channel with M-branch MRC diversity.

The average bit-error-rate against the average received SNR per bit for BPSK modulation in various fading channel conditions obtained by an appropriate choice of $k$ and $m$. For $k = 1$ as the diversity receiver increases the bit-error-rate performance

improves for same values of SNR but for $k = 5$ as the diversity receiver increases average bit-error-rate performance improves much faster than $k = 1$ as shown in Figure 6.1.
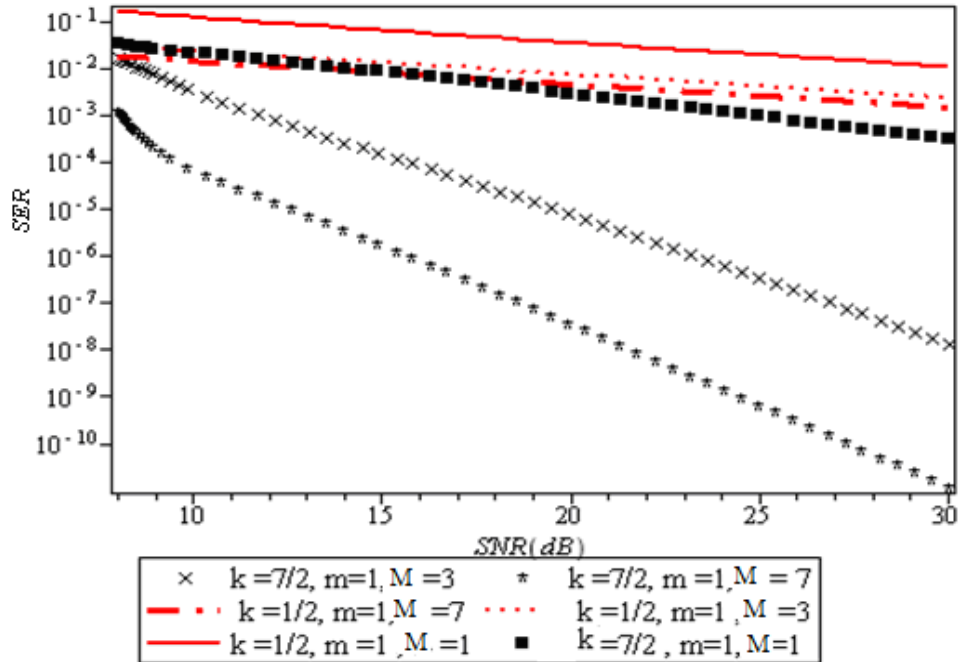


**Figure 6.2** Average SER versus SNR for *M*-QAM modulation scheme over generalized-fading channel with M-branch MRC diversity.

The simulation results are also included as shown to match exactly with the analytical results obtained from the mathematical Equations. Figure 6.2 shows the average symbol-error-rate versus SNR for 4-QAM modulation scheme, although Equation (6.20) is provided in an infinite series form, which converges rapidly and steadily requiring very few terms for the desired accuracy. Figure 6.3 shows the outage probability versus SNR plot for the threshold = 25dB.

As the diversity increases the symbol rate improve significantly as shown in Figure 6.2 for chosen value of *m* and *k* and this improvement is more significant as *k* increases. As the value of *k* increases, the outage probability remains constant over large range of SNR as shown in Figure 6.3.
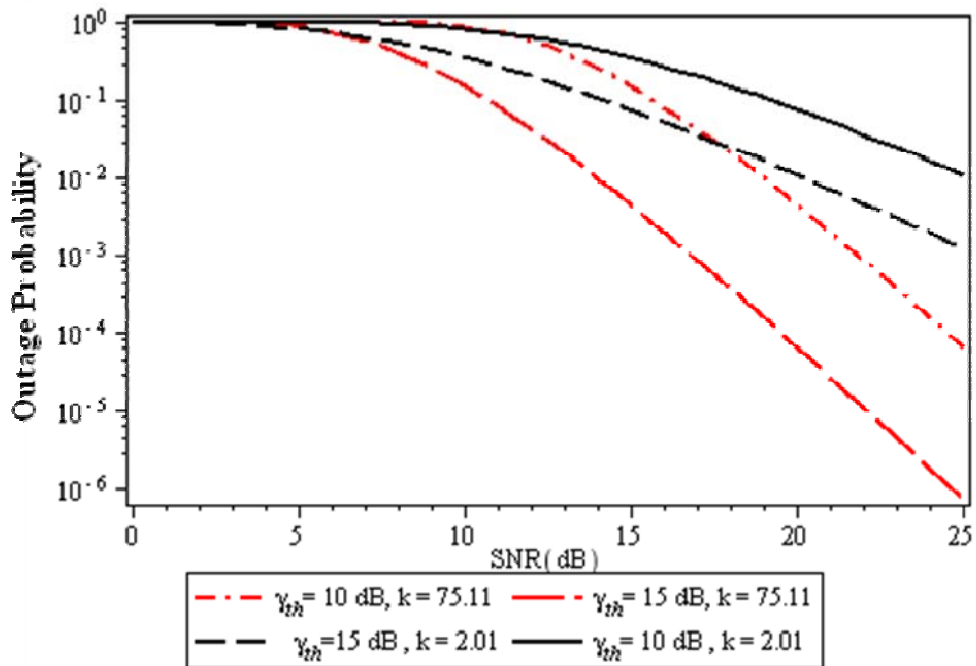
**Figure 6.3** Outage probabilities versus SNR for generalized K - fading channel with M-branch MRC diversity.

## 6.6 CONCLUSION

In this Chapter, we have investigated the generalized-K distribution by using simple MGF based approach. We have obtained a novel MGF for generalized-K fading channel with M-branch MRC diversity. In the expression of MGF, the Meijer's G function has been used. Also, the obtained MGF function is used to evaluate the bit-error-rate of BPSK/BFSK modulation and symbol-error-rate of *M*-QAM modulation schemes. The Average bit-error-rate expression of BPSK/BFSK is given in the Equation (6.13) for *M* = 1 the Equation (6.13) is similar with [165 Equation (8)] and also the average symbol-error-rate expression for *M*-QAM modulation scheme that is given by Equation (6.20) is novel. We also derived an expression for the outage probability. These mathematical expressions are very useful for modeling the wireless communication system.

# ANALYSIS OF CHANNEL CAPACITY OF GENERALIZED-K FADING BASED ON MARGINAL MOMENT GENERATING FUNCTION

## 7.1 INTRODUCTION

The received signal over a wireless channel is usually characterized by the joint effect of two independent random processes such as small scale fading due to the arrival of multiple, randomly delayed, reflected and scattered signal components at the receiver side and large scale fading due to shadowing from various obstacles in the propagation path. Therefore, it is useful for various wireless system designers to have a general statistical model that encompasses both of these random processes. To model the small-scale fading channel, various fading models such as Rayleigh, Rician and Nakagami have been proposed in [2]. In addition to the multipath fading in the wireless environment, the quality of signal is also affected due to the shadowing from various obstacles in the propagation path. The Nakagami-$m$ and Rayleigh-lognormal (R-L) are well known composite statistical distribution to model the multipath and shadowing [160-166]. As these distributions don't have closed-form mathematical solution, so it is difficult to use it. However, they have been approximated by the Generalized-K distribution [163] and K-distribution [160]. The diversity combining [167-173] is an effective technique for mitigating the detrimental effects of the multipath fading and shadowing in the wireless mobile channels.

In general, the channel capacity in fading environment is a complex expression in terms of the channel variation in time and/or frequency depending upon the transmitter's and/or receiver's knowledge of the channel side information. For the various channel side information assumptions that have been proposed, several definitions of the channel capacity have been provided. These definitions depend on the different employed power and rate adaptation policies and the existence, or not, an outage probability [22]. Earlier, the channel capacity has been studied by various researchers for different fading environment [104-110]. In [104], Goldsmith and Varaiya have examined the channel capacity of the Rayleigh fading channels under

different adaptive transmission techniques. Lee [105] has derived an expression for the channel capacity of a Rayleigh fading channel. In [106], Gunther has extended the results presented in [105] by deriving the channel capacity of Rayleigh fading channels under diversity scheme. Alouini and Goldsmith in [107] have derived the channel capacity of Rayleigh fading channels under different diversity schemes and different rate adaptation and transmit power schemes. Other fading channels like K-fading, Nakagami, Weibull, Rician, and Hoyt fading channels were studied in [108-112]. As per best of author's knowledge, the ref. [113, 114] is the main article, which deals with the channel capacity on generalized–K fading. In [113], the channel capacity under different diversity schemes and different rate adaptation and transmit power schemes for K-fading channel has been derived. However, in [113] has limitation that the channel capacity has been analyzed only for special value of the shaping parameter that is m = 2 and moreover in [113], for calculation of channel capacity under the optimal rate constant ($C_{ora}$) policy, author shows two methods for calculation of ($C_{ora}$), first method involves Lommel function and second method shows that, when $k$ is an integer plus one half, the capacity can be expressed in the term of the more familiar sine and cosine integrals. These two methods as discussed above having complex expression for the channel capacity. In [114], the channel capacity under different diversity schemes and different rate adaptation and transmit power schemes for K-fading channel has been derived. For computation of the $C_{ORA}$, in [114] Efthymoglou et al have been taken the approximate value by calculating limit at ($a \rightarrow 1$) and formula for $C_{ORA}$ is valid for non-integer value of shaping parameters $k$ and $m$. If $k$ and $m$ are integers then formula for $C_{ORA}$ fails. In [111, 112], the characteristics function (CF) is developed for computing the ergodic channel capacity. In [112, 115], the moment generating function based (MGF) approach is proposed for computation of the channel capacity only for $C_{ORA}$ scheme by using numerical techniques. In [116], a novel MGF based approach is developed for evaluation of the channel capacity for various rate adaptations and transmit power. In [116], the integral is evaluated by using mainly two type of numerical technique and both the numerical techniques are lengthy and much more complex.

In this chapter, we have presented MGF based channel capacity analysis over Generalized-K fading channel with M-branch maximal-ratio combining (MRC)

diversity. The main contribution of this chapter consists in the evaluation the MGF function and the derived MGF function is used to evaluate a closed-form expression for the channel capacity under optimal rate adaptation (ORA) and channel inversion with fixed rate (CIFR). The derived results are obtained in the terms of well known Meijer G function, which can be easily implemented using Maple or Mathematica software.

## 7.2 GENERALIZED-K FADING CHANNEL MODEL

The channel model for M-branch MRC diversity receiver operating over a generalized-K fading channel is similar with Section 6.4 in the previous chapter and the probability density function (PDF) is given by Equation (6.8) in same chapter.

### 7.2.1 MARGINAL MOMENT GENERATING FUNCTION

In this Section, marginal MGF is evaluated of SNR of M-branch MRC diversity as Equation (5.2) and further it is used to obtain the channel capacity. The marginal MGF is defined as [155]:

$$\hat{M}(s,\gamma_0) = \int_{\gamma_o}^{\infty} e^{-s\gamma} f_\gamma(\gamma) d\gamma \tag{7.1}$$

By substituting the value of $f_\gamma(\gamma)$ from Equation (6.8) in Equation (7.1), we get:

$$\hat{M}(s,\gamma_0) = \int_{\gamma_o}^{\infty} \frac{2}{\Gamma(mL)\Gamma(k)} (\Xi)^{(\alpha+1)/2} (\gamma)^{(\alpha-1)/2} K_\beta \left[ 2\sqrt{\Xi\gamma} \right] d\gamma \tag{7.2}$$

By putting $2\sqrt{\Xi\gamma} = t$ and after some mathematical manipulation, the Equation (7.2) can be written as:

$$\hat{M}(s,\gamma_0) = \frac{1}{(2)^{\alpha-1}\Gamma(mL)\Gamma(k)} \int_{2\sqrt{\Xi\gamma_o}}^{\infty} t^\alpha e^{-(t^2)s/4\Xi} K_\beta(t) dt \tag{7.3}$$

By expressing $K_\beta(t) = \dfrac{\left| I_{-\beta}(t) - I_\beta(t) \right|}{\sin\pi\beta}$ form [149] and putting it in Equation (7.3), we get:

$$\hat{M}(s,\gamma_0) = \frac{1}{(2)^{\alpha-1}\Gamma(mL)\,\Gamma(k)} \int\limits_{2\sqrt{\Xi\gamma_o}}^{\infty} t^{\alpha}\, e^{-(t^2)s/4\Xi}\, \frac{\left[I_{-\beta}(t)-I_{\beta}(t)\right]}{\sin\pi\beta}\, dt \tag{7.4}$$

From [149], by expressing $I_{-\beta}(t)$ and $I_{\beta}(t)$ as:

$$I_{-\beta}(t) = \sum_{p=0}^{\infty} \frac{1}{p!\,\Gamma(k-\beta+1)}\left(\frac{t}{2}\right)^{-\beta+2k} \quad \text{and} \tag{7.5}$$

$$I_{\beta}(t) = \sum_{k=0}^{\infty} \frac{1}{p!\,\Gamma(k+\beta+1)}\left(\frac{t}{2}\right)^{\beta+2k} \tag{7.6}$$

By putting the value of $I_{-\beta}(t)$ and $I_{\beta}(t)$ from the Equation (7.5) and (7.6), respectively in the Equation (7.4), we get:

$$\hat{M}(s,\gamma_0) = \frac{1}{(2)^{\alpha-1}\Gamma(mL)\,\Gamma(k)\sin\pi\beta} \int\limits_{2\sqrt{\Xi\gamma_o}}^{\infty} t^{\alpha}\, e^{-(t^2)s/4\Xi}\left( \sum_{p=0}^{\infty} \frac{1}{p!\,\Gamma(p-\beta+1)}\left(\frac{t}{2}\right)^{-\beta+2p} - \sum_{k=0}^{\infty} \frac{1}{p!\,\Gamma(p+\beta+1)}\left(\frac{t}{2}\right)^{\beta+2p} \right) dt$$
$$\tag{7.7}$$

By changing the order of integration in Equation (7.7), we get:

$$\hat{M}(s,\gamma_0) = \frac{1}{(2)^{\alpha-1}\Gamma(mL)\,\Gamma(k)\sin\pi\beta}\left( \sum_{p=0}^{\infty} \frac{1}{p!\,\Gamma(p-\beta+1)(2)^{-\beta+2k}} \int\limits_{2\sqrt{\Xi\gamma_o}}^{\infty} t^{\alpha-\beta+2p}\, e^{-(t^2)s/4\Xi}\, dt - \right.$$

$$\left. \sum_{p=0}^{\infty} \frac{1}{p!\,\Gamma(p+\beta+1)(2)^{\beta+2p}} \int\limits_{2\sqrt{\Xi\gamma_o}}^{\infty} t^{\alpha+\beta+2p}\, e^{-(t^2)s/4\Xi}\, dt \right) \tag{7.8}$$

Say $I_1 = \int\limits_{2\sqrt{\Xi\gamma_o}}^{\infty} t^{\alpha-\beta+2p}\, e^{-(t^2)s/4\Xi}\, dt$ \hfill (7.9)

$$I_2 = \int\limits_{2\sqrt{\Xi\gamma_o}}^{\infty} t^{\alpha+\beta+2p}\, e^{-(t^2)s/4\Xi}\, dt \tag{7.10}$$

Now evaluation of $I_1$ as given by Equation (7.9), is obtained as given below:

$$I_1 = \int\limits_{2\sqrt{\Xi\gamma_o}}^{\infty} t^{\alpha-\beta+2p}\, e^{-(t^2)s/4\Xi}\, dt$$

Using [149 Equation (3.381.3)] and after some mathematical manipulation, the Equation (7.9) can be expressed as:

$$I_1 = (2)^{\alpha-\beta+2p}(\Xi)^{\frac{\alpha-\beta+2p+1}{2}}(s)^{-\frac{(\alpha-\beta+2p+1)}{2}}\Gamma\left(\frac{\alpha-\beta+2p+1}{2},\gamma_0 s\right) \tag{7.11}$$

Similarly, $I_2$ can be expressed as given below:

$$I_2 = (2)^{\alpha+\beta+2p}(\Xi)^{\frac{\alpha+\beta+2p+1}{2}}(s)^{-\frac{(\alpha+\beta+2p+1)}{2}}\Gamma\left(\frac{\alpha+\beta+2p+1}{2},\gamma_0 s\right) \tag{7.12}$$

By substituting the value of $I_1$ and $I_2$ in Equation (7.8), marginal MGF can be expressed as:

$$\hat{M}(s,\gamma_0) = \frac{1}{\Gamma(mL)\,\Gamma(k)\sin\pi\beta}\left(\sum_{p=0}^{\infty}\frac{2}{p!\Gamma(p-\beta+1)}(\Xi)^{\frac{\alpha-\beta+2p+1}{2}}(s)^{-\frac{(\alpha-\beta+2p+1)}{2}}\Gamma\left(\frac{\alpha-\beta+2p+1}{2},\gamma_0 s\right)-\right.$$

$$\left.\sum_{p=0}^{\infty}\frac{1}{p!\Gamma(p+\beta+1)}(\Xi)^{\frac{\alpha+\beta+2p+1}{2}}(s)^{-\frac{(\alpha+\beta+2p+1)}{2}}\Gamma\left(\frac{\alpha+\beta+2p+1}{2},\gamma_0 s\right)\right) \tag{7.13}$$

If we put lower limit $\gamma_0 = 0$ in Equation (7.13), then marginal MGF changes to MGF. MGF for generalized-K fading channel is similar with Equation (6.10) as discussed in the previous chapter.

## 7.3 MARGINAL MGF-BASED CHANNEL CAPACITY ANALYSIS

The channel capacity has been used as the fundamental information theoretic performance measure to predict the maximum information rate of a communication system. It is extensively used as the basic tool for the analysis and design of new and more efficient techniques to improve the spectral efficiency of modern wireless communication systems and to gain insight into how to counteract the detrimental effects of the multipath fading propagation via opportunistic and adaptive communication methods. The main reason for the analysis of the spectral efficiency over fading channels is represented by the fact that most framework described in various literature make use of the so-called PDF based approach of the received SNR to be applied, which is a task that might be very cumbersome for most system setups and often require to manage expression including series. It is also well known that a prior knowledge of channel state information at the transmitter may be exploited to

improve the channel capacity such that in the low SNR regime, the maximum achievable data rate of a fading channel might be much larger than when there is no fading. The MGF and CF based approaches have extensively been used for analyzing average bit error rate probability and outage probability. Alouini et al [170] have also pointed out the complexity of using and generalizing MGF and CF based approaches for channel capacity computation. Moreover, the application of the PDF based approach for channel capacity computation turns out to be in evident counter tendency with recent advances on performance analysis of digital communication over fading channels. Several researchers [171-174] have clearly shown the potential of using either an MGF or CF–based approach for simplifying the analysis in most situation of interest with the computation of important performance parameters where the application of PDF based approach seems impractical. Recent advances on the performance analysis of digital communication systems in fading channels has recognized the potential importance of the MGF or Laplace transforms as a powerful tools for simplifying the analysis of diversity communication systems. This led to simple expressions to average bit and symbol-error-rate for wide variety of digital communication scheme on fading channels including multipath reception with correlated diversity [173-174]. Key to these developments was the transformation of the conditional error-rate expressions into different equivalent forms in which the conditional variable appears only as an exponent. In this section, we have proposed some alternative expressions for the channel capacity computation relying on the knowledge of the MGF, $M_\gamma(.)$ of $\gamma$. We have obtained novel expression for $C_{ORA}, C_{CIFRr}$, $C_{OPRA}$ and $C_{TCIFR}$ schemes using a novel marginal MGF based channel capacity analysis approach.

### 7.3 .1 OPTIMAL RATE ADAPTATION

When transmitter power remains constant, usually as a result of channel state information being available at receiver side, the channel capacity with optimal rate adaptation ($C_{ORA}$) in the terms of MGF based approach can be expressed as [112]:

$$C_{ORA} = \frac{1}{\ln(2)} \int_0^\infty \frac{e^{-s}(1 - M(s))}{s} ds \qquad (7.14)$$

$$I_3 = \frac{1}{\ln(2)} \int_0^\infty \frac{e^{-s}}{s}\, ds \tag{7.15}$$

and

$$I_4 = -\frac{1}{\ln(2)} \int_0^\infty \frac{e^{-s} M(s)}{s}\, ds \tag{7.16}$$

From (7.15) by putting the values $M(s)$ in $I_4$ that is Equation (7.16), we get:

$$I_4 = -\frac{1}{\ln(2)} \int_0^\infty \frac{e^{-s}\, \dfrac{(\Xi/s)^{\frac{\alpha+1}{2}}}{\Gamma(mL)\Gamma(k)}\, G_{1\ \ 2}^{2\ \ 1}\!\left[\frac{\Xi}{s}\,\middle|\, \begin{matrix} (1-\alpha)/2 \\ \beta/2 \quad -\beta/2 \end{matrix}\right]}{s}\, ds \tag{7.17}$$

By putting $s = \Xi t$ and after some mathematical manipulation, the Equation (7.17) can be expressed as:

$$I_4 = -\frac{(\Xi)^{\frac{\alpha+1}{2}}}{\ln(2)\Gamma(mL)\Gamma(k)} \int_0^\infty e^{-\Xi t}\, t^{-\left(\frac{\alpha+3}{2}\right)} G_{1\ \ 2}^{2\ \ 1}\!\left[\frac{1}{t}\,\middle|\, \begin{matrix} (1-\alpha)/2 \\ \beta/2 \quad -\beta/2 \end{matrix}\right] dt \tag{7.18}$$

In order to make integral more simpler by using [157 Equation (8.2.2.14)], we get:

$$G_{1\ \ 2}^{2\ \ 1}\!\left[\frac{1}{t}\,\middle|\, \begin{matrix} (1-\alpha)/2 \\ \beta/2 \quad -\beta/2 \end{matrix}\right] = G_{1\ \ 2}^{2\ \ 1}\!\left[t\,\middle|\, \begin{matrix} 1-\beta/2 \quad 1+\beta/2 \\ (\alpha+1)/2 \end{matrix}\right] \tag{7.19}$$

The Equation (7.18) can be expressed as:

$$I_4 = -\frac{(\Xi)^{\frac{\alpha+1}{2}}}{\ln(2)\Gamma(mL)\Gamma(k)} \int_0^\infty e^{-\Xi t}\, t^{-\left(\frac{\alpha+3}{2}\right)} G_{1\ \ 2}^{2\ \ 1}\!\left[t\,\middle|\, \begin{matrix} 1-\beta/2 \quad 1+\beta/2 \\ (\alpha+1)/2 \end{matrix}\right] dt \tag{7.20}$$

From [25 Equation (2.24.3.1)], the Equation (7.20) can be expressed as:

$$I_4 = -\frac{(\Xi)^{\frac{\alpha+1}{2}}}{\ln(2)\Gamma(mL)\Gamma(k)}\, G_{1\ \ 3}^{2\ \ 1}\!\left[\frac{1}{\Xi}\,\middle|\, \begin{matrix} 1+(\alpha+1)/2 \quad 1-\beta/2 \quad 1+\beta/2 \\ (\alpha+1)/2 \end{matrix}\right] \tag{7.21}$$

Expression $I_3$ shown in the Equation (7.15), is singular is at zero and diverging between 0 to 1. So after approximation, Equation (7.15) can be expressed as:

$$I_3 = \frac{1}{\ln(2)} \int_1^\infty \frac{e^{-s}}{s}\, ds \tag{7.22}$$

From [23] the above integral can be written as:

$$I_3 = \frac{0.21938}{\ln(2)} \tag{7.23}$$

By substituting results of eq. (7.21) and (7.23) in (7.14), $C_{ORA}$ can be expressed as:

$$C_{ORA} = \frac{1}{\ln(2)} \left[ 0.21938 - \frac{(\Xi)^{\frac{\alpha+1}{2}}}{\Gamma(mL)\Gamma(k)} G_{1\ \ 3}^{2\ \ 1} \left[ \frac{1}{\Xi} \middle| \begin{matrix} 1+(\alpha+1)/2 & 1-\beta/2 & 1+\beta/2 \\ (\alpha+1)/2 & & \end{matrix} \right] \right] \tag{7.28}$$

$$C_{ORA} \approx -\frac{1}{\ln(2)} \frac{(\Xi)^{\frac{\alpha+1}{2}}}{\Gamma(mL)\Gamma(k)} G_{1\ \ 3}^{2\ \ 1} \left[ \frac{1}{\Xi} \middle| \begin{matrix} 1+(\alpha+1)/2 & 1-\beta/2 & 1+\beta/2 \\ (\alpha+1)/2 & & \end{matrix} \right] \tag{7.29}$$

The above expression for the capacity with ORA policy evaluates correctly for arbitrary non-integer values of shaping parameters $k$ and $m$ whereas the limit for these special values can be obtained numerically, an approach for evaluation of $C_{ORA}$ through this is much simpler than [113] and [114]. The Equation (7.29) is also valid for non-integer value of $k$ and $m$. The channel capacity with optimal rate adaptation ($C_{ORA}$) can be calculated in closed-form, by using another method in the terms of MGF based approach as [116]:

$$C_{ORA} = \frac{1}{\ln(2)} \int_0^\infty E_i(-s) M_\gamma^{(1)}(s) ds \tag{7.30}$$

where $E_i(\cdot)$ denotes the exponential integral function defined in [157] and $M_\gamma^{(1)}(s)$ is the first derivative of MGF. By expressing $E_i(-s)$ as [157 Equation (8.4.11.1)] and by putting value Equation (6.10) in the Equation (7.30), we get:

$$I_5 = -\frac{(\Xi)^{\frac{\alpha+1}{2}}}{\Gamma(mL)\Gamma(k)} \int_0^\infty G_{1\ \ 2}^{2\ \ 0} \left[ s \middle| \begin{matrix} 1 \\ 0 & 0 \end{matrix} \right] \frac{d}{ds} \left( (s)^{-(\alpha+1)/2} G_{1\ \ 2}^{2\ \ 1} \left[ \frac{\Xi}{s} \middle| \begin{matrix} (1-\alpha)/2 & \\ \beta/2 & -\beta/2 \end{matrix} \right] \right) ds \tag{7.31}$$

By using [157 Equation (8.2.1.35)] along with [157 Equation (8.2.1.14)] and by putting $s = \Xi t$, the integral given in Equation (7.31), can be expressed as:

$$I_5 = \frac{1}{\Gamma(mL)\Gamma(k)} \int_0^\infty (t)^{-(\alpha+3)/2} G_{1\ \ 2}^{2\ \ 0} \left[ \Xi t \middle| \begin{matrix} 1 \\ 0 & 0 \end{matrix} \right] G_{2\ \ 1}^{1\ \ 2} \left[ t \middle| \begin{matrix} 1-\beta/2 & 1+\beta/2 \\ 1+(\alpha+1)/2 & \end{matrix} \right] dt \tag{7.32}$$

From [157 Equation (2.24.1)], the integral $I_5$ in Equation (7.32), can be expressed as:

$$I_5 = \frac{(\Xi)^{\frac{\alpha+1}{2}}}{\Gamma(mL)\Gamma(k)} G_{4\ 2}^{1\ 4}\left[\frac{1}{\Xi}\middle|\begin{array}{cccc}1-\beta/2 & 1+\beta/2 & 1+(\alpha+1)/2 & 1+(\alpha+1)/2\\ 1+(\alpha+1)/2 & (\alpha+1)/2 & &\end{array}\right] \tag{7.33}$$

By putting $I_5$ in (7.30), $C_{ORA}$ can be expressed as:

$$C_{ORA} = \frac{1}{\ln(2)}\frac{(\Xi)^{\frac{\alpha+1}{2}}}{\Gamma(mL)\Gamma(k)} G_{4\ 2}^{1\ 4}\left[\frac{1}{\Xi}\middle|\begin{array}{cccc}1-\beta/2 & 1+\beta/2 & 1+(\alpha+1)/2 & 1+(\alpha+1)/2\\ 1+(\alpha+1)/2 & (\alpha+1)/2 & &\end{array}\right] \tag{7.34}$$

## 7.3.2 OPTIMAL SIMULTANEOUS POWER AND RATE ADAPTATION

The channel capacity in case of optimal simultaneous power and rate adaptation policy is evaluated numerically by using standard software like Mapple and Mathematica similarly as discussed in Chapter 5. To obtain the optimal cut-off SNR, $\gamma_\circ$, we need to solve MMGF based Equation (5.34) as given below.

$$\frac{\hat{M}(0,\gamma_\circ)}{\gamma_\circ} - \int_0^\infty \hat{M}(s,\gamma_\circ)\,ds = 1 \tag{7.35}$$

$$I_6 = \int_0^\infty \hat{M}(s,\gamma_0)\,ds \tag{7.36}$$

$$I_7 = \frac{\hat{M}(0,\gamma_\circ)}{\gamma_\circ} = \frac{1-P_{out}(\gamma_\circ)}{\gamma_\circ} \tag{7.37}$$

By substituting value of $\hat{M}(s,\gamma_0)$ from Equation (7.13) in Equation (7.36), we get:

$$I_6 = \int_0^\infty \frac{1}{\Gamma(mM)\Gamma(k)\sin\pi\beta}\left(\sum_{p=0}^\infty \frac{2}{p!\Gamma(p-\beta+1)}(\Xi)^{\frac{\alpha-\beta+2p+1}{2}}(s)^{-\frac{(\alpha-\beta+2p+1)}{2}}\Gamma\left(\frac{\alpha-\beta+2p+1}{2},\gamma_0 s\right) - \right.$$

$$\left.\sum_{p=0}^\infty \frac{1}{p!\Gamma(p+\beta+1)}(\Xi)^{\frac{\alpha+\beta+2p+1}{2}}(s)^{-\frac{(\alpha+\beta+2p+1)}{2}}\Gamma\left(\frac{\alpha+\beta+2p+1}{2},\gamma_0 s\right)\right)ds \tag{7.38}$$

where

$$I_8 = \int_0^\infty (s)^{-\frac{(\alpha-\beta+2p+1)}{2}}\Gamma\left(\frac{\alpha-\beta+2p+1}{2},\gamma_0 s\right)ds \text{ and} \tag{7.39}$$

$$I_9 = \int_0^\infty (s)^{-\frac{(\alpha+\beta+2p+1)}{2}} \Gamma\left(\frac{\alpha+\beta+2p+1}{2}, \gamma_0 s\right) ds \qquad (7.40)$$

By putting the value from [157 Equation (8.4.16.2)] along with [157 Equation 2.24.2.1] in Equation (7.39), $I_8$ can be written as:

$$I_8 = (\gamma_0)^{\frac{(\alpha-\beta+2p-1)}{2}} \frac{\Gamma\left(\frac{1-(\alpha-\beta+2p)}{2}\right)}{\Gamma\left(1+\frac{1-(\alpha-\beta+2p)}{2}\right)} \qquad (7.41)$$

Similarly,

$$I_9 = (\gamma_0)^{\frac{(\alpha+\beta+2p-1)}{2}} \frac{\Gamma\left(\frac{1-(\alpha+\beta+2p)}{2}\right)}{\Gamma\left(1+\frac{1-(\alpha+\beta+2p)}{2}\right)} \qquad (7.42)$$

By substituting value of $I_8$ and $I_9$ from Equation (7.41) and (7.42), respectively to Equation (7.38), we get:

$$I_6 = \frac{1}{\Gamma(mM)\Gamma(k)\sin\pi\beta} \left( \sum_{p=0}^\infty \frac{2}{p!\Gamma(p-\beta+1)}(\Xi)^{\frac{\alpha-\beta+2p+1}{2}} \frac{\Gamma\left(\frac{1-(\alpha-\beta+2p)}{2}\right)}{\Gamma\left(1+\frac{1-(\alpha-\beta+2p)}{2}\right)} \right.$$
$$\left. - \sum_{p=0}^\infty \frac{2}{p!\Gamma(p+\beta+1)}(\Xi)^{\frac{\alpha+\beta+2p+1}{2}} \frac{\Gamma\left(\frac{1-(\alpha+\beta+2p)}{2}\right)}{\Gamma\left(1+\frac{1-(\alpha+\beta+2p)}{2}\right)} \right) \qquad (7.43)$$

For the evaluation of integral $I_7$, $P_{out}(\gamma_\circ)$ evaluated is evaluated first. From Equation (5.51) along with (6.8), $P_{out}(\gamma_\circ)$ can be expressed as:

$$P_{out}(\gamma_\circ) = \int_0^{\gamma_\circ} \frac{2(\gamma)^{(\alpha-1)/2}(\Xi)^{(\alpha+1)/2}}{\Gamma(mM)\Gamma(k)} K_\beta\left[2\sqrt{\Xi\gamma}\right] d\gamma$$

$$P_{out}(\gamma_\circ) = 1 - \int_{\gamma_\circ}^\infty \frac{2(\gamma)^{(\alpha-1)/2}(\Xi)^{(\alpha+1)/2}}{\Gamma(mM)\Gamma(k)} K_\beta\left[2\sqrt{\Xi\gamma}\right] d\gamma \qquad (7.44)$$

By replacing $K_\beta(\cdot)$ as [157 Equation (8.4.23.1)] and applying [157 Equation 2.24.2.3] in the Equation (7.44) can be expressed as:

$$P_{out}(\gamma_\circ) = 1 - \frac{(\Xi\gamma_\circ)^{(\alpha+1)/2}}{\Gamma(mM)\Gamma(k)} G_{1\ 3}^{3\ 0}\left[\begin{array}{ccc} 1-(\alpha+1)/2 \\ -(\alpha+1)/2 & \beta/2 & -\beta/2 \end{array}\right] \tag{7.45}$$

From Equation (7.37), integral $I_7$ can be expressed as:

$$I_7 = \frac{(\Xi\gamma_\circ)^{(\alpha+1)/2}}{\gamma_\circ\,\Gamma(mM)\Gamma(k)} G_{1\ 3}^{3\ 0}\left[\begin{array}{ccc} 1-(\alpha+1)/2 \\ -(\alpha+1)/2 & \beta/2 & -\beta/2 \end{array}\right] \tag{7.46}$$

By putting result $I_6$ and $I_7$ in Equation (7.35), we get:

$$\frac{(\Xi\gamma_\circ)^{(\alpha+1)/2}}{\gamma_\circ\,\Gamma(mM)\Gamma(k)} G_{1\ 3}^{3\ 0}\left[\begin{array}{ccc} 1-(\alpha+1)/2 \\ -(\alpha+1)/2 & \beta/2 & -\beta/2 \end{array}\right] - \frac{1}{\Gamma(mM)\Gamma(k)\sin\pi\beta} \times$$
$$\left(\sum_{p=0}^{\infty}\frac{2}{p!\Gamma(p-\beta+1)}(\Xi)^{\frac{\alpha-\beta+2p+1}{2}}\frac{\Gamma\left(\frac{1-(\alpha-\beta+2p)}{2}\right)}{\Gamma\left(1+\frac{1-(\alpha-\beta+2p)}{2}\right)} - \sum_{p=0}^{\infty}\frac{2}{p!\Gamma(p+\beta+1)}(\Xi)^{\frac{\alpha+\beta+2p+1}{2}}\frac{\Gamma\left(\frac{1-(\alpha+\beta+2p)}{2}\right)}{\Gamma\left(1+\frac{1-(\alpha+\beta+2p)}{2}\right)}\right) = 1 \tag{7.47}$$

In order to get optimal cut-off SNR, $\gamma_\circ$, Equation (7.47) is evaluated numerically.

### 7.3.3 CHANNEL INVERSION WITH FIXED RATE

The channel capacity for channel inversion with fixed rate ($C_{CIFR}$) scheme by using MGF based approach is used to obtain Equation (5.47), which is:

$$C_{CIFR} = \log_2\left(1 + \frac{1}{\int_0^\infty M(s)\,ds}\right) \tag{7.48}$$

For evaluation of $I_{10}$, by substituting the value M(s) from Equation (6.10) to the Equation (7.48), we get:

$$I_{10} = \int_0^\infty M(s)\,ds = \int_0^\infty \frac{(\Xi/s)^{\frac{\alpha+1}{2}}}{\Gamma(mM)\Gamma(k)} G_{1\ 2}^{2\ 1}\left[\frac{\Xi}{s}\left|\begin{array}{cc} (1-\alpha)/2 \\ \beta/2 & -\beta/2 \end{array}\right.\right]ds \tag{7.49}$$

By putting t = 1/s in Equation (7.49) and by using [157 Equation 2.24.2.1], Equation (7.49), can be expressed as:

$$I_{10} = \frac{\Xi \Gamma\big((\alpha + \beta - 1)/2\big)\Gamma\big((\alpha - \beta - 1)/2\big)}{\Gamma(mM)\Gamma(k)}$$

$$C_{CIFR} = \log_2\left(1 + \frac{\Gamma(mM)\Gamma(k)}{\Xi \Gamma\big((\alpha + \beta - 1)/2\big)\Gamma\big((\alpha - \beta - 1)/2\big)}\right) \tag{7.50}$$

So now the channel capacity for channel inversion with fixed rate scheme is:

For M = 1 and if *m* is an integer in the Equation (7.50), we get:

$$C_{CIFR} = \log_2\left(1 + \frac{\bar{\gamma}\,(m-1)(k-1)}{km}\right) \tag{7.51}$$

The above Equation is similar with [113 Equation (29)] and [114 Equation (27)]. The approach for the derivation of this Equation has been discussed in [113] and [114] is quite complicated where as the approach presented in chapter is very simple.

### 7.3.4 TRUNCATED CHANNEL INVERSION

The channel capacity for $C_{TCIFR}$ scheme is evaluated by using Equation (5.54) as:

$$C_{TCIFR} = \log_2\left(1 + \frac{1}{\int_0^\infty \hat{M}(t,\gamma_0)\,dt}\right)\left\{\hat{M}(0,\gamma_0)\right\}$$

From Equation (7.43) and from (7.45), $C_{TCIFR}$ can be expressed as

$$C_{TCIFR} = \log_2\left(1 + \frac{1}{\frac{1}{\Gamma(mL)\Gamma(k)\sin \pi\beta}\left(\sum_{p=0}^{\infty}\frac{2}{p!\Gamma(p-\beta+1)}(\Xi)^{\frac{\alpha-\beta+2p+1}{2}}\frac{\Gamma\left(\frac{1-(\alpha-\beta+2p)}{2}\right)}{\Gamma\left(1+\frac{1-(\alpha-\beta+2p)}{2}\right)} - \sum_{p=0}^{\infty}\frac{2}{p!\Gamma(p+\beta+1)}(\Xi)^{\frac{\alpha+\beta+2p+1}{2}}\frac{\Gamma\left(\frac{1-(\alpha+\beta+2p)}{2}\right)}{\Gamma\left(1+\frac{1-(\alpha+\beta+2p)}{2}\right)}\right)}\frac{(\Xi\gamma_\circ)^{(\alpha+1)/2}}{\Gamma(mM)\Gamma(k)}G_{1\ 3}^{3\ 0}\left[\begin{array}{c|ccc} & 1-(\alpha+1)/2 \\ & -(\alpha+1)/2 & \beta/2 & -\beta/2\end{array}\right]\right) \tag{7.64}$$

### 7.4 RESULT AND DISCUSSION

In this section, we have presented some numerical results for the channel capacity with MRC diversity over generalized-K fading channel. The proceeding performed

under infrequent light and frequent heavy shadowing. The corresponding slandered deviations ($\sigma$) of lognormal shadowing is 0.115 to 0.806, respectively. The parameter $k$ for generalized-K fading can be computed by using moment matching approach [114, 169], that lies from $k = 1.093$ to $k = 75.11$. Figure 7.1 shows the channel capacity for optimal rate adaptation ($C_{ORA}$) versus SNR ($\bar{\gamma}$) in case of heavy shadowing ($k = 1.0931$, $m = 2$) and light shadowing ($k = 75.11$, $m=2$). As the $M$ increases form $M = 1$ to $M = 3$ channel capacity improves significantly. Figure 7.2 shows the plot of channel capacity for optimal rate adaptation ($C_{ORA}$) versus fading parameter for various values of average SNR per branch such as ($\bar{\gamma}$) = 5 dB, 10 dB and 15 dB. From the figure it is clear that as fading parameter increases, the channel capacity improves slightly and it becomes constant after certain value. Figure 7.3 depicts the channel capacity for optimal rate and power adaptation ($C_{OPRA}$) versus SNR ($\bar{\gamma}$) plot in light shadowing (k = 75.11, m =2) and heavy shadowing ($k = 1.0931$, $m = 2$) for $M = 1$, 3. By focusing on the effect shadowing, particularly in case of heavy shadowing ($k =1.0931$) the channel capacity degrades significantly as shown in Figure 7.3 and it improves with the increase of $M$. Figure 7.4 shows the channel capacity for channel inversion with fixed rate ($C_{CIFR}$) as a function SNR ($\bar{\gamma}$) for light shadowing ($k = 75.11$, $m =2$) and heavy shadowing ($k = 1.0931$, $m = 2$).

For heavy shadowing, the channel capacity ($C_{CIFR}$) improves less with increase of SNR ($\bar{\gamma}$) and for light shadowing ($C_{CIFR}$) increases rapidly. Figure 7.5 shows the plot of channel capacity for channel inversion with fixed rate ($C_{CIFR}$) versus fading parameter, m, for various values of the average SNR per branch such as ($\bar{\gamma}$) = 5 dB, 10 dB and 15 dB. The channel capacity improves slightly with increase of fading parameters and it becomes constant after certain values of $m$. Figure 7.6 shows dependence of Channel capacity with truncated channel inversion ($C_{TCIFR}$) on cutoff SNR ($\gamma_0$), for various values of SNR ($\bar{\gamma}$) and shadowing, k. All curves shows that ($C_{TCIFR}$) is maximized for an optimal value of cutoff SNR and optimal cut-off rate increases with the increase of SNR ($\bar{\gamma}$). Figure 7.7 shows the dependency of channel capacity with truncated channel inversion ($C_{TCIFR}$) on MRC diversity receivers at various values of shadowing, as the number of diversity receivers increases the

channel capacity improves significantly. In the Figure 7.8, comparison of the channel capacity of proposed MGF based method and PDF based method [113] for various value of shadowing parameters and diversity receivers is shown.
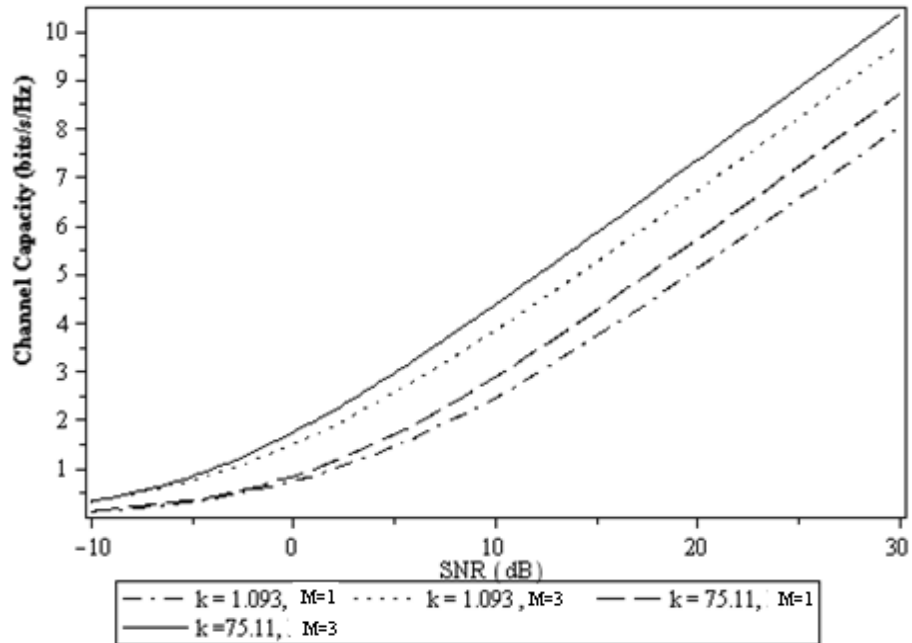


**Figure 7.1** The channel capacity for optimal rate adaptation ($C_{ORA}$) versus SNR for heavy shadowing ($k = 1.0931$) and light shadowing ($k = 75.11$).
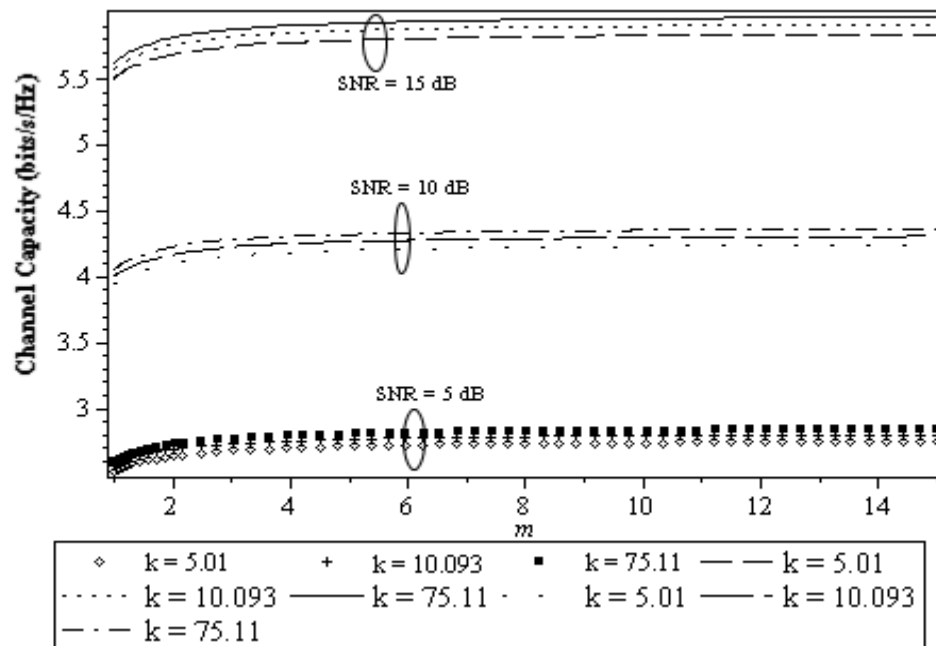


**Figure 7.2** The channel capacity for optimal rate adaptation ($C_{ORA}$) versus fading parameter.

The PDF based approach which is discussed in detail in [113] is only valid for fixed value of the shaping parameter (i.e. $m = 2$) but the MGF based proposed method discussed in this chapter is valid for any arbitrary chosen values of the shaping parameter $m$.
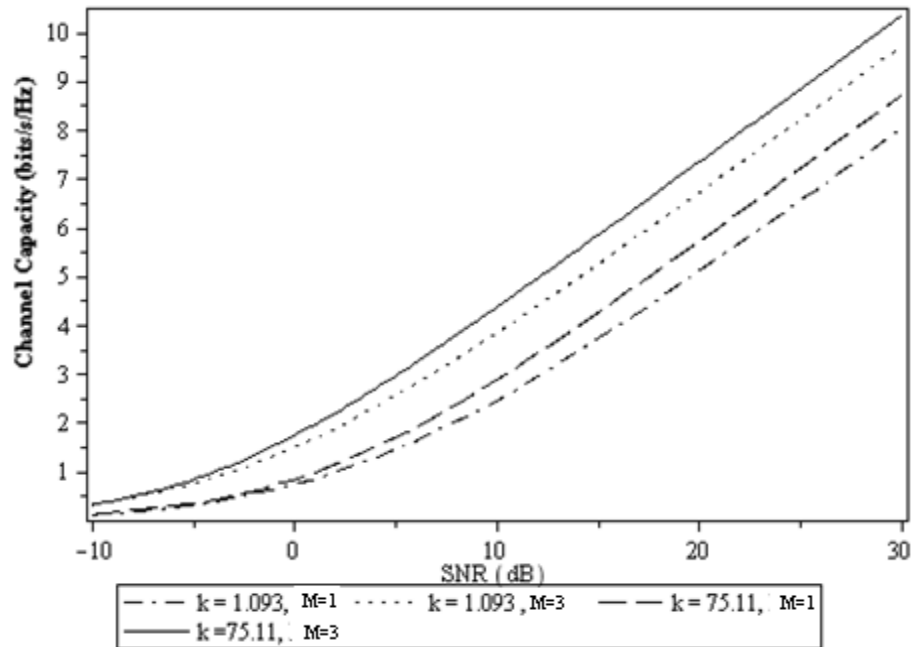


**Figure 7.3** The channel capacity for optimal rate and power adaptation $(C_{OPRA})$ versus SNR plot for heavy shadowing (k = 1.0931) and light shadowing (k = 75.11).
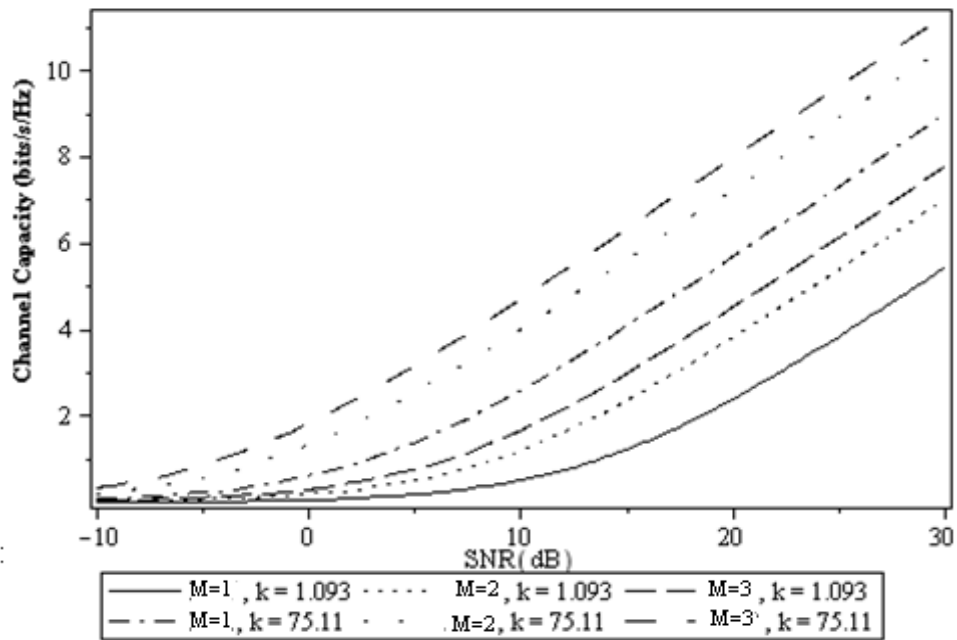


**Figure 7.4** The channel capacity for channel inversion with fixed rate $(C_{CIFR})$ versus SNR for light shadowing (k = 75.11) and heavy shadowing (k = 1.0931).
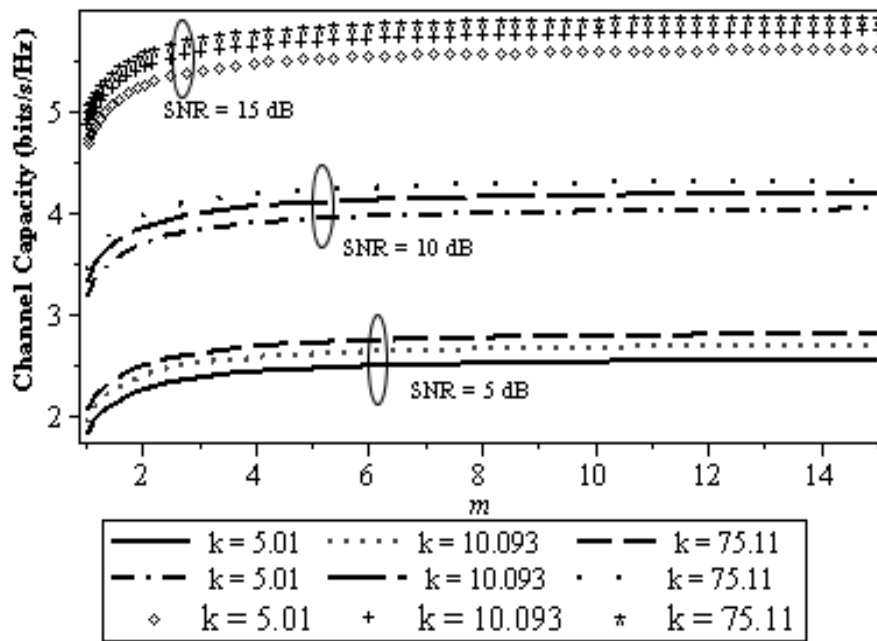
**Figure 7.5** The channel capacity for channel inversion with fixed rate $(C_{CIFR})$ versus fading parameter.
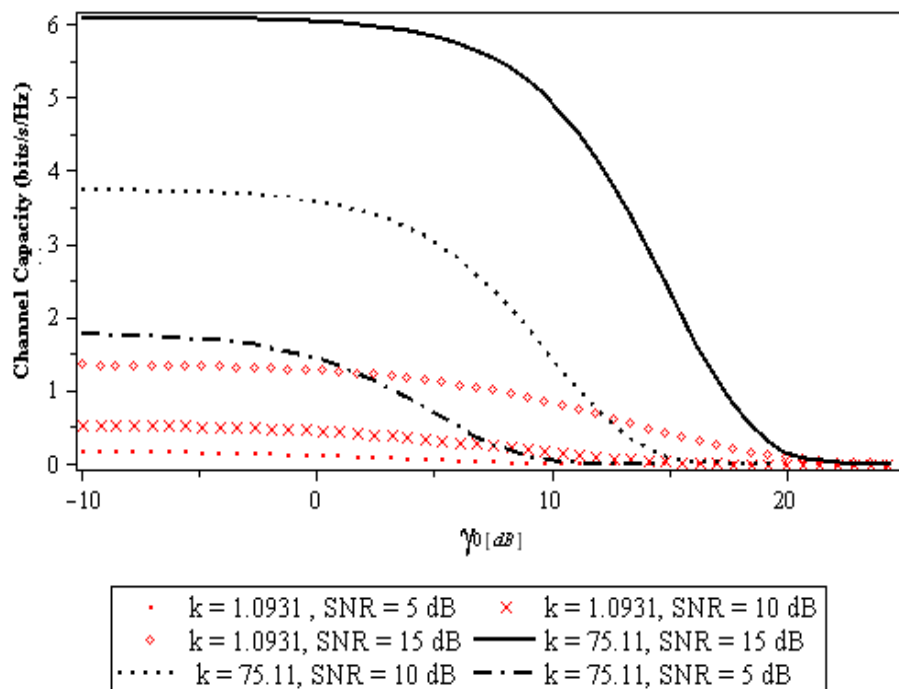


**Figure 7.6** The channel capacity with truncated channel inversion $(C_{TCIFR})$ versus cut-off SNR $(\gamma_0)$, MRC diversity $(M = 1)$.
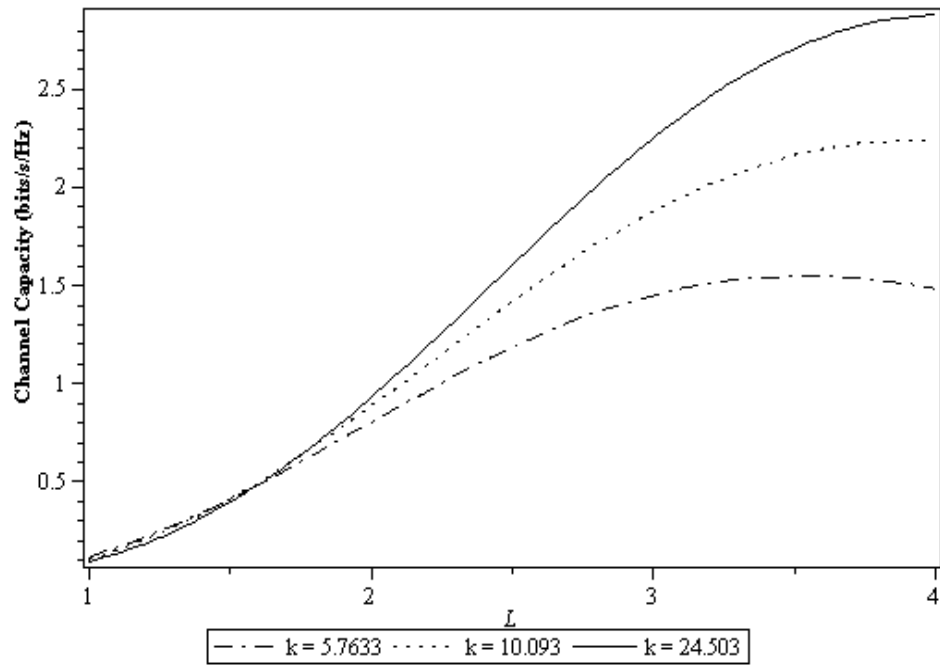
**Figure 7.7** The channel capacity with truncated channel inversion ($C_{TCIFR}$) versus MRC diversity, cutoff $(\gamma_0)$ = 10 dB and average SNR $(\bar{\gamma})$ =15 dB for various values of shadowing parameters.
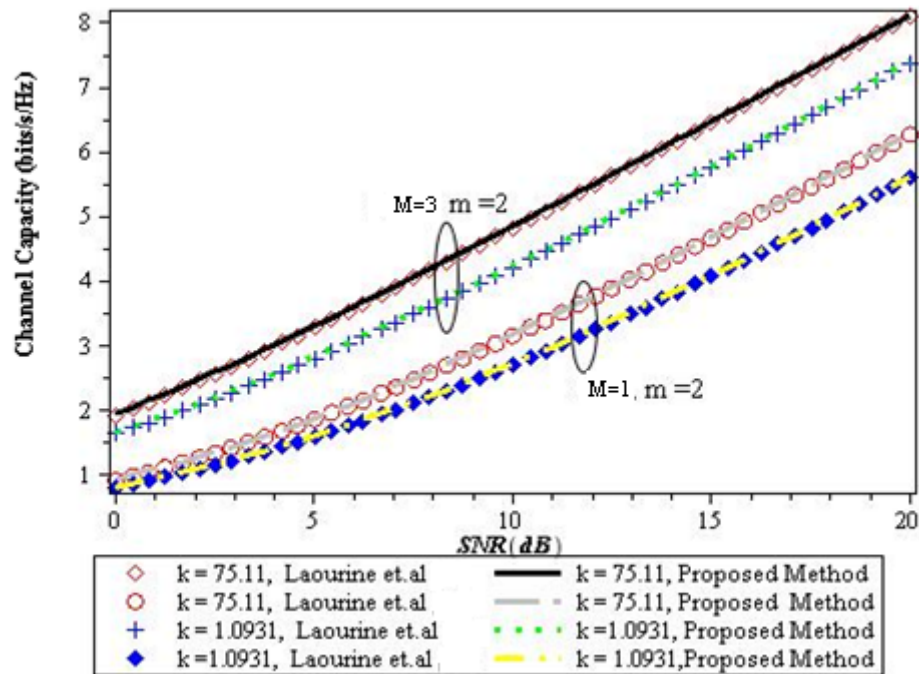


**Figure 7.8** Comparison of channel capacity for optimal rate adaptation ($C_{ora}$) with proposed method and PDF based method [113].
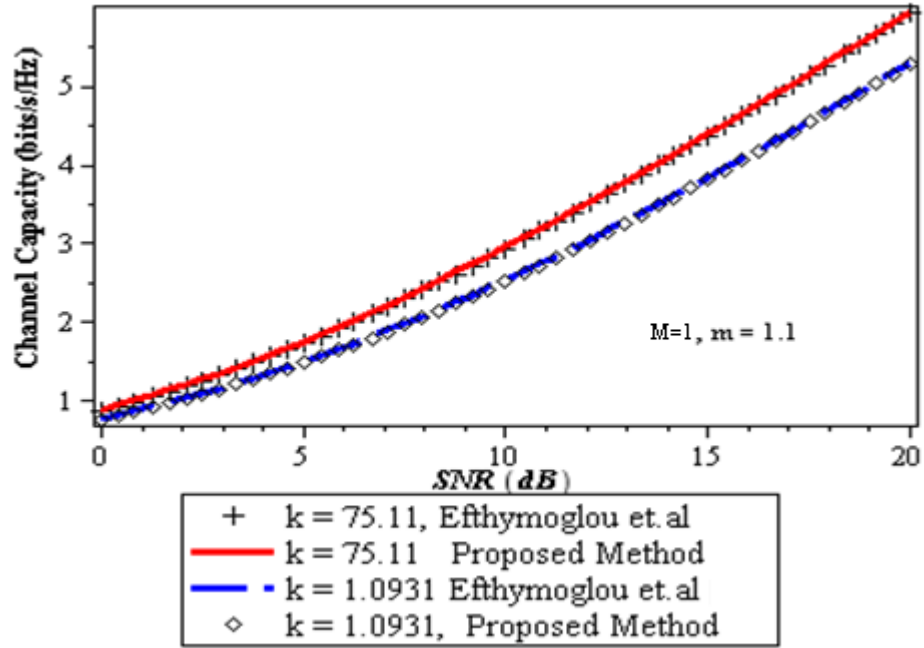
**Figure 7.9** Comparison of the channel capacity for optimal rate adaptation ($C_{ora}$)) with proposed method and PDF based method [114].

The Figure 7.9 shows the comparison of channel capacity of the proposed MGF based method and PDF based method as reported in [114]. The PDF based method in approximates ($C_{ora}$) at $a = 1$ and also approach is valid only for non-integer value of $k$ and $m$.

## 7.5 CONCLUSION

In this Chapter, we have obtained the mathematical expression for the marginal MGF for generalized-K fading channel with M-branch MRC diversity. Also, the obtained marginal MGF function is used to evaluate channel capacity under different adaptation policies. We derived the expression of channel capacity with optimal rate adaptation ($C_{ORA}$) which valid for arbitrary value of the shaping parameters k and m. We also derived expression for capacity for channel inversion with fixed rate ($C_{CIFR}$). The $C_{ORA}$ and $C_{CIFR}$ is very easily calculated using MGF based approach and for $M = 1$, $C_{CIFR}$ is calculated by using Equation (25) is similar with [113 eq. 29] and [114 eq. 27]. In this work, we also derived marginal MGF based channel capacity for truncated channel inversion ($C_{TCIFR}$) and for optimal rate and power adaptation ($C_{OPRA}$) schemes for Generalized-K fading channel, which is novel and can be applied to other fading channels also.

# CONCLUSION AND FUTURE SCOPE

Physical layer design is a very important part of the communication system and has a profound impact on the feasibility of the communication processes at the higher layers. OFDM-based transmission is a promising candidate to achieve high data rates via collective usage of a large number of subcarrier bands. This modulation technique allows digital data to be transmitted over a radio channel by using a large number of narrow bandwidth subcarriers and offer several advantages over other transmission technologies such as high spectral efficiency, robustness to fading channel, immunity to impulse interference, and capability of handling very strong multi-path fading and frequency selective fading without having to provide powerful channel equalization. However, one of the major disadvantages of OFDM communication is its sensitivity against carrier frequency offset, which causes inter-carrier interference and degrades the performance of the system. The carrier frequency offset is caused by the mismatch of frequencies between the oscillators of transmitter and receiver, or by the Doppler spread due to the relative movement between the transmitter and receiver as well as phase noise arises predominantly due to imperfections of the local oscillator in the transceiver. However, the ICI induced by phase noise and timing offset can be completely compensated or corrected. Since the Doppler spread or frequency shift is random, so we can only mitigate its impact in the system. A simple and most effective method, which is known as self-cancellation scheme, reduces the ICI at the cost of transmission rate with little additional computational complexity.

In this thesis, we have investigated an efficient ICI cancellation technique and developed a novel mathematical model to improve the bit-error-rate and carrier-to-interference ratio compared to the other techniques as reported in literature. In the proposed OFDM system, at the transmitter, IFFT is performed for first part of the data and FFT for the second part of data. At the receiver, FFT is performed for first part of the data and IFFT for the second part of data. These combined operation forms an ICI cancellation scheme for the OFDM system. We analyze the subcarrier index before

and after cancellation of the frequency offset and discuss the carrier-to-interference ratio. The average carrier-to-interference power ratio is used as the ICI level indicator and theoretically carrier-to-interference ratio expression is derived for the proposed scheme. The proposed scheme provides significant carrier-to-interference ratio improvement, which has been studied theoretically and supported by simulations.

A repeated correlative coding scheme is also proposed to combat ICI caused by the frequency offset in OFDM communication systems. This proposed scheme combine two ideas of the well-known methods, which are the coding of adjacent subcarriers with antipodal of the same data symbol (ICI self-cancellation) and correlative coding. A mathematical expression for the carrier-to-interference ratio by using this proposed repeated correlative coding scheme is derived. The carrier-to-interference ratio for proposed scheme is significantly improved compared to the correlative coding as well as self-cancellation scheme. The bit-error-rate of proposed scheme is also compared with the ICI self-cancellation scheme and correlative coding scheme, which is comparable to that of the ICI self-cancellation scheme and much better than correlative coding scheme. The proposed theoretical analysis and simulation results prove that the ICI caused by multicarrier frequency offset can be cancelled efficiently by using the proposed repeated correlative coding scheme for the OFDM communication system. However, to statistically model the wireless channels, it is a very common practice to consider two independent propagation models, the small-scale propagation model for random amplitude and phase variations and large-scale propagation model for power (shadowing and path loss) variation. Several distributions have been discussed to model the small-scale fading such as the Rayleigh, Rician and Nakagami-m in detail. The Rayleigh and Rician distributions are used to characterize the channel envelop of faded signal over small geographical areas or short term fades.

Recently, the Nakagami-m fading channel model has received considerable attention due to its great flexibility and accuracy. In studying the performance of wireless communication system, it is usually assumed that two signals are independent of one another, however, there are number of real-life scenario in which this assumption is not valid. Therefore, the effect of correlated fading on the performance of a diversity combining receiver has received a great deal of research

interest. We have analyzed the performance of correlated Nakagami-m fading channel by using the maximal-ratio combining diversity at the receiver. A closed-form mathematical expression is derived for the average bit-error-rate, symbol-error-rate and outage probability for various modulation scheme in terms of the higher transcendental function such as Appell hypergeometric function by using the well-known moment generating function based approach with arbitrary fading index for OFDM communication systems. The diversity path greater than two (M ≥ 2) at the receiver hence the average bit-error-rate performance of the OFDM system is improved significantly. The proposed mathematical analysis is used to study various novel performance evaluation results with parameters of interest such as fading severity and correlation coefficients, which is very significant for the design consideration of the OFDM communication systems.

In the wireless communication systems, the multipath fading of the signal is important phenomena, which limits the channel capacity. We have investigated the marginal moment generating function (MMGF) for the correlated Nakagami-$m$ fading channel by using maximal-ratio combining diversity scheme at receiver for the computation of the channel capacity for various adaptive transmission schemes such as: 1) optimal simultaneous power and rate adaptation, 2) optimal rate adaptation with constant transmit power, 3) channel inversion with fixed rate, and 4) truncated channel inversion with fixed rate. An analytical expression for the channel capacity as a function of signal-to-noise ratio over the correlated Nakagami-$m$ fading channel with maximal-ratio combining diversity at the receiver is obtained, which is valid for arbitrary value of the fading parameters. We have also analyzed the effect of correlation on the channel capacity. Due to their simple forms, these results offer a useful analytical tool for the accurate performance evaluation of the various communication systems of practical interest. In addition to multipath fading, the quality of signal in the wireless communication environment is also affected due to shadowing from various obstacles in propagation path. The Nakagami-$m$ and Rayleigh-lognormal (Suzuki) are well known composite statistical distribution to model the multipath fading and shadowing. The Gamma probability density function (PDF) was proposed for shadowing instead of the lognormal and the resultant PDF is called generalized-K distribution for the shadowed fading channel and the $K$-

distribution when the short term fading is modeled by using the Rayleigh instead of the Nakagami-m PDF. The K-distribution is derived as a special case of the generalized-K distribution by letting $m = 1$. The generalized-K distribution fading model characterizes the confined effect of fast and slow fading in the received signal by using two shaping parameters.

We have also investigated a simple and novel MMGF based channel capacity analysis approach over generalized-K fading channel with maximal-ratio combining diversity. Initially, an analytical expression for the MMGF of received signal-to-noise ratio with M-branch maximal-ratio combining diversity is obtained and utilizes it to derive the mathematical expression for the channel capacity under the different power and rate adaptation policies for arbitrary value of shaping parameters. The result of proposed methods is compared with other reported literature to support the analysis. We have derived the expression for the channel capacity with optimal rate adaptation ($C_{ORA}$) which is valid for arbitrary values of the shaping parameters $k$ and $m$. Moreover, we derived an expression for the capacity for channel inversion with fixed rate ($C_{CIFR}$). The $C_{ORA}$ and $C_{CIFR}$ are very easily computed by using the MGF based approach. We also derived the marginal MGF based channel capacity for truncated channel inversion with fixed rate ($C_{TCIFR}$) and channel capacity for optimal rate and power adaptation ($C_{OPRA}$) schemes for the Generalized-K fading channel, which is a simple and novel approach that can be applied to other fading channels also.

Multicarrier techniques, such as OFDM support huge data rates that are robust to channel impairments. However, with a growing demand for spectrum access, it may be difficult for any single transmission to obtain a large contiguous frequency spectrum block in dynamic spectrum access environment. Spectrum management is further complicated when considering world-wide operations. Moreover, there might be measurement-based controls on the spectrum usage, such as temporal, spectral, or energy characteristics, that would constrain the availability of the contiguous frequencies. Currently, spectrum allotment operates by providing each new service with its own fixed frequency block. Demand for access to spectrum has been growing dramatically, and is likely to continue to grow in the foreseeable future. OFDM-based transmission is a promising candidate for a flexible spectrum pooling system in dynamic spectrum access environment, where the implementation achieves high data

rates via collective usage of a large number of subcarrier bands. This modulation technique allows digital data to be transmitted over a radio channel by using a large number of narrow bandwidth subcarriers. Usually, these subcarriers are regularly spaced in frequency, forming a contiguous block of spectrum. Moreover, it is possible to turn-off subcarriers corresponding to the spectrum occupied by the incumbent users in order to avoid any interference to existing transmissions, thereby enabling secondary utilization of the unused portions of the spectrum to improve the spectrum utilization efficiency as well as mitigate apparent spectrum scarcity problem. The growing interest of studying OFDM-based cognitive radios is due to the apparent scarcity of the large spectral bandwidth for high data rate communications. OFDM based cognitive radios can handle this apparent spectrum scarcity and enable high data rate communications utilizing aggregate non-contiguous bands of spectrum.

# REFERENCES

[1] R. W. Chang, "Synthesis of band-limited orthogonal signals for multichannel data transmission," *Bell Systems Technical Journal*, vol. 46, no. 12, pp. 1775–1796, Dec. 1966.

[2] R. Prasad, "OFDM for Wireless Communications," Artech House: Boston, 2004.

[3] S. B. Weinstein and P.M. Ebert, " Data transmission by frequency division multiplexing using discrete Fourier transform" *IEEE Trans*. on *Commun*., vol. 19, pp. 628-634, Oct.1971.

[4] S. Sesia, I. Toufik and M. Baker, "LTE – the UMTS Long Term Evolution: From Theory to Practice," John Wiley and Sons: New York, 2009.

[5] H. Holma and A. Toskala, "LTE for UMTS-OFDMA and SC-FDMA Based Radio Access," John Wiley and Sons: New York, 2009.

[6] L. Cimini, "Analysis and simulation of a digital mobile channel using orthogonal frequency division multiplexing," *IEEE Trans. on Commun.*, vol. 33, no. 7, pp. 665–675, July 1985.

[7] F. Classen and H. Meyr, "Frequency synchronization algorithms for OFDM systems suitable for communication over frequency selective fading channels," *Proceedings of IEEE Veh. Technology Conf.* (VTC 94), Stockholm, Sweden, pp. 1655–1659, 8–10 Jun. 1994.

[8] S. C. Surender and R. M. Narayanan "UWB noise-OFDM netted radar: physical layer design and analysis," *IEEE Trans. on Aerospace and Electronic Systems*, vol. 47, no. 2, pp. 1380-1400, April 2011.

[9] L. Hanzo, M. M¨unster, B. Choi, and T. Keller, "OFDM and MC-CDMA for Broadband Multi-user Communications, WLANs and Broadcasting," John Wiley and IEEE Press, 2003.

[10] H. Schulze and C. Luders, "Theory and Applications of OFDMA and CDMA", John Wiley & Sons, Ltd: Chichester, UK, 2005.

[11] S. H. Han and J. H. Lee, "An overview of peak-to-average power ratio reduction techniques for multicarrier transmission," *IEEE Trans. on Wireless Commun.*, vol. 12, no. 2, pp. 56-65, Apr. 2005.

[12] J. Armstrong, "Peak-to-average power reduction for OFDM by repeated clipping and frequency domain filtering," *Electron. Lett.*, vol. 38, no. 5, pp. 246-247, Feb. 2002.

[13] L. Wang and C. Tellambura, "A simplified clipping and filtering technique for PAR reduction in OFDM systems," *IEEE Signal Process. Lett.*, vol. 12, no. 6, pp. 453-456, June 2005

[14] D. C. Cox, "Wireless personal communications: What is it?" *IEEE Pers. Commun. Mag.*, pp. 20–35, April 1995.

[15] T. S. Rappaport, "Wireless Communications – Principles and Practice," 2nd ed., Prentice-Hall: Englewood Cliffs, NJ, 2001.

[16] J. D. Vriendt, P. Lainé, C. Lerouge, and X. Xu, "Mobile network evolution: a revolution on the move," *IEEE Commun. Mag.*, pp. 104–11, April 2002.

[17] W. Stallings, "Wireless Communications and Networks," 2nd ed., Prentice-Hall: Englewood Cliffs, NJ, 2005.

[18] K. Pahlavan and P. Krishnamurthy, "Principles of Wireless Networks: A Unified Approach," Prentice-Hall: Englewood Cliffs, NJ, 2002.

[19] W. C. Jakes, Jr., "Microwave Mobile Communications," Wiley: New York, 1974 [reprinted by IEEE Press].

[20] M. Paetzold, "Mobile Fading Channels: Modelling, Analysis, and Simulation," 1st Edition. John Wiley & Sons: New York, 2002

[21] D. Parsons, "The Mobile Radio Propagation Channel," Wiley: New York, 1994.

[22] M. K. Simon and M.-S. Alouni, "Digital communication over fading channels: a unified approach to performance analysis," 2nd ed., Wiley: Hoboken, 2005.

[23] G. L. Turin, "A statistical model for urban multipath propagation," *IEEE Trans. on Vehicular Technology*, vol. 21, no. 1, pp. 1-9, 1972.

[24] W. Braun and U. Dersch, "A physical mobile radio channel model," *IEEE Trans. on Vehicular Technology*, vol. 40, no. 2, pp. 472–482, May 1991.

[25] T. K. Sarkar, Z Ji, K. Kim, A. Medour, and S. P. Magdalena, "A survey of various propagation models for mobile communication," *IEEE Antennas and Propagation Magazine*, vol. 45, no. 3, pp.51-82, Jun. 2003.

[26] A. Papoulis, "Probability, Random Variables, and Stochastic Processes," McGraw-Hill: New York, 1984.

[27] S. O. Rice, "Mathematical analysis of random noise," *Bell System Technical Journal*, vol. 23, no. 1, pp. 282–332, 1944.

[28] M. Nakagami, "The m-distribution — a general formula of intensity distribution of rapid fading," in *Statistical Methods in Radio Wave Propagation*, W. G. Hoffman, ed. Oxford, U.K.: Pergamon, 1960.

[29] B. Sklar, "Digital Communications – Fundamentals and Applications," Prentice-Hall: Englewood Cliffs, NJ, 1988.

[30] A. Goldsmith, "Wireless Communications," Cambridge University Press: New York, 2005.

[31] G. L. Stuber, "Principles of Mobile Communication," Kluwer: Norwell, MA, 2001.

[32] A. Coulson, A. Williamson, and R. Vaughan, "A statistical basis for lognormal shadowing effects in multipath fading channels," *IEEE Trans. on Commun.*, vol. 46, no. 4, pp. 494–502, Apr. 1998.

[33] D. C. Cox, R. Murray and A. Morris, "800 MHz attenuation measured in and around suburban houses," *AT &T Bell Laboratory Technical Journal*, vol. 63, no. 6, pp. 921-954, Jul. 1984.

[34] H. L. Bertoni, "Radio Propagation for Modern Wireless Systems", Upper Saddle River, NJ, Prentice Hall PTR, 2000.

[35] J. Bingham, "Multicarrier modulation for data transmission: an idea whose time has come," *IEEE Commun. Mag.*, vol. 28 no. 5 pp. 5–14, May 1990.

[36] A. R. S. Bahai, B. R. Saltzberg, and M. Ergen, "Multi-Carrier Digital Communications – Theory and Applications of OFDM," $2^{nd}$ ed., Springer-Verlag: New York, 2004.

[37] C. Eklund, R. B. Marks, K. L. Stanwood, and S. Wang, "IEEE Standard 802.16: a technical overview of the wireless MAN 326 air interface for broadband wireless access," *IEEE Commun. Mag.*, pp. 98–107, June 2002.

[38] J. M. Cioffi, "Digital Communications," Chap. 4: Multichannel Modulation, unpublished course notes, available at http: //www.stanford.edu /class/ee379c/.

[39] A. H. Ballard "A new multiplex technique for communication systems," *IEEE Trans. on Power Apparatus and Systems*, vol. 85, no. 10, pp. 1054 – 1059, Oct. 1966.

[40] Z. Wang, X. Ma, and G. B. Giannakis, "OFDM or single-carrier block transmissions?," *IEEE Trans. Commun.*, vol. 53, no. 3, pp. 380–94, March 2004.

[41] S. Kaider, "Performance of multi-carrier CDM and COFDM in fading channels," *Proc. IEEE Globecom Conf.*, Dec. 1999, Honolulu, Hawaii USA, pp. 847–851.

[42] H. Sampath, S. Talwar, J. Tellado, V. Erceg, and A. Paulraj, "A fourth-generation MIMO-OFDM broadband wireless system: design, performance, and field trial results," *IEEE Commun. Mag.*, pp. 143–9, Sept. 2002.

[43] R. C. V. Macario, "Modern Personal Radio Systems," IEE Telecommunication Series 33 (The Institution of Electrical Engineers), London, UK, 1996.

[44] M. Schwartz, "Mobile Wireless Communication," Cambridge University Press, Cambridge, 2005.

[46] J. E. Padgett, C. G. Gunther, and T. Hattori, "Overview of wireless personal communications," *IEEE Commun. Mag.*, pp. 28–41, Jan. 1995.

[47] Vijay K. Garg, "Wireless Communication and Networking," $1^{st}$ ed., Elsevier Inc.: London, 2007.

[48] H. Holma and A. Toskala, "WCDMA FOR UMTS: Radio Access for Third Generation Mobile Communications," $3^{rd}$ ed., John Wiley & sons: New York, 2004.

[49] H. Holma and A. Toskala, "WCDMA FOR UMTS: HSPA Evolution and LTE," 5th ed., John Wiley & Sons: New York, 2010.

[50] The mobile broadband evolution: 3GPP release and beyond, 3G Americas, Feb. 2009.

[51] J. Ahn and H. S. Lee, "Frequency domain equalization of OFDM signal over frequency nonselective Rayleigh fading channels," *Electron. Lett.*, vol. 29, no. 16, pp. 1476–1477, 1993.

[52] R. Li and G. Stette, "Time-limited orthogonal multicarrier modulation schemes," *IEEE Trans. Commun.*, vol. 43, no. 234, pp. 1269–1272, 1995.

[53] T. Pollet, M. V. Bladel, and M. Moeneclaey, "BER sensitivity of OFDM systems to carrier frequency offset and Wiener phases noise," *IEEE Trans. Commun.*, vol. 43, no. 234, pp. 191–193, 1995.

[54] Y. Zhao and S.-G. Haggman, "Inter-carrier interference self-cancellation scheme for OFDM mobile communication systems," *IEEE Trans. Commun.*, vol. 49, pp. 1185-1191, 2001.

[55] Y. Zhao, J.-D. Leclercq, and S.-G. Haggman, "Inter-carrier interference compression in OFDM communication systems by using correlative coding," *IEEE Commun. Lett.*, vol. 2, pp. 214–216, 1998.

[56] P. H. Moose, "A technique for orthogonal frequency division multiplexing frequency offset correction," *IEEE Trans. Commun.*, vol. 42, no. 10, pp. 2908-2914, Oct. 1994.

[57] J. Armstrong, "Analysis of new and existing methods of reducing intercarrier interference due to carrier frequency offset in OFDM", *IEEE Trans. Commun.*, vol. 47, no. 3 , pp. 365-369, Mar. 1999.

[58] C. Muschallik, "Improving an OFDM reception using an adaptive Nyquist windowing," *IEEE Trans. Consumer Electron.*, vol. 42, no. 8, pp. 259-269, Aug. 1996.

[59] V. K. Dwivedi and G Singh, "Improved BER analysis of OFDM communication system on correlated Nakagami fading channel," *Proc. Int. Conf. on Recent Advances in Microwave Theory and Applications*, India, Nov. 2008, pp.536-539.

[60] Vivek K. Dwivedi and G. Singh, "A novel bit error rate analysis and improved ICI reduction method in OFDM communication systems," *Journal of Infrared, Millimeter and Terahertz Waves*, vol. 30, no. 11, pp. 1123-1242, 2009.

[61] H.-G. Yeh and Y.-K.Chang, "A conjugate operation for mitigating intercarrier interference of OFDM systems," *Proc. Vehicular Technology Conference*, 2004, Atlanta, vol. 6, pp. 3965-3969, Sept. 26-29, 2004.

[62] Wei Bai and Y. Kim, "Effects of correlative coding on OFDM systems for intercarrier interference suppression," *IEEE Trans. Veh. Technology*, vol. 56, no. 6, pp. 3732-3738, 2007.

[63] Y. Zhang and H. Liu, "Frequency-domain correlative coding for MIMO-OFDM systems over fast fading channels," *IEEE Commun. Lett.*, vol. 10, pp. 347–349, 2006.

[64] Y. Zhang and H. Liu, "Decision-feedback receiver for quasi-orthogonal space-time coded OFDM using correlative coding over fast fading channels," *IEEE Trans. on Wireless Commun.*, vol. 5, no. 11, pp. 3017–3022, Nov. 2006.

[65] N. C. Beaulieu and P. Tan, "On the use of correlative coding for OFDM," *Proc. of IEEE Int. Conf. on Communication* (ICC 2007), June 24–28, 2007, pp. 756–761.

[66] K. Sathananathan and C. Tellambura, "Forward error correction codes to reduce inter-carrier interference in OFDM," *Proc. of IEEE Int. Symp. on Circuits and Systems* (ISCAS 2001), vol. 4, pp. 566-569, May 2001.

[67] U. Tureli, D. Kivanc and H. Liu, "Experimental and analytical studies on a high-resolution OFDM carrier frequency offset estimator", *IEEE Trans. Veh. Technol.*, vol. 50, no. 2, pp. 629-643, Mar. 2001.

[68] M. J. Fernandez-Getino Garcia, O. Edfors and J. M. Paez-Borrallo, "Frequency offset correction for coherent OFDM in wireless systems," *IEEE Trans. Cons. Elect.*, vol. 47, no. 1, pp. 187-193, Feb. 2001.

[69] V. K. Dwivedi and G Singh, "An efficient BER analysis of OFDM systems with ICI conjugate cancellation method," *PIERS Proceeding*, Cambridge, USA, July 2-6, 2008, pp. 166-171.

[70] A. Sahin, and H. Arslan, "Edge windowing for OFDM based systems," *IEEE Commun. Lett.*, vol. 5, no. 11 , pp. 1208 – 1211, Nov. 2011.

[71] R. Song and S. Leung, "A novel OFDM receiver with second order polynomial Nyquist window functions," *IEEE Commun. Lett.*, vol. 9, no. 5, pp. 391-393, May 2005.

[72] L. E. Franks, "Further results on Nyquist's problem in pulse transmission," *IEEE Trans. Commun. Technol.*, vol. 16, no. 4, pp. 337-340, Apr. 1968.

[73] S. H. M¨uller-Weinfurtner, "Optimum Nyquist windowing in OFDM receivers," *IEEE Trans. Commun.*, vol. 49, pp. 417-420, Mar. 2001.

[74] N. C. Beaulieu, C. C. Tan, and M. O. Damen, "A better than Nyquist pulse," *IEEE Commun. Lett.*, vol. 5, no. 9, pp. 367-368, Sept. 2001.

[75] J. Lee, H. Lou, D. Toumpakaris, and J. M. Cioffi, "SNR analysis of OFDM systems in the presence of carrier frequency offset for fading channels," *IEEE Trans. Wireless Commun*, vol**.** 5, no. 12, pp. 3360 - 3364, Dec. 2006.

[76] A. J. Coulson, "Maximum likelihood synchronization for OFDM using a pilot symbol: Algorithm," *IEEE J. Sel. Areas Commun.*, vol. 19, no. 12, pp. 2486–2494, 2001.

[77] Y. C. Wu, and E. Serpedin, "Data-aided maximum likelihood symbol timing estimation in MIMO correlated fading channels," *Proceedings of IEEE* Acoustics, Speech, and Signal Processing (ICASSP), vol. 4, pp. 829-832, 2004.

[78] Y. C. Wu and E. Serpedin, "Low-complexity feed forward symbol timing estimator using conditional maximum-likelihood principles," *IEEE Commun. Lett.*, vol. 8, no. 3, pp. 168-170, Mar. 2004.

[79] Y. C. Wu and E. Serpedin, "Unified analysis of a class of blind feed forward symbol timing estimators employing second-order statistics," *IEEE Trans. on Wireless Commun.*, vol. 5, no. 4, pp. 737-742, Apr. 2006.

[80] X. Li, Y. C. Wu, and E. Serpedin, "Timing synchronization in decode and forward cooperative communication systems," *IEEE Trans. Signal Processing*, vol. 57, no. 4, pp. 1444-1455, Apr. 2009.

[81] J. Chen, Y. C. Wu, S. Ma, and T. S. Ng, "Joint CFO and channel estimation for multiuser MIMO-OFDM systems with optimal training sequences," *IEEE Trans. Signal Processing*, vol. 56, no. 8, pp. 4008-4019, Aug. 2008.

[82] H. Minn, M. Zeng, and V. K. Bhargava, "On timing offset estimation for OFDM systems," *IEEE Commun. Lett.*, vol. 4, pp. 242–244, July 2000.

[83] T. Hwang, C. Yang, G. Wu, S. Li, and G. Ye Li, "OFDM and its wireless applications: a survey," *IEEE Trans. on Veh. Tech*, vol. 58, no. 4, pp. 1673-1694, May 2009.

[84] P. J. Crepeau, "Asymptotic performance of M-ary orthogonal modulation in generalized fading channels," *IEEE Trans. on Commun.*, vol. 36, no. 11, pp. 1246 – 1248, Nov. 1988.

[85] A. Annamalai, C. Tellambura, and V. K. Bhargava, "Exact evaluation of maximal-ratio and equal-gain diversity receivers for M-ary QAM on Nakagami fading channels," *IEEE Trans. Commun.*, vol. 47, no. 9, pp. 1335 – 1344, Sept. 1999.

[86] A. Annamalai, C. Tellambura and V. K. Bhargava, "Unified analysis of equal-gain diversity on Rician and Nakagami fading channels," *Proc. IEEE Wireless Commun. and Networking Conf.* (WCNC' 99), New Orleans, LA, September 21-24, 1999, vol. 1, pp. 10-14.

[87] B. Glance and L. J. Greenstein, "Frequency-selective fading effects in digital mobile radio with diversity combining," *IEEE Trans. Commun.*, vol. 31, no. 9, pp. 1085 – 1094, Sept. 1983.

[88] M. K. Simon and M.-S. Alouini, "A unified performance analysis of digital communication with dual selection combining diversity over correlated Rayleigh and Nakagami-m fading channels," *IEEE Trans. Commun.*, vol. 47, no. 1, pp. 33 – 43, Jan. 1999.

[89] G. L. Turin, "On optimal diversity reception," *IRE Trans. Inf. Theory*, vol. 7, no. 7, pp. 154 – 167, July 1961.

[90] M. A. Blanco and K. J. Zdunek, "Performance and optimization of switched diversity systems for the detection of signals with Rayleigh fading," *IEEE Trans. Commun.*, vol. 27, no. 12, pp. 1887 – 1895, Dec. 1979.

[91] A. A. Abu-Dayya and N. C. Beaulieu, "Analysis of switched diversity systems on generalized-fading channels," *IEEE Trans. Commun.*, vol. 42, no. 11, pp. 2959 – 2966, Nov. 1994.

[92] E. A Neasmith and N.C Beaulieu, "New results on selection diversity," *IEEE Trans. on Commun.*, vol. 46 , no. 5 .pp. 695 – 704, 1998.

[93] A. A. Abu-Dayya and N. C. Beaulieu, "Switched diversity on microcellular Ricean channels," *IEEE Trans. Veh. Technol.*, vol. 43, no. 4, pp. 970–976, Nov. 1994.

[94] T. Eng, N. Kong, and L. B. Milstein, "Comparison of diversity combining techniques for Rayleigh-fading channels," *IEEE Trans. Commun.*, vol. 44, no. 9, pp. 1117 – 1129, Sept. 1996.

[95] E. K. Al-Hussaini and A. M. Al-Bassiouni, "Performance of MRC diversity systems for the detection of signals with Nakagami fading," *IEEE Trans. Commun.*, vol. 33, no. 12**,** pp. 1315–1319, Dec. 1985.

[96] D. V. Bandjur, M. C. Stefanovic, and M. V. Bandjur, "Performance analysis of SSC diversity receiver over correlated Ricean fading channels in presence of co-channel interference," *Electronics Lett.*, vol. 44, no. 9, pp. 587–588, 2008.

[97] G. Rui, L. J. Lin and J. Yang, "Performance analysis of BPSK for MIMO-OFDM in Nakagami-m fading channels," *Proc. Int. Symp. Intelligent Signal Processing and Comm. Systems*, 13-16 Dec. 2005, Hong Kong, pp. 109-112.

[98] V. A. Aalo, "Performance of maximal-ratio diversity systems in a correlated Nakagami fading environment," *IEEE Trans. Commun.*, vol. 43, no. 8**,** pp. 2360–2369, Aug. 1995.

[99] P. M. Shankar, "Performance analysis of diversity combining algorithms in shadowed fading channels," *Wireless Personal Communications*, vol. 37, no. 1-2, pp. 61-72, 2006.

[100] P. Theofilakos, A. G. Kanatasand and G. P. Efthymoglou, "Performance of generalized selection combining receivers in *K*-fading channels," *IEEE Commun. Lett.*, vol. 12, no. 11, pp. 816-818, Nov.2008.

[101] P. S. Bithas, P. T. Mathiopoulos, and S A. Kotsopoulos, "Diversity reception over generalized-K ($K_G$) fading channels," *IEEE Trans. Wireless Commun.*, vol. 6, no. 12, pp. 4238 – 4243, Dec. 2007.

[102] P. S. Bithas, N. C. Sagias, P. T. Mathiopoulos, G. K. Karagiannidis, and A. A. Rontogiannis, "On the performance analysis of digital communications over generalized-K fading channels," *IEEE Commun. Lett.*, vol. 5, no. 10, pp. 353–355, May 2006.

[103] A. Conti, M. Z. Win, M. Chiani, and J. H. Winters, "Bit error outage for diversity reception in shadowing environment," *IEEE Commun. Lett.*, vol. 7, no. 1, pp. 15–17, Jan. 2003.

[104] A. Goldsmith and P. Varaiya, "Capacity of fading channels with channel side information," *IEEE Trans. Inform. Theory*, vol. 43, no. 6, pp. 1896–1992, Nov. 1997.

[105] W. C. Y. Lee. "Estimate of channel capacity in Rayleigh fading environment," *IEEE Trans. on Veh. Technol.*, vol. 93, no. 39, pp. 187-189, Aug. 1990.

[106] C. G. Gunther, "Comment on estimate of channel capacity in Rayleigh fading environment," *IEEE Trans. on Veh. Technol.*, vol. 45, no. 2, pp. 401-403, May 1996.

[107] M. S. Alouini and A. J. Goldsmith, "Capacity of Rayleigh fading channels under different adaptive transmission and diversity-combining techniques," *IEEE Trans. on Veh. Technol.*, vol. 48, no. 4, pp. 1165-1181, Jul. 1999.

[108] S. Khatalin and J. P. Fonseka, "Capacity of correlated Nakagami-m fading channels with diversity combining techniques," *IEEE Trans. on Veh. Technol.* vol. 55, no. 1, pp. 142-150, Jan. 2006.

[109] G. K. Karagiannidis N. C. Sagias, and G. S. Tombras, "New results for the Shannon channel capacity in generalized fading channels," *IEEE Commun. Lett.,* vol. 9, no. 2, pp. 97-99, Feb. 2005.

[110] S. Khatalin and J. P. Fonseka, "On the channel capacity in Rician and Hoyt fading environment with MRC diversity," *IEEE Trans. on Veh. Technol.*, vol. 55, no. 1, pp. 137-141, Jan. 2006.

[111] Q. T. Zhang and D. P. Liu, "Simple capacity formulas for correlated SIMO Nakagami channels," *Proc. IEEE Veh. Technol. Conf.*, Jeju Korea, Apr. 2003, vol. 1, pp. 554 – 556.

[112] K. A. Hamdi, "Capacity of MRC on correlated Rician fading channels," *IEEE Trans. Commun.*, vol. 56, no. 5, pp. 708 – 711, May 2008.

[113] A. Laourine, M.S. Alouini, S. Affes,and A. St´ephenne, "On the capacity of generalized-*K* fading channels," *IEEE Trans. on Wireless Commun.*, vol. 7, no. 7, pp. 2441-2445, Jul. 2008.

[114] G. P. Efthymoglou, N. Y. Ermolova, and V. A. Aalo, "Channel capacity and average error rates in generalized-K fading channels," *IET Commun.*, vol. 4, no. 11, pp. 1364–1372, July ,2010.

[115] R. C. Palat, A. Annamalai and J. H. Reed, "An efficient method for evaluating information outage probability and ergodic capacity of OSTBC system," *IEEE Commun. Lett.*, vol. 12, no. 3, pp. 191– 193, Mar. 2008.

[116] M. Di Renzo, F. Graziosi and F. Santucci, "Channel capacity over generalized fading channels: a novel MGF-based approach for performance analysis and design of wireless communication systems," *IEEE Trans. Veh. Technol.*, vol. 59, no.1, pp. 127-149, Jan. 2010.

[117] T. M. Schmidl and D. C. Cox, "Robust frequency and timing synchronization for OFDM," *IEEE Trans. Commun.*, vol. 45, no. 12, pp. 1613 – 1621, Dec. 1997.

[118] J.-J. van de Beek, M. Sandell, and P. O. Biijesson, "ML estimation of time and frequency offset in OFDM systems," *IEEE Trans. Signal Process*, vol. 45, no. 7, pp. 1800-1805, July 1997.

[119] Vivek K. Dwivedi and G. Singh, "A LMMSE approach for frequency offset estimation in OFDM system," *Proc. Int. Conf. on Intelligent Systems and Networks* (ISN-2008), India, pp. 264-266.

[120] Vivek K. Dwivedi and G. Singh "Inter-carrier interference cancellation in OFDM systems" *Proc. National Conference on Wireless and Optical Communication* (WOC-2007), India, pp. 245-248.

[121] Y.-D. Lee, D.-H. Park and H.-K. Song, **"**Improved channel estimation and mai robust schemes for wireless OFDMA system," *Progress In Electromagnetic Research*, vol. 81, pp. 213–223, 2008.

[122] K Sathananthan and C. Tellambura, "Probability of error calculation of OFDM systems with frequency offset," *IEEE Trans. Comm.*, vol. 49, no.11, pp. 1884-1888, Nov. 2001.

[123] R. Nee and R. Prasad, "OFDM for Wireless Multimedia Communications," Artech House: Boston, March 2000.

[124] Y. Zhao and S.-G. Haggman, "BER analysis of OFDM communication systems with inter carrier interference," *Proc. Int. Conf. on Communication Technology* (ICCT), Oct. 1998, Beijing, China, vol. 2, pp. 22-24.

[125] H. Kang, Y. Kim, W. Hwang and K. Kim, "BER performance of OFDM system with the polynomial self cancellation scheme for OFDM mobile communication systems," *Proc IEEE APCC/OECC*, Beijing, China, Oct. 1999, vol. 1, pp. 701-704.

[126] K. Sathananantan and R. M. A. P. Rajatheva, "Analysis of OFDM in presence of frequency offset and method to reduce performance degradation," *Proc. IEEE Globcom.*, 2000, San Fransisco, CA, Nov. 2000, vol. 1, pp.72-76.

[127] Yu Fu and C. C. Ko, "Theoretical BER analysis of OFDM system with ICI self cancellation," *Proc. 5th Int. Symposium on Wireless Personal Multimedia Communication*, Honolulu, HI, USA, Oct. 2002**,**vol. 3, pp. 991-994.

[128] K. Chang, Y. Han, J. Ha, and Y. Kim, "Cancellation of ICI by Doppler effect in OFDM systems," *Proc. Vehicular Technology Conf.* 2006, Melbourne, Australia, May 2006, vol. 3, pp. 1411 – 1415.

[129] Y.-H. Peng, Y.-C. Kuo, G.-R. Lee**,** and J.-H. Wen, "Performance analysis of a new ICI-self-cancellation-scheme in OFDM systems," *IEEE Trans. Consumer Electronics*, vol. 53, no. 4, pp. 1333-1338, Nov. 2007.

[130] H.C. Wu, Y. Wu, "A new ICI matrices estimation scheme using Hadamard sequence for OFDM systems," *IEEE Trans. on Broadcasting*, vol. 51 , no. 3 , pp. 305 – 314, 2005.

[131] J. G. Proakis, "Digital Communications," Fourth Edition: McGraw-Hill Series, New York, 2001.

[132] H. T. Hui, "The performance of the maximum ratio combining method in correlated Rician fading channel for antenna diversity signal combining," *IEEE Trans. Antenna Propag.*, vol. 53, no. 3, pp. 958-964, Mar. 2005.

[133] Y. Miyagaki, N. Morinaga and T. Namekawa, "Error probability characteristics for CPSK signal through m-distributed fading channel," *IEEE Trans. Commun.*, vol. 26, no. 1, pp. 88–89, Jan. 1978.

[134] G. Fedele, L. Izzo, and M. Tanda, "Dual diversity reception of M–ary DPSK signals over Nakagami fading channels," *Proc. IEEE PIMRC Toronto*, Canada, Sept. 26–29, 1995, pp. 1195–1201.

[135] P. Lombardo, G. Fedele, and M. M. Rao, "MRC performance for binary signals in Nakagami fading with general branch correlation model," *IEEE Trans. Commun.*, vol. 47, pp. 44–52, Jan. 1999.

[136] J. Salz and J.Winters, "Effect of fading correlation on adaptive arrays in digital mobile radio," *IEEE Trans. Veh. Technol.*, vol. 43, pp. 1049–1057, Nov. 1994.

[137] F. Adachi, M. T. Feeney, J. D. Parsons, and A. G. Wllamson, "Cross correlation between the envelopes of 900 MHz signals received at a mobile radio base station site," *Proc. Inst. Elect. Eng.*, vol. 133, pp. 506–512, Oct. 1986.

[138] P. S. Bithas and P. T. Mathiopoulos, "Performance analysis of SSC diversity receivers over correlated ricean fading satellite channels," *EURASIP Journal on Wireless Communications and Networking*, vol. 2007, Article ID 25361, 9 pages, 2007.

[139] P. S. Bithas, P. T. Mathiopoulos, and G. K. Karagiannidis, "Switched diversity receivers over correlated Weibull fading channels," *Proc. Int. Workshop on Satellite and Space Communications* (IWSSC '06), Spain, Sept. 2006, pp. 143– 147.

[140] A. Scaglione, S. Barbarossa, and G. B. Giannakis, "Optimal adaptive precoding for frequency-selective Nakagami-m fading channels," *Proc. 52$^{nd}$ IEEE Vehicular Technology Conf.*, Boston, MA, USA, Sep. 2000, vol. 3, pp. 1291-1295.

[141] Y. Gong and K. B. Letaief, "Performance of space time Trellis coding over Nakagami fading channels," *Proc. 51$^{st}$ IEEE Vehicular Technology Conf.*, Rhodes, Aug. 2001, vol. 2, pp. 1405-1409.

[142] V. A. Aalo and J. Zhang, "Average error probability of optimum combining with a co-channel interferer in Nakagami fading," *Proc. Wireless Communications and Networking Conf.*, Chicago, IL, Aug. 2000, vol. 1, pp. 376-381.

[143] M. Z. Win, G. Chrisikos and J. H. Winters, "MRC performance for M-ary modulation in arbitrarily correlated Nakagami fading channels," *IEEE Commun. Lett*, vol. 4, no. 10, pp. 301-303, Oct. 2000.

[144] Z. Kang, K. Yao, and F. Lorenzelli, "Nakagami-m fading modeling the frequency domain for OFDM system analysis," *IEEE Commun*. Lett., vol. 7, no. 10, pp. 484-486, Oct. 2003.

[145] Z. Du, J. Cheng and N. C. Beaulieu, "Error rate of OFDM signals on frequency selective Nakagami-m fading channel," *Proc. Global Telecommunications Conf.*, Dallas, Texas , vol. 6, Nov. 2004, pp. 3994 – 3998.

[146] Z. Du, J. Cheng and N. C. Beaulieu, "Accurate error-rate performance analysis of OFDM on frequency-selective Nakagami-m fading channels," *IEEE Trans. Commun*, vol. 54, no.2, pp. 319 - 328, Feb. 2006.

[147] J. N. Pierce and S. Stein, "Multiple diversity with non independent fading," *Proc. IRE.*, ,pp. 89-104, 1960.

[148] D. G. Brennan, "Linear diversity combining techniques," *Proc. IRE*, vol. 47, pp. 1075-1102, June 1959.

[149] I. S. Gradshteyn and I. M. Ryzhik, "Table of Integrals, Series, and Products," 7$^{th}$ Ed., Academic Press: San Diego, 2007.

[150] D. B. Dacosta and M. D. Yacoub, "Moment generating functions of generalized fading distributions and applications," *IEEE Comm. Lett.*, vol. 12, no. 2, pp. 112-114, Feb. 2008.

[151] M. S. Alouini and A. J. Goldsmith, "A unified approach for calculating error rates of linearly modulated signals over generalized fading channels," IEEE Trans. Commun., vol. 47, no. 9 , pp. 1324-1334, Sep. 1999.

[152] A. Erdelyi, "Higher Transcendental Function", New York: McGraw Hill, Vol. I, 1953.

[153] R. K. Mallik, M. Z. Win, J. W. Shao, M.-S. Alouini, and A. J. Goldsmith, "Channel capacity of adaptive transmission with maximal-ratio combining in correlated Rayleigh fading," *IEEE Trans. Wireless Commun.*, vol. 3, no. 4, pp. 1124–1133, Jul. 2004.

[154] S. Y. Park, D. J. Love, and D. H. Kim, "Capacity limits of multi-antenna multicasting under correlated fading channels," *IEEE Trans. on Commun.*, vol. 58, no. 7, pp. 2002-2013, Jul. 2010.

[155] P. Theofilakos, A. G. Kanatas and G. P. Efthymoglou, "Performance of generalized selection combining receivers in K-fading channels," *IEEE Commun. Lett.*, vol. 12, no. 11, pp. 816-818, Nov.2008.

[156] M. Abramowitz and I. A. Stegun, Eds., "Handbook of Mathematical Functions: with Formulas, Graphs, and Mathematical Tables," Dover Publications: New York, 1970.

[157] A. P. Prudnikov, Y. A. Brychkov, and O. I. Marichev, "*Integrals and Series: More Special functions*," vol. 3, Gordon and Breach Science, New York, 1990,

[158] A.Abdi and M. Kaveh, "On the utility of gamma PDF in modeling shadow fading (slow fading)," *Proc. of IEEE Vehicular Technology Conference* (VTC), Houston, vol. 3, Jul. 1999, pp. 2308 - 2312.

[159] J. Salo, L. Vuokko, H. M. El-Sallabi, and P. Vainikainen, "An additive model as a physical basis for shadow fading," *IEEE Trans. on Veh. Technology*, vol. 56, no. 1, pp. 13–26, Jan. 2007.

[160] P. M. Shankar, "Error rates in generalized shadowed fading channels," *Wireless Personal Communications*, vol. 28, no. 4, pp. 233–238, Feb.2004.

[161] A. Abdi and M. Kaveh, "K-distribution: an appropriate substitute for Rayleigh-lognormal distribution in fading-shadowing wireless channels," *Electron. Lett.*, vol. 34, no. 9, pp. 851– 852, Apr. 1998.

[162] A. Abdi and M. Kaveh, "Comparison of DPSK and MSK bit error rates for *K* and Rayleigh-Lognormal fading distributions," *IEEE Commun. Lett.*, vol. 4, no. 4, pp. 122–124, Apr. 2000.

[163] S. Al-Ahmadi and H. Yanikomeroglu, "The ergodic and outage capacities of distributed antenna systems in generalized-K fading channels," *Proc. 21ˢᵗ IEEE Int. Symp. on Personal Indoor and Mobile Radio Communication* (PIMRC), 26-30 Sept. 2010, pp. 662 – 666.

[164] T. S. B. Reddy, R. Subadar, and P. R. Sahu, "Outage probability of SC receiver over exponentially correlated K fading channels," *Electron. Lett.*, vol. 14, no. 2, pp. 118– 120, Feb. 2010.

[165] H. Mehdi, K. C. Teh, and K. H. Li, "Multiuser detectors for band-limited direct sequence code- division multiple-access systems with multi tone jamming and generalised-K fading," *IET Commun.*, vol. 4 , no. 17, pp. 2021 – 2031, 2010.

[166] Vivek K. Dwivedi and G. Singh, "Analysis of channel capacity of Generalized - K fading with maximal-ratio combining diversity receivers," *Proc. of IEEE Int. Conference on Communication Systems and Network Technol.* (CSNT-2011), 3-5 Jun. 2011, India, pp. 550-552.

[167] H. Boche and E. A. Jorswieck, "On the ergodic capacity as a function of the correlation properties in systems with multiple transmit antennas without CSI at the transmitter," *IEEE Trans. Commun.*, vol. 52, no. 10, pp. 1654-1657, Oct. 2004.

[168] Vivek K. Dwivedi and G. Singh,"Error-rate analysis of OFDM for correlated Nakagami-m fading channel by using maximal-ratio combining diversity,"

*International Journal of Microwave and Wireless Technol.*, vol. 3, no. 6, pp. 717-726, Dec. 2011.

[169] I. M. Kostic, "Analytical approach to performance analysis for channel subject to shadowing and fading," *IEE Proc.*, vol. 152, no. 6, pp. 821–827, Dec. 2005.

[170] M.-S. Alouini, A. Abdi, and M. Kaveh, "Sum of gamma variates and performance of wireless communication systems over Nakagami-m fading channels," *IEEE Trans. Veh. Technol.*, vol. 50, no. 6, pp. 1471–1480, Nov. 2001.

[171] A. Annamalai, C. Tellambura, and V. K. Bhargava, "A general method for calculating error probabilities over fading channels," *IEEE Trans. Commun.*, vol. 53, no. 5, pp. 841–852, May 2005.

[172] Y.-C. Ko, M.-S. Alouini, and M. K. Simon, "Outage probability of diversity systems over generalized fading channels," *IEEE Trans. Commun.*, vol. 48, no. 11, pp. 1783–1787, Nov. 2000.

[173] A. Annamalai, C. Tellambura, and V. K. Bhargava, "Simple and accurate methods for outage analysis in cellular mobile radio systems — a unified approach," *IEEE Trans. Commun.*, vol. 49, no. 2, pp. 303–316, Feb. 2001.

[174] V. V. Veeravalli, "On performance analysis for signaling on correlated fading channels," *IEEE Trans. Commun.*, vol. 49, no. 11, pp. 1879-1883, Nov. 2001.